

What's in a wave?

Marcus Jan van Houwelingen

What's in a wave?

Cover picture: Nucleus Medical Media

© 2010 Marc van Houwelingen

Thesis Erasmus Medical Center, Rotterdam

All rights reserved. No part of this book may be reproduced or transmitted in any form or by any means, without prior written permission of the author.

ISBN 978-94-6169-056-2

Printed by Optima Grafische Communicatie

What's in a wave?

Wat zit er in in een golf?

Proefschrift

ter verkrijging van de graad van doctor aan
de Erasmus Universiteit Rotterdam
op gezag van de rector magnificus

Prof.dr. H.G. Schmidt

en volgens besluit van het College voor Promoties

De openbare verdediging zal plaatsvinden op donderdag
11 mei 2011 om 15:30 uur

door

Marcus Jan van Houwelingen

geboren te Eindhoven



Promotiecomissie

Promotor: Prof.dr. D.J.G.M. Duncker
Prof.dr.ir. A.P.G. Hoeks

Overige leden: Prof.dr. W.J. van der Giessen
Dr. A.H. van den Meiracker
Prof.dr. F.W. Prinzen

Copromotor: Dr. D. Merkus

The studies in this thesis have been conducted at the Biophysics department, Maastricht University, The Netherlands and the Laboratory for Experimental Cardiology, Erasmus MC Faculty, The Netherlands

The studies described in this thesis were financially supported by Dräger Medical B.V. and SenterNovem of the Dutch Ministry of Economic Affairs (TSGE3162, KWR09134)

The publication of this thesis was financially supported by Dräger Medical B.V.

Content

Chapter 1	General introduction	7
Chapter 2	The onset of ventricular isovolumic contraction as reflected in the carotid artery distension waveform	31
Chapter 3	Coronary-aortic interaction during ventricular isovolumic contraction	49
Chapter 4	Initiation of ventricular contraction as reflected in the arterial tree	65
Chapter 5	Arterial determination of the left ventricular isovolumic contraction period in the assessment of hemorrhagic shock severity	85
Chapter 6	General discussion and conclusion	103
Summary		123
Samenvatting		129
Dankwoord		135
Curriculum Vitae		143
List of publications		147
PhD portfolio		151

Chapter 1

General introduction

1.1 Introduction

In western society, cardiovascular disease is one of the leading causes of death. An appropriate lifestyle and therapeutic interventions can delay the deterioration of cardiovascular disease. As a result, early detection of cardiovascular disease has received significant attention. Two of the oldest cardiovascular signals measured are blood pressure [1] and ECG [2]. These measures provide (non-) invasive estimates of cardiac and vascular function. With technical advances, the entire arterial blood pressure waveform (figure 1) became available to clinicians, allowing a major step forward in the recognition of cardiovascular disease. For example, the arterial blood pressure waveform allows for the determination of vascular stiffness, which has been shown to be an early predictor of the development of hypertension [3] and risk for myocardial infarction [4]. The arterial blood pressure waveform is also used in the early detection of shock [5, 6], guiding immediate treatment with the administration of fluids and/or vaso-active agents. Hence the evaluation of the arterial blood pressure waveform has become part of daily clinical practice.

The shape and amplitude of the arterial blood pressure waveform are the result of the intricate interaction of numerous systems (figure 2). It therefore contains a vast amount of information about the interaction of these systems. Research into the analysis of the arterial blood pressure waveform is still ongoing. So far, it has resulted in numerous applications that can aid in an earlier detection of cardiac and/or vascular dysfunction [6-9]. The non-invasive assessment of the arterial blood pressure waveform, which has recently become available through technical advances, has intensified research into the constituents of the arterial blood pressure waveform, and has expanded diagnostic applications [10-13]. Possibly more important, non-invasive assessment allows for access to the arterial blood pressure wave of a patient earlier in the care

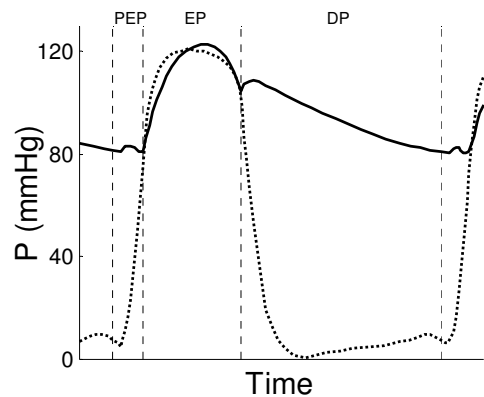


Figure 1. Representative aortic (solid line) and left ventricular pressure (dotted line). The vertical lines indicate the intervals of the Pre-Ejection Period (PEP), Ejection Period (EP) and Diastole (DP)

pathway. This allows for a faster assessment of the condition of a patient, next to a decreased patient discomfort compared to an invasive arterial pressure measurement.

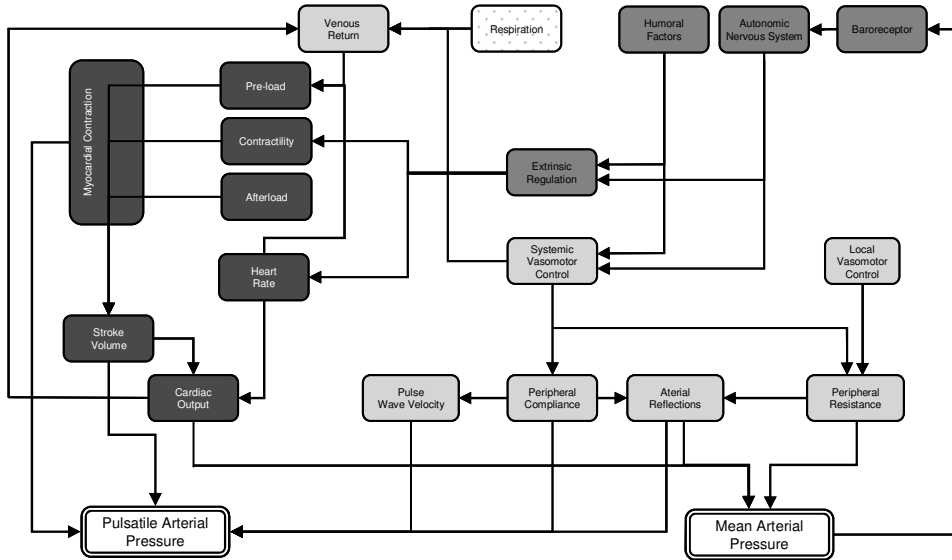


Figure 2. Schematic overview of the determinants of the pulsatile and mean component of the arterial pressure wave. Dark grey blocks indicate a cardiac origin, light grey blocks a vascular origin, middle grey blocks a neuro-humoral origin and the dotted block a respiratory origin.

The main research question in this thesis is whether additional information on the cardio-vascular interaction can be derived from the arterial pressure waveform. It is therefore important to understand the interaction between the various parts of the cardiovascular system and how this interaction is reflected in the amplitude and timing features of the arterial blood pressure waveform. The following sections will introduce how the cardiovascular subsystems, as shown in figure 2, are related to the timing and amplitude properties of the arterial blood pressure waveform. Additionally, the effect of hemorrhagic shock on the subsystems and the resulting change in amplitude and/or timing properties of the arterial pressure waveform will be used as an illustrative example of cardiovascular dysfunction.

The cardiovascular system consists of the heart and both the systemic and pulmonary circulation. The heart connects both circulations in a single closed loop and drives the flow of blood. The pulmonary circulation is contained within the thorax, while the systemic circulation supplies organs both in- and outside of the thorax. Consequently, the systemic circulation is much more accessible for

measurements on the cardiovascular system and is usually readily available for the clinician. For that reason we will focus on cardiovascular information that can be derived from the systemic arterial pressure waveform.

1.2 Cardiac influence on the arterial pressure wave

The phasic cardiac contraction ejects blood into the vascular bed resulting in a steady (mean) and pulsatile arterial pressure component. During ventricular contraction (systole), which onset is defined by the Q-top of the ECG, 60-70% of the blood contained within the left ventricle is ejected into the aorta [14, 15] (figure 3, bottom left panel). Prior to ejection, left ventricular contraction causes left ventricular intra-cavity pressure to rise, whilst the mitral valve located between the left atrium and ventricle prevents blood from flowing back into the atrium. Only when left ventricular pressure surpasses aortic pressure, the aortic valve opens allowing ejection of blood [14]. The early systolic interval between the Q-top of the ECG and the aortic valve opening is referred to as the pre-ejection period (PEP, figure 3). PEP can be subdivided into two intervals. The first interval spans the time from the Q-top of the ECG to closure of the mitral valve and represents the electro-mechanical delay [16] (EMD, figure 3). The second interval constitutes the isovolumic contraction period (IC, figure 3) and

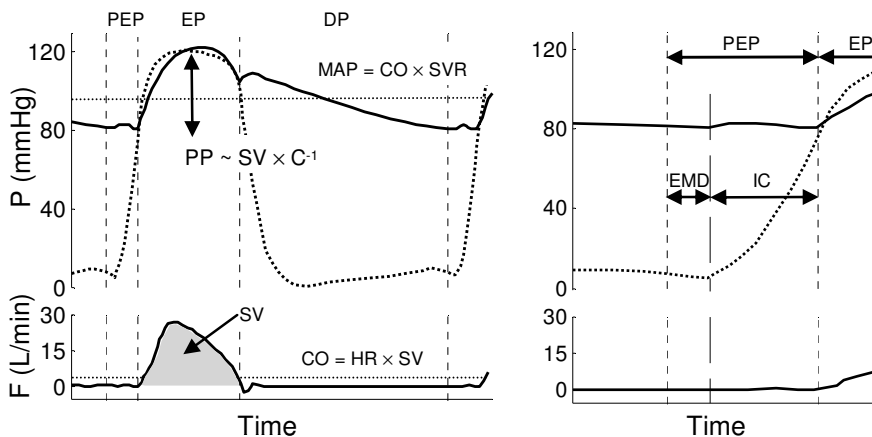


Figure 3. The left panels show the left ventricular (dotted curve) and the aortic (solid curve) pressure, together with left ventricular volume outflow. The systolic phase consists of the pre-ejection period (PEP) and ejection period (EP), and is followed by the diastolic phase (DP), indicated by the vertical dotted lines. The right panels show an enlargement of the early systolic phase, where the subdivision of PEP into the electro mechanical delay (EMD) and isovolumic contraction period (IC) is indicated with a vertical dashed line. Area under the flow curve during PEP and EP represents stroke volume (SV, in grey, bottom left panel). The relation between pulse pressure (PP) and stroke volume via arterial compliance (C) is indicated in the top left panel. The relation between mean arterial pressure (MAP, horizontal dotted line), cardiac output (CO) and systemic vascular resistance (SVR) is indicated in the same panel. In the bottom left panel the relation between stroke volume and cardiac output via heart rate is indicated with a horizontal dotted line.

refers to the time between mitral valve closure and the onset of ejection. During the isovolumic contraction period left ventricular pressure increases under influence of the contracting ventricle [16, 17], preparing the heart for ejection. In the second part of systole, left ventricular pressure increases above aortic pressure level, causing the ejection of blood (i.e. stroke volume, which is the area under the systolic part of the volume flow curve in figure 3 bottom left panel) into the aorta. This results in an increase in arterial pressure as the aorta accommodates the ejected volume. The ejection phase (EP) ends with the closure of the aortic valve due to ventricular relaxation [14] (figure 3). During the diastolic phase left ventricular relaxation causes its transmural pressure to drop, allowing the ventricle to be filled with blood from the pulmonary venous system via the left atrium (DP, figure 3). This loads the left ventricle for ejection of stroke volume during the next cardiac cycle.

1.2.1 Stroke volume influence on arterial pressure waveform

The ejection of stroke volume is responsible for the pulsatile behavior of the arterial pressure wave, where the compliant arterial tree cushions the increase in arterial pressure by an increasing volume [14] (figure 3). Ejection of stroke volume into the arterial tree is responsible for the phasic increase in pressure (pulse pressure, PP, figure 3), whereas flow to the periphery results in the deflation of the central arteries and a gradual drop in arterial pressure during diastole. Consequently, the compliant arterial tree acts as a temporary buffer for the stroke volume causing the systemic vascular bed to be perfused over the entire cardiac cycle [14]. Mean arterial pressure (MAP, figure 3) is therefore related to systemic vascular resistance and the average volume flow of blood (cardiac output CO, figure 3). Cardiac output equals the product of heart rate and stroke volume. Therefore, changes in stroke volume can affect both mean and pulsatile amplitude of the arterial blood pressure (figure 3). Stroke volume depends on left ventricular preload, contractility and afterload [14]. These will be described in more detail with respect to their distinct influences on the timing and amplitude characteristics of the arterial pressure waveform in the following sections.

Preload

Left ventricular preload is defined as the stretch of the left ventricular myocardium at the end of its diastolic phase [14]. It is therefore related to the left ventricular filling pressure and diastolic compliance [14]. Initially, the relaxing left ventricle will receive blood from pulmonary veins via the left atrium. Left atrial contraction enhances blood volume flow into the left ventricle, resulting in an increased left ventricular filling pressure and diastolic volume. Within certain

limits, increasing stretch (preload) of the left ventricular myocardium enhances the tension generated during isometric contraction [14, 18], which allows for a larger stroke volume [19]. The intrinsic mechanism of the heart to increase stroke volume as a result of an increased preload is known as the Frank-Starling mechanism [20] (figure 4).

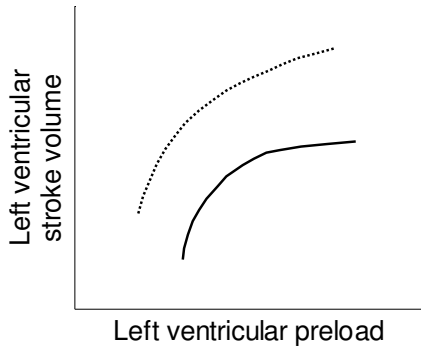


Figure 4. Frank-Starling relation of the left ventricle, where the solid line indicates a normal relation and the dotted line the effect of an increase in ventricular contractility.

The increase in preload, and hence stroke volume, will not only increase pulse pressure (see section 1.3.1), but will also increase the ejection period and shorten the isovolumic contraction period [17]. In the face of a constant heart rate the change in pre-ejection period negates the changes in ejection period resulting in a virtually unaltered duration of ventricular systole [16, 17]. Figure 5 shows the effect of an increased preload on the left ventricular pressure-volume relation and the arterial pressure waveform.

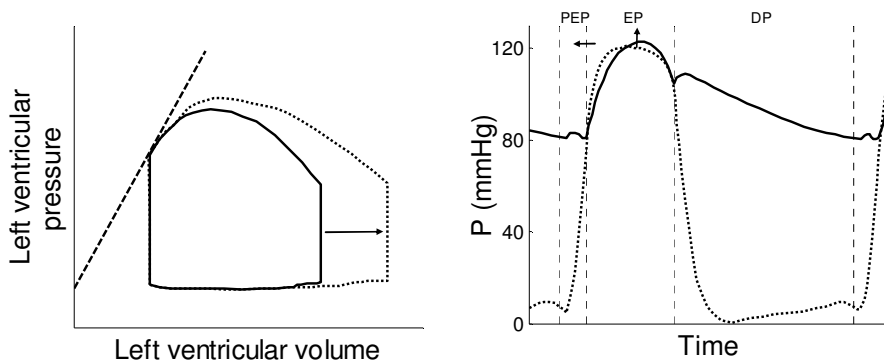


Figure 5. Left panel shows the effect of an increase in preload on the pressure-volume relationship (dotted line) as compared to a normal preload (solid line). The straight dashed line indicates the end systolic pressure volume relation. The right panel shows the effect of an increase in preload on the amplitude and timing characteristics of the left ventricular and arterial pressure waveform (arrows).

Contractility

Myocardial contractility is defined as the intrinsic contractile force generated by the myocardium for contraction, independent of the preload. Consequently, an increase in contractility (e.g. by extrinsic regulation or inotropic medication) will

result in an increased stroke volume (figure 6, left panel, dotted line). The increased contractility will further result in an earlier onset of the upstroke of the arterial pressure due to an increased rate of pressure build-up in the left ventricle [14]. The increased rate of left ventricular pressure build-up will also result in an increased ejection rate of stroke volume and hence a steeper systolic upslope of the arterial pressure wave and a higher pulse pressure [14]. Consequently increases in contractility will decrease the ejection time despite the increase in stroke volume. Therefore, duration of total systole will decrease [17, 21, 22].

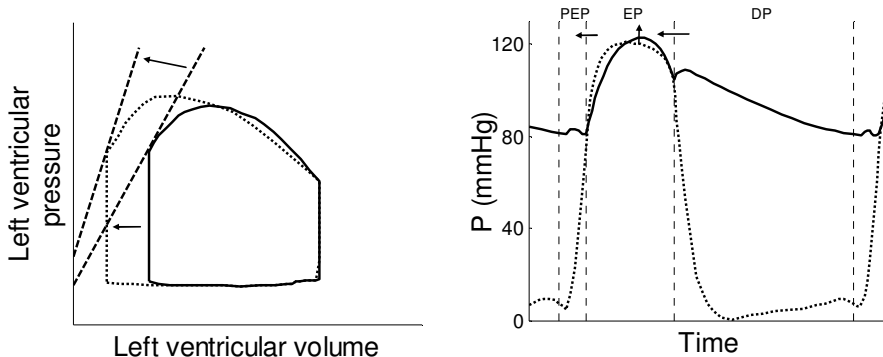


Figure 6. Left panel shows the effect of an increase in contractility on the pressure-volume relationship (dotted line) as compared to a normal contractility (solid line). The increase in contractility leads to an increase in slope of the end systolic pressure volume relation (straight dashed lines, increase indicated with an arrow). The right panel shows the effect of an increase in contractility on the amplitude and timing properties of the left ventricular and arterial pressure waveform (arrows).

Afterload

Afterload is defined as the stress required of the ventricular myocardium to eject blood [14]. Afterload is therefore directly related to the arterial blood pressure (as left ventricular pressure should exceed the aortic pressure for the aortic valve to open) as well as to the end diastolic volume [14]. An increased afterload will decrease stroke volume [14]. Moreover, it will decrease the ejection period and increase the pre-ejection period [17] (figure 7). Therefore the net influence of an increased afterload on the duration of systole is hard to predict.

Heart rate

Provided that diastolic filling time is sufficient, increases in heart rate will result in a higher mean arterial pressure via the increased cardiac output [14, 23]. It will further result in a decrease in both the isovolumic contraction and ejection period, and hence results in a decrease in the systolic phase duration [17].

Increased heart rate will decrease stroke volume only when the diastolic period is too short for the heart to fill adequately [23]. Therefore, there is an optimum in

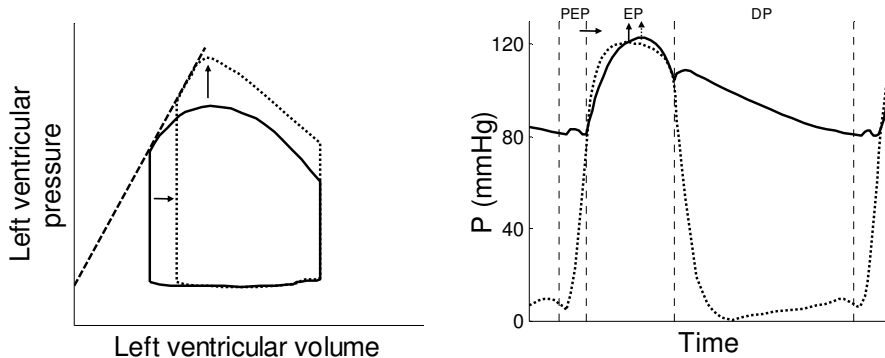


Figure 7. Left panel shows the effect of an increase in afterload on the pressure-volume relationship (dotted line) as compared to a normal contractility (solid line). The straight dashed line indicates the end systolic pressure volume relation. The right panel shows the effect of an increase in afterload (dotted arrow) on the amplitude and timing properties of the left ventricular and arterial pressure waveform (solid arrows).

heart rate to obtain a maximum mean arterial pressure. Heart rates above that optimum will decrease mean arterial again. Moreover, arterial pulse pressure will decrease with heart rates above the optimum due to the decreased stroke volume.

1.2.2 Cardiac motion

Myocardial contraction and the associated cardiac motion may perturb the arterial pressure waveform via the connection between the moving heart and the aorta. It has been shown that compression of the coronary vascular bed due to contraction generates a pressure wave traveling from the coronary vascular bed towards the aorta [24-27]. This pressure wave might well influence the shape of the aortic pressure waveform. Myocardial contraction is even able to reverse temporarily coronary artery blood volume flow with a more pronounced reversed volume flow during exercise [28, 29]. Assuming this retrograde volume flow reaches the aorta, the addition of volume to the aortic foot volume could also intermittently increase aortic pressure.

As described above, left ventricular contraction causes the aortic pressure to increase during ejection of blood. However, changing left ventricular intra-cavity blood pressure and intra-cavity flow may additionally influence the arterial pressure waveform prior to aortic valve opening. During isovolumic contraction, the movement of the left ventricular myocardium redirects intra-ventricular blood volume towards its outflow tract [30]. The redirected blood will, hence, exert a

force against the aortic valve during the isovolumic contraction period. Subsequent valve displacement and deformation possibly may perturb the aortic pressure waveform [31, 32]. Additionally, movement of the myocardial tissue could result in radial and longitudinal forces on the foot of the aorta [33-35], possibly contributing to the aortic pressure perturbation.

1.3 Systemic vascular influence on the arterial pressure wave

Although the heart is the origin of the systemic arterial pressure wave, the shape and average value of the systemic arterial pressure waveform depend on the vascular properties of the systemic circulation [14, 20]. Both the arterial and venous contribute to the amplitude and timing characteristics of the arterial pressure waveform. Their specific contributions will be discussed in the following sections.

1.3.1 Influence of the arterial tree on the arterial pressure wave

The shape and average value of the arterial pressure wave depends on the compliance of the arterial tree and peripheral resistance [20, 36, 37]. The combined effect of arterial resistance and compliance can be represented by the arterial impedance. Spatial mismatches in impedance have a specific impact on the arterial pressure waveform and will therefore be described separately [36].

Arterial tree compliance

The pulsatile amplitude of the arterial pressure waveform (pulse pressure) is related to the compliance of the arterial tree, which acts as a buffer for the left ventricular stroke volume, and the systemic vascular resistance (see next section). A highly compliant arterial tree can expand easier to accommodate the stroke volume with only a small pressure increase from minimum diastolic to maximum systolic pressure, as compared to a stiff arterial tree, where the same stroke volume causes a higher pressure increase [14] (figure 8). Consequently, a lower arterial compliance increases left ventricular afterload [38] (see section 1.2.1).

The compliance of arteries depends on the ratio of their elastin and collagen content [14, 36]. As a consequence the relation between volume and pressure in an artery (i.e. arterial compliance) is curvilinear [39]. Therefore, at a higher

mean arterial pressure and arterial lumen volume, injection of a specific stroke volume will result in an augmented increase in pulse pressure [36]. Next to the elastin and collagen content of the arteries, vascular smooth muscle cells modulate the compliance of the arterial tree [14]. Vascular smooth muscle cells contract under influence of neurohumoral activation, decreasing arterial compliance and increasing arterial resistance.

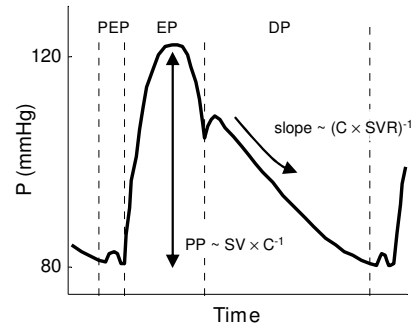


Figure 8. Influence of arterial compliance (C) on pulse pressure (PP) during ejection of stroke volume (SV) and rate of decay during diastole. SVR represents systemic vascular resistance.

The compliant arterial tree acts as buffer for the left ventricular stroke volume. Therefore, arterial compliance is one of the two determinants in the rate of decay of the arterial pressure wave during diastole. The other determinant is the blood volume flow towards the periphery, which is determined by the systemic vascular resistance [40] (figure 8). Next to the rate of pressure decay during diastole, the compliant nature of the arterial tree also affects timing properties of the arterial pressure waveform. It is responsible for the gradual transmission of the initial pressure pulse wave, generated by injection of stroke volume, over the arterial tree [14, 36]. From figure 9 it can be appreciated that the onset of arterial systole, recorded at the level of the canine aortic-iliac bifurcation (28 cm from the heart), occurs later than the onset of arterial systole near the aortic valve (0 cm from the heart) [36, 41]. The measurement location is therefore important to consider in the timing analysis of the arterial pressure wave when related to e.g. the ECG.

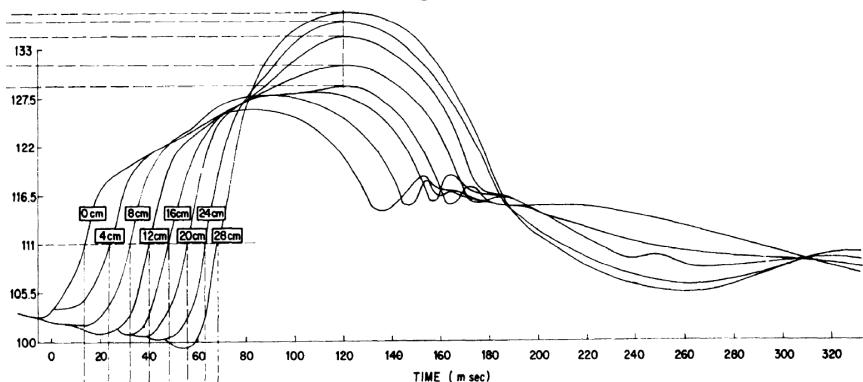


Figure 9. Synchronous blood pressure recording made at a series of sites along the aorta in a dog, starting from the descending aorta (0 cm) (from [41]).

The speed of a pressure wave (pulse wave velocity, PWV) in a vessel can be calculated using the Bramwell-Hill equation [36] (Equation 1), assuming a long wavelength compared to the vessel diameter (which is related to its volume), a small wall thickness compared to vessel diameter and a linear pressure-volume relationship.

$$PWV = \sqrt{\frac{1}{\rho} \frac{\Delta P}{\Delta V}} \cdot V \quad \text{Equation 1}$$

In Equation 1 ρ represents blood mass density, ΔP the change in transmural pressure due to a change in intra-vessel volume ΔV (their ratio effectively represents the inverse of the compliance of the vessel), and V the diastolic volume of the vessel, which depends on diastolic pressure and compliance of the vessel. Consequently, when arteries become less compliant for example with age [38, 42, 43] or hypertension [7, 44], pulse wave velocity will increase. The increased pulse wave velocity will not only affect timing properties of the arterial pressure waveform, but also its amplitude, resulting in an increase in ventricular afterload [38] (see below).

Arterial tree resistance

Systemic vascular resistance can be calculated by dividing mean arterial pressure by cardiac output [14] (figure 10). It is predominantly determined by the arterioles, which are the smallest arteries prior to the capillary bed [14]. Both local and systemic factors influence arteriolar resistance to match local volume flow to the demand of the tissue. The rate of blood volume outflow from the arterial reservoir through the arterioles together with the arterial compliance determines the rate of decay of the arterial blood pressure slope during diastole [40] (figure 10). Moreover, arteriolar resistance contributes to the generation of reflections through mismatches in arterial impedance, affecting both amplitude and timing properties of the arterial pressure waveform [45] (see below).

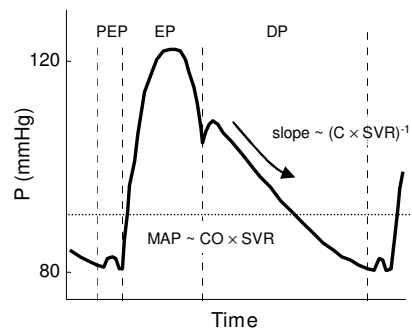


Figure 10. Influence of systemic vascular resistance (SVR) on mean arterial pressure (MAP) with a specific cardiac output (CO) and rate of decay during diastole. C represents arterial compliance.

Arterial tree impedance

Arterial impedance is the frequency-dependent combination of arterial compliance and resistance and varies with vessel size and structure. Wave reflections occur at any site where vessel impedances do not match, which is likely to occur at bifurcations [36]. The amplitude of the reflection is related to the degree of mismatch in impedance between connected arterial segments. How a reflection contributes to the measured arterial pressure waveform depends on vascular properties of the measurement site [39, 46], amplitude of reflection [36], distance from the reflection site to the measurement site and pulse wave velocity [36] (figure 11). Reflection sites close to the heart, like the one at the level of the aortic-renal bifurcation, can generate reflections that return to the heart during the ejection phase [47]. Only in subjects with stiff arteries (high pulse wave velocity), reflections with a more peripheral origin, e.g. from the aortic-iliac level, may arrive during systole [38]. Reflections that return to the heart during systole will augment aortic systolic pressure and therefore increase left ventricular afterload [14, 38].

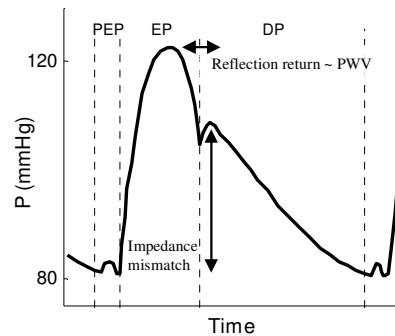


Figure 11. Influence of reflections caused by arterial impedance mismatches on the arterial blood pressure wave. An increased mismatch increases reflection amplitude (vertical arrow). Changes in arrival time of the dicrotic wave related to changes in pulse wave velocity (PWV) affect the ejection period (EP, horizontal arrow)

Reflections can aid in the assessment of the cardiovascular system. The pressure perturbation occurring in early diastole due to a peripheral reflection contributes to aortic valve closure and explains the dicrotic notch [48]. This allows for the determination of the ejection period of the heart by arterial pressure waveform timing analysis (figure 11). The ejection period is a valuable marker in the assessment of left ventricular myocardial performance [12, 49-51]. Another example of the use of reflections in the assessment of the cardiovascular status is the use of an early reflection that causes a shoulder in the systolic pulse pressure. It is used to calculate the augmentation index, a marker for arterial stiffness [47, 52].

1.3.2 Influence of the venous system on the arterial pressure wave

Blood from the capillary vascular bed collects in the venous system, from which it is transported back to the heart. The venous system is highly compliant and therefore contains most of the circulating blood volume. Neurohumoral control of this volume allows for the control of systemic venous return by means of vasoconstriction or dilatation [14]. An increase in venous return translates into an increased right heart output, which results in an increased left ventricular preload and stroke volume [14]. With the increased left ventricular stroke volume mean arterial pressure and pulse pressure also increase, as described in sections 1.2.1 and 1.3.1.

Venous return can be restricted by an increased intra-pleural pressure (e.g. due to positive pressure ventilation). The increased intra-pleural pressure raises the intra-thoracic vena cava pressure and, as a consequence, decreases volume flow from outside of the thorax to the heart [53]. The decrease in right heart preload in combination with an increased afterload decreases right ventricular stroke volume [6]. The latter will subsequently result in a decreased left ventricular preload and stroke volume [54].

The decrease in venous return and its subsequent effects as described above dominates the ventilation induced change in left ventricular stroke volume in the healthy heart [6]. Increased intra-pleural pressure also transiently increases left ventricular stroke volume by squeezing blood from the pulmonary vascular bed towards the left ventricle [55]. Moreover, increased intra-pleural pressure decreases left ventricular afterload and, hence, facilitates left ventricular ejection [56]. These two mechanisms cause the initial increase in stroke volume following the onset of increased intra-pleural pressure, but contribute far less to the variation in stroke volume or pulse pressure compared to the effect of the decrease in venous return [6]. Finally, Denault et al. [57] showed that the increased intra-pleural pressure increased left ventricular contractility and heart rate via sympathetic activation. However, when normal left ventricular contractility is preserved, the influence of changes in cardiac contractility on the arterial pressure waveform are only minor [57]. Moreover, diastolic filling will be influenced only at very high heart rates [23]. Therefore, the effect of ventilation induced changes in contractility and heart rate on stroke volume and pulse pressure is also considered to be minimal.

A decrease in intra-pleural pressure enhances venous return to the right heart, which results in an increased right ventricular stroke volume. The increase in

right ventricular output will initially be used to fill the pulmonary vascular bed followed by an augmented left ventricular venous return.

From the above follows that cyclic changes in intra-pleural pressures due to positive pressure ventilation result in cyclic changes in the arterial pressure wave [6, 58] (figure 12).

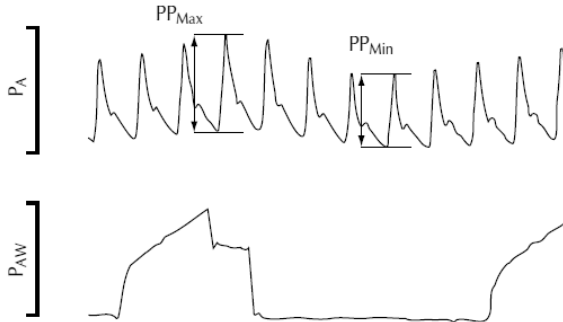


Figure 12. Influence of ventilation on arterial pressure (from [58]). P_A shows the arterial pressure over a ventilation cycle P_{AW} . PP_{Max} indicates maximum pulse pressure that occurs during inspiration, PP_{Min} indicates minimum pulse pressure that occurs during expiration.

1.4 Neurohumoral influence on the arterial pressure wave

The neurohumoral systems, i.e. the autonomic nervous system and release of humoral factors, have a direct influence on the arterial blood pressure. Their influence is exerted through control of heart rate, local and systemic control of vasoconstriction and control of fluid balance [14]. The exact mechanisms are beyond the scope of this thesis.

1.5 The effect of hemorrhagic shock on the arterial pressure wave

Hemorrhage causes a reduction in circulating blood volume and consequently a decrease in left ventricular preload. The reduction in preload results in a reduced stroke volume and cardiac output, inducing systemic hypotension. This situation is termed hemorrhagic shock [59]. In response to a drop in systemic arterial pressure, neurohumoral control increases heart rate and systemic vasoconstriction [14]. Constriction of the venous system initially counteracts the hemorrhage mediated drop in preload and hence cardiac output. Together with the increased total systemic vascular resistance, a severe drop in systemic arterial pressure is therefore prevented [14]. Arterial vasoconstriction reduces arterial compliance, increasing the slope of the curvilinear volume–pressure relation of the large arteries [14]. However, this decrease in compliance is likely

counteracted by the hemorrhagic shock mediated decrease in arterial pressure (which increases compliance). This assumption is based on the notion that pulse wave velocity, an indicator for vascular stiffness, does not change under influence of hemorrhage [45, 60, 61]. Dark et al. [45] showed that during hemorrhagic shock early reflections caused by splanchnic vasoconstriction augment the arterial pressure wave and, hence, increase the afterload of the heart. They concluded that changes in impedance, as a consequence of a sympathetic response to hemorrhage, are mediated through changes in arterial resistance rather than arterial compliance [45]. With progressing hemorrhage, venous return will drop to such extent that neurohumoral mediated changes in the cardiovascular system do not suffice, eventually resulting in a drop of mean arterial pressure.

Figure 13 shows the effect of a graded hemorrhagic shock on the cardiovascular subsystems that determine the characteristics of the arterial blood pressure waveform, i.e. shape, amplitude and timing.

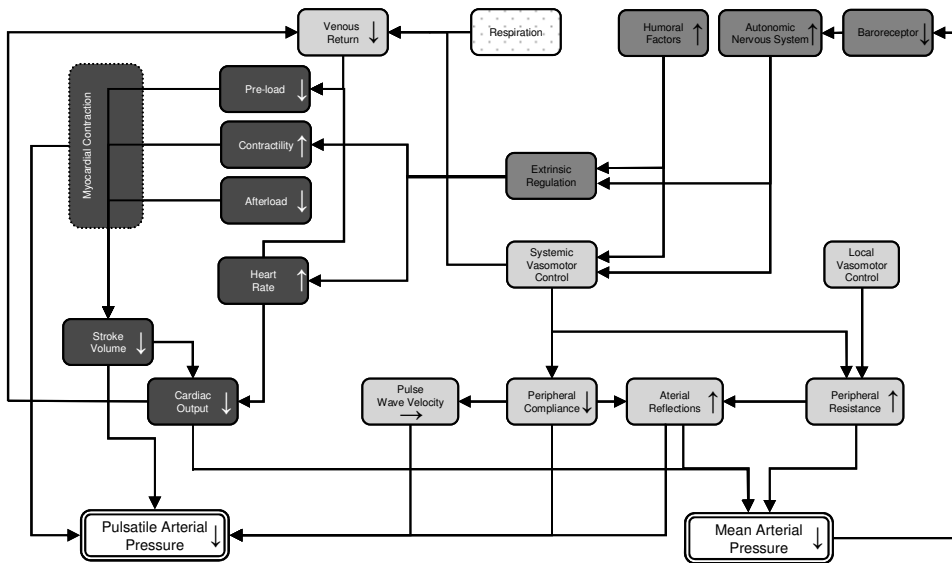


Figure 13. the effects of hemorrhage on the determinants of the shape and amplitude of the arterial pressure wave. Changes due to hemorrhage are indicated with arrows, ↑ indicates an increase, ↓ a decrease and → no change.

Indicators of right or left ventricular preload, like right atrial pressure or pulmonary artery occlusion pressure, are frequently used in the decision whether or not to give fluids to a patient with an acute circulatory failure [6, 62]. The pre-ejection period is, similar to stroke volume and pulse pressure, related to preload (see section 1.2.1). The advantage of the pre-ejection period over the

right atrial pressure or pulmonary artery occlusion pressure is that it can be obtained non-invasively. Chan et al. [60] was able to show that in healthy volunteers a progressive central hypovolemia evoked by a head-up tilt increased the pre-ejection period of the heart while mean arterial blood pressure was maintained. However, with progression of hemorrhagic shock, cardiac contractility increases, thereby shortening the pre-ejection period [17, 63]. Moreover, a drop in afterload has a further decreasing effect on the pre-ejection period [17]. Consequently, hemorrhagic shock affects the pre-ejection period via multiple pathways [63]. In general, static indicators that relate to ventricular preload have proven to poorly predict whether a patient will respond favorably to fluid expansion [6, 62]. The low predictive value follows from the unknown working point of the heart on its Frank-Starling curve [6] (figure 4).

Using positive pressure ventilation one may cyclically perturb left ventricular preload and consequently stroke volume (see section 1.3.2). When operating on the steep slope of the Frank-Starling curve the ventilation induced variation in stroke volume will be larger in magnitude as compared to when operating on the flat slope (figure 14). The concomitant ventilation induced variation in pulse pressure will change accordingly. It has been shown that the amplitude of the relative ventilation induced variation in stroke volume and arterial pulse pressure reflects the fluid status of a hemorrhagic shock patient and is able to predict whether a patient will benefit from fluid expansion or not [6, 10, 58, 64, 65].

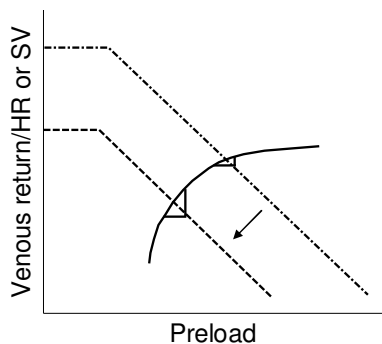


Figure 14. Frank-Starling curve in relation to venous return. The influence of a changing working point on the Frank-Starling curve, due to hemorrhage, on stroke volume (SV) in the face of an unchanged ventilation induced preload variation. The working point is determined by the relation between venous return divided by HR and preload (dash-dotted line), which shifts downwards under influence of hemorrhage (dashed line).

Using the relative rather than the absolute variation supports the determination of a subject-independent threshold value to discriminate between responders and non-responders. Bendjelid et al. [10] showed in cardiac surgery patients that the pre-ejection period, assessed from the pressure waveform in the radial artery, decreased during inspiration and increased during expiration as a consequence of ventilation induced changes in preload. Similar to the pulse

pressure and stroke volume variation, the relative variation in pre-ejection period was shown to be able to predict whether a patient is fluid responsive or not [10, 66]. The benefit of analysis of timing rather than the amplitude characteristics is that it allows the use of a (non-invasive) substitute for the arterial pressure waveform (e.g. the ultrasound derived arterial distension waveform). The only requirement for such substitute is that there exists a monotone ascending relationship between it and the pressure waveform, which preserves the timing properties of the arterial pressure waveform.

1.6 Aim and outline of this thesis

Although the arterial blood pressure measurement is part of daily clinical practice, and the blood pressure waveform has been investigated intensely for additional and valuable information [6-9], it still contains unused information (figure 15). As indicated before, the main research question in this thesis is whether additional information on the cardio-vascular interaction can be derived from the arterial pressure waveform, assessed either in the (ascending) aorta or peripherally (e.g. in the carotid artery). In chapter 2 we describe the observation of a small but persistent perturbation found in the late diastolic phase of the carotid distension waveform, i.e. the change in arterial diameter that is closely related to the carotid pressure waveform. A similar perturbation was also found in the aortic pressure waveform in patients who received an artificial aortic valve. This perturbation was related to the subsequent systolic phase, providing information on the current heart cycle. Figure 15 shows an example of the perturbation occurring in the aortic pressure waveform.

In order to relate the observed pressure perturbation to cardiac and vascular function, its origin needs to be known, which we set out to investigate in chapter 3 and 4. Specifically, chapter 3 disproves a possible role of the coronary system as hypothesized in chapter 2 to be the most likely origin of the perturbation. Chapter 4 investigates the timing properties of the perturbation onset in relation to other relevant cardiac timing properties. It further elucidates the origin of the perturbation by addressing specific aspects of the ventricular pressure waveform and cardiac motion at the time of the onset of the perturbation.

Having established that the onset of the pressure perturbation coincides with the onset of the left ventricular isovolumic contraction, its clinical applicability is examined in chapter 5. Here, a proof of concept is given for the applicability of the onset of the pressure perturbation in the field of shock treatment. Moreover,

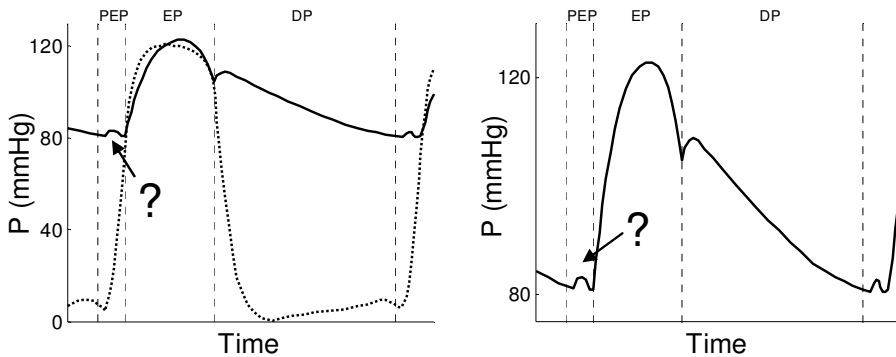


Figure 15. Left panel shows left ventricular (dotted line) and aortic pressure (solid line). Right panel shows the enlarged aortic pressure from left panel. The Pre-Ejection Period (PEP), Ejection Period (EP) and Diastole (D) are indicated by vertical dotted lines. Just prior to the onset of aortic systole a small pressure perturbation is indicated, of which the origin will be discussed in this thesis.

its performance is compared to the applicability of three other predictors of fluid responsiveness in that chapter. Chapter 5 aims to prove a close relation between the timing properties of the pressure perturbation and frequently used invasive predictors of fluid responsiveness. Because the pressure perturbation can be sensed non-invasively in peripheral arteries, it has the potential of a non-invasive marker, potentially shortening the time required to detect a compromised circulation (i.e. shock).

1.7 References

1. Salvetti A: **A centenary of clinical blood pressure measurement: a tribute to Scipione Riva-Rocci.** *Blood Press* 1996, **5**(6):325-326.
2. Moukabary T: **Willem Einthoven (1860-1927): Father of electrocardiography.** *Cardiol J* 2007, **14**(3):316-317.
3. Van Merode T, Hick PJ, Hoeks AP, Rahn KH, Reneman RS: **Carotid artery wall properties in normotensive and borderline hypertensive subjects of various ages.** *Ultrasound Med Biol* 1988, **14**(7):563-569.
4. Safar ME, Levy BI, Struijker-Boudier H: **Current perspectives on arterial stiffness and pulse pressure in hypertension and cardiovascular diseases.** *Circulation* 2003, **107**(22):2864-2869.
5. Berkenstadt H, Margalit N, Hadani M, Friedman Z, Segal E, Villa Y, Perel A: **Stroke volume variation as a predictor of fluid responsiveness in patients undergoing brain surgery.** *Anesth Analg* 2001, **92**(4):984-989.
6. Michard F, Teboul JL: **Using heart-lung interactions to assess fluid responsiveness during mechanical ventilation.** *Crit Care* 2000, **4**(5):282-289.
7. Blacher J, Safar ME: **Large-artery stiffness, hypertension and cardiovascular risk in older patients.** *Nat Clin Pract Cardiovasc Med* 2005, **2**(9):450-455.

8. Huang H, Ye JY, Li YR, Wang XY, Zhang YH, Wang JY, Ding X, Li HG, Han DM: **Pulse transit time for quantifying inspiratory effort in patients with obstructive sleep apnea.** *ORL J Otorhinolaryngol Relat Spec*, **73**(1):53-60.
9. Tomiyama H, Yamashina A: **Non-invasive vascular function tests: their pathophysiological background and clinical application.** *Circ J*, **74**(1):24-33.
10. Bendjelid K, Suter PM, Romand JA: **The respiratory change in preejection period: a new method to predict fluid responsiveness.** *J Appl Physiol* 2004, **96**(1):337-342.
11. Nelson MR, Stepanek J, Cevette M, Covalciuc M, Hurst RT, Tajik AJ: **Noninvasive measurement of central vascular pressures with arterial tonometry: clinical revival of the pulse pressure waveform?** *Mayo Clin Proc*, **85**(5):460-472.
12. Reesink KD, Hermeling E, Hoerberigs MC, Reneman RS, Hoeks AP: **Carotid artery pulse wave time characteristics to quantify ventriculoarterial responses to orthostatic challenge.** *J Appl Physiol* 2007, **102**(6):2128-2134.
13. Oliver JJ, Webb DJ: **Noninvasive assessment of arterial stiffness and risk of atherosclerotic events.** *Arterioscler Thromb Vasc Biol* 2003, **23**(4):554-566.
14. Boron WF, Boulpaep EL: **Medical Physiology**, 2 edn. Philadelphia: Elsevier Saunders; 2005.
15. Hiscock SC, Evans MJ, Morton RJ, Hall DO: **Investigation of normal ranges for left ventricular ejection fraction in cardiac gated blood pool imaging studies using different processing workstations.** *Nucl Med Commun* 2008, **29**(2):103-109.
16. Weissler AM, Harris WS, Schoenfeld CD: **Systolic time intervals in heart failure in man.** *Circulation* 1968, **37**(2):149-159.
17. Wallace AG, Mitchell JH, Skinner NS, Sarnoff SJ: **Duration of the phases of left ventricular systole.** *Circ Res* 1963, **12**:611-619.
18. Frank O: **Dynamik de Herzmuskels.** *Z Biol* 1895, **32**:370:447.
19. Starling E: **The Linacre Lecture on the Law of the Heart Given at Cambridge, 1915.** 1918.
20. Guyton ACH, J.E.: **Textbook of medical physiology**, 10 edn: W.B. Saunders Company; 2000.
21. Tournadre JP, Muchada R, Lansiaux S, Chassard D: **Measurements of systolic time intervals using a transoesophageal pulsed echo-Doppler.** *Br J Anaesth* 1999, **83**(4):630-636.
22. Boudoulas H: **Systolic time intervals.** *Eur Heart J* 1990, **11 Suppl I**:93-104.
23. Sugimoto T, Sagawa K, Guyton AC: **Effect of tachycardia on cardiac output during normal and increased venous return.** *Am J Physiol* 1966, **211**(2):288-292.
24. Davies JE, Whinnett ZI, Francis DP, Manisty CH, Aguado-Sierra J, Willson K, Foale RA, Malik IS, Hughes AD, Parker KH *et al*: **Evidence of a dominant backward-propagating "suction" wave responsible**

- for diastolic coronary filling in humans, attenuated in left ventricular hypertrophy.** *Circulation* 2006, **113**(14):1768-1778.
25. Siebes M, Kolyva C, Verhoeff BJ, Piek JJ, Spaan JA: **Potential and limitations of wave intensity analysis in coronary arteries.** *Med Biol Eng Comput* 2009, **47**(2):233-239.
 26. Sun YH, Anderson TJ, Parker KH, Tyberg JV: **Wave-intensity analysis: a new approach to coronary hemodynamics.** *J Appl Physiol* 2000, **89**(4):1636-1644.
 27. Sun YH, Anderson TJ, Parker KH, Tyberg JV: **Effects of left ventricular contractility and coronary vascular resistance on coronary dynamics.** *Am J Physiol Heart Circ Physiol* 2004, **286**(4):H1590-1595.
 28. Chilian WM, Marcus ML: **Effects of coronary and extravascular pressure on intramyocardial and epicardial blood velocity.** *Am J Physiol* 1985, **248**(2 Pt 2):H170-178.
 29. Bender SB, van Houwelingen MJ, Merkus D, Duncker DJ, Laughlin MH: **Quantitative analysis of exercise-induced enhancement of early- and late-systolic retrograde coronary blood flow.** *J Appl Physiol*, **108**(3):507-514.
 30. Sengupta PP, Khandheria BK, Korinek J, Jahangir A, Yoshifuku S, Milosevic I, Belohlavek M: **Left ventricular isovolumic flow sequence during sinus and paced rhythms: new insights from use of high-resolution Doppler and ultrasonic digital particle imaging velocimetry.** *J Am Coll Cardiol* 2007, **49**(8):899-908.
 31. Lansac E, Lim HS, Shomura Y, Lim KH, Rice NT, Goetz W, Acar C, Duran CM: **A four-dimensional study of the aortic root dynamics.** *Eur J Cardiothorac Surg* 2002, **22**(4):497-503.
 32. Thubrikar M, Piepgrass WC, Shaner TW, Nolan SP: **The design of the normal aortic valve.** *Am J Physiol* 1981, **241**(6):H795-801.
 33. Sengupta PP, Tajik AJ, Chandrasekaran K, Khandheria BK: **Twist mechanics of the left ventricle: principles and application.** *JACC Cardiovasc Imaging* 2008, **1**(3):366-376.
 34. Buckberg GD, Mahajan A, Jung B, Markl M, Hennig J, Ballester-Rodes M: **MRI myocardial motion and fiber tracking: a confirmation of knowledge from different imaging modalities.** *Eur J Cardiothorac Surg* 2006, **29 Suppl 1**:S165-177.
 35. Remme EW, Lyseggen E, Helle-Valle T, Opdahl A, Pettersen E, Vartdal T, Ragnarsson A, Ljosland M, Ihlen H, Edvardsen T *et al*: **Mechanisms of preejection and postejction velocity spikes in left ventricular myocardium: interaction between wall deformation and valve events.** *Circulation* 2008, **118**(4):373-380.
 36. Fung YC: **Biomechanics**, vol. *Circulation*, 2 edn. La Jolla: Springer; 1996.
 37. Boron W, Boulpaep E: **Medical Physiology.** Philadelphia: Elsevier Saunders; 2005.
 38. Franklin SS: **Hypertension in older people: part 1.** *J Clin Hypertens (Greenwich)* 2006, **8**(6):444-449.

39. Langewouters GJ, Wesseling KH, Goedhard WJ: **The static elastic properties of 45 human thoracic and 20 abdominal aortas in vitro and the parameters of a new model.** *J Biomech* 1984, **17**(6):425-435.
40. Westerhof N, Stergiopulos N, Noble MIM: **Snapshots of hemodynamics.** New York: Springer; 2010.
41. Olson RM: **Aortic blood pressure and velocity as a function of time and position.** *J Appl Physiol* 1968, **24**(4):563-569.
42. Tomiyama H, Yamashina A, Arai T, Hirose K, Koji Y, Chikamori T, Hori S, Yamamoto Y, Doba N, Hinohara S: **Influences of age and gender on results of noninvasive brachial-ankle pulse wave velocity measurement--a survey of 12517 subjects.** *Atherosclerosis* 2003, **166**(2):303-309.
43. Lee HY, Oh BH: **Ageing and arterial stiffness.** *Circ J*, **74**(11):2257-2262.
44. Greenwald SE: **Ageing of the conduit arteries.** *J Pathol* 2007, **211**(2):157-172.
45. Dark P, Little R, Nirmalan M, Purdy J: **Systemic arterial pressure wave reflections during acute hemorrhage.** *Crit Care Med* 2006, **34**(5):1497-1505.
46. Pythoud F, Stergiopulos N, Bertram CD, Meister JJ: **Effects of friction and nonlinearities on the separation of arterial waves into their forward and backward components.** *J Biomech* 1996, **29**(11):1419-1423.
47. Segers P, Qasem A, De Backer T, Carlier S, Verdonck P, Avolio A: **Peripheral "oscillatory" compliance is associated with aortic augmentation index.** *Hypertension* 2001, **37**(6):1434-1439.
48. Lewis RP, Rittogers SE, Froester WF, Boudoulas H: **A critical review of the systolic time intervals.** *Circulation* 1977, **56**(2):146-158.
49. Hasegawa M, Rodbard D, Kinoshita Y: **Timing of the carotid arterial sounds in normal adult men: measurement of left ventricular ejection, pre-ejection period and pulse transmission time.** *Cardiology* 1991, **78**(2):138-149.
50. Chen SC, Chang JM, Liu WC, Tsai JC, Chen LI, Lin MY, Hsu PC, Lin TH, Su HM, Hwang SJ *et al*: **Significant correlation between ratio of brachial pre-ejection period to ejection time and left ventricular ejection fraction and mass index in patients with chronic kidney disease.** *Nephrol Dial Transplant*.
51. Middleton PM, Chan GS, O'Lone E, Steel E, Carroll R, Celler BG, Lovell NH: **Changes in left ventricular ejection time and pulse transit time derived from finger photoplethysmogram and electrocardiogram during moderate haemorrhage.** *Clin Physiol Funct Imaging* 2009, **29**(3):163-169.
52. Nichols WW, Singh BM: **Augmentation index as a measure of peripheral vascular disease state.** *Curr Opin Cardiol* 2002, **17**(5):543-551.
53. Morgan BC, Martin WE, Hornbein TF, Crawford EW, Guntheroth WG: **Hemodynamic effects of intermittent positive pressure respiration.** *Anesthesiology* 1966, **27**(5):584-590.

54. Scharf SM, Brown R, Saunders N, Green LH: **Hemodynamic effects of positive-pressure inflation.** *J Appl Physiol* 1980, **49**(1):124-131.
55. Brower R, Wise RA, Hassapoyannes C, Bromberger-Barnea B, Permutt S: **Effect of lung inflation on lung blood volume and pulmonary venous flow.** *J Appl Physiol* 1985, **58**(3):954-963.
56. Pinsky MR, Matuschak GM, Klain M: **Determinants of cardiac augmentation by elevations in intrathoracic pressure.** *J Appl Physiol* 1985, **58**(4):1189-1198.
57. Denault AY, Gorcsan J, 3rd, Pinsky MR: **Dynamic effects of positive-pressure ventilation on canine left ventricular pressure-volume relations.** *J Appl Physiol* 2001, **91**(1):298-308.
58. Gunn SR, Pinsky MR: **Implications of arterial pressure variation in patients in the intensive care unit.** *Curr Opin Crit Care* 2001, **7**(3):212-217.
59. Hardaway RM, 3rd: **Monitoring of the patient in a state of shock.** *Surg Gynecol Obstet* 1979, **148**(3):339-345.
60. Chan GS, Middleton PM, Celler BG, Wang L, Lovell NH: **Change in pulse transit time and pre-ejection period during head-up tilt-induced progressive central hypovolaemia.** *J Clin Monit Comput* 2007, **21**(5):283-293.
61. Quinsac C, Heil M, Jackson A, Dark P: **Instantaneous versus average wave speed calculation in large mammals under acute hemorrhage.** *Conf Proc IEEE Eng Med Biol Soc* 2007, **2007**:971-972.
62. Godje O, Peyerl M, Seebauer T, Lamm P, Mair H, Reichart B: **Central venous pressure, pulmonary capillary wedge pressure and intrathoracic blood volumes as preload indicators in cardiac surgery patients.** *Eur J Cardiothorac Surg* 1998, **13**(5):533-539; discussion 539-540.
63. Bendjelid K: **Pre-ejection period, contractility and preload. A fascinating riddle.** *J Clin Monit Comput* 2007, **21**(6):387.
64. Perel A, Pizov R, Cotev S: **Systolic blood pressure variation is a sensitive indicator of hypovolemia in ventilated dogs subjected to graded hemorrhage.** *Anesthesiology* 1987, **67**(4):498-502.
65. Reuter DA, Felbinger TW, Schmidt C, Kilger E, Goedje O, Lamm P, Goetz AE: **Stroke volume variations for assessment of cardiac responsiveness to volume loading in mechanically ventilated patients after cardiac surgery.** *Intensive Care Med* 2002, **28**(4):392-398.
66. Feissel M, Badie J, Merlani PG, Faller JP, Bendjelid K: **Pre-ejection period variations predict the fluid responsiveness of septic ventilated patients.** *Crit Care Med* 2005, **33**(11):2534-2539.

Chapter 2

The onset of ventricular isovolumic contraction as reflected in the carotid artery distension waveform

Marc J. Van Houwelingen, Paul J. Barenbrug, M. Christianne Hoeberigs, Robert S. Reneman, and Arnold P. G. Hoeks. **The onset of ventricular isovolemic contraction as reflected in the carotid artery distension waveform** *Ultrasound in Med. & Biol.*, Vol. 33, No. 3, pp. 371–378, 2007.

The onset of ventricular isovolumic contraction as reflected in the carotid artery

Abstract

The blood pressure waveform carries information about the cardiac contraction and the impedance characteristics of the vascular bed. Here, we demonstrate that the start of isovolumic ventricular contraction is persistently reflected as an inflection point in the pressure wave as recorded in the aortic root (TP_{IC}) as well as in the carotid artery distension waveform (TD_{IC}) as it travels down the arterial tree. In a group of six patients with normal pressure gradients across the aortic valve after valve replacement, the TP_{IC} had a small delay with respect to the onset of isovolumic ventricular contraction (<10 ms). In a group ($n = 21$) of young presumably healthy volunteers, the inflection point occurred persistently in the carotid distension waveform, as recorded by means of ultrasound, before the systolic foot (intersubject delay between inflection point and systolic foot: $\text{mean} \pm \text{SD} = 40.0 \pm 9.4$ ms, intrasubject SD 4.6 ms). Retrograde coronary blood flow during isovolumic ventricular contraction may be the origin of the persistent end-diastolic pressure and distension perturbation. This study shows that the duration of the isovolumic contraction can be reliably extracted from the carotid artery distension waveform.

2.1 Introduction

Because of the obvious relation between the heart and the vascular system, the analysis and interpretation of the blood pressure waveform as recorded at peripheral sites with respect to cardiac action have attracted a lot of attention [1-4]. The time relationship between the electrocardiogram (ECG) and the peripheral pressure waveform provides useful information about cardiac contraction. For proper interpretation, it is essential to be informed directly or indirectly of the time delay between the R-top of the ECG and the onset of cardiac contraction, known as the pre-ejection period (PEP). Correction for PEP is necessary on an individual basis, for example, if the transit time of the pressure pulse from the heart to a peripheral recording site is referenced to the ECG. For a pressure wave covering 0.6 m with an assumed propagation speed of 6 m/s, the transit time will be about 0.1 s. By using the R-top of the ECG as reference, the PEP will increase the observed transit time by 50 to 60 ms and will, without correction, lead to an underestimation of the pulse wave velocity by 30% to 40%. The relevance of the onset of cardiac contraction for the relation between cardiac action and interpretation of the peripheral pressure waveform prompts the need for an easily applicable measurement technique. In a clinical environment, noninvasive techniques, such as phonocardiography or cardiac ultrasound Doppler registrations, can be used to identify specific phases of the cardiac cycle and quantify myocardial performance [5-8]. These techniques require selective audio signal postprocessing [7] and manual identification of the relevant time points. An alternative is offered by blood pressure waveforms measured at distal sites of the arterial tree with applanation tonometry. Drawbacks of the applanation tonometry technique are the need for a stiff background to compress the artery [9], as well as a lean skin to avoid cushioning of the pressure pulse, making this technique unsuitable for major arteries close to the heart or in obese subjects. In manual applanation tonometry, unsteadiness of the hand is another source of error [10]. Techniques that use peripheral sites, e.g., brachial, radial or digital arteries, to derive information about central phenomena are subject to criticism because the pressure waveform changes along the arterial tree [11]. Using generalized transfer functions, it is possible to suppress this alteration and to reconstruct aortic pressure waveforms from peripheral pressure registrations [12-14]. Because the transfer function is based on a statistical average of many subjects, individual information about the shape of the pressure waveform will be disguised [15]. Further, the transfer function does not account for the nonlinear propagation of the pulse wave velocity as a function of distending pressure [16]. As a consequence, the quality of the time information derived

from the reconstructed aortic pressure waveform is degraded by the reconstruction process [12, 15]. Ultrasound techniques solve some of the drawbacks related to direct measurement of the blood pressure waveform because it can be used at sites without any stiff background, making it suitable for investigating sites close to the heart, e.g., the common carotid artery. Dedicated analysis of the reflected radiofrequency ultrasound signals results in a diameter waveform with a high temporal and spatial resolution [17]. Because of the direct relationship between blood pressure and artery diameter [16, 18, 19], temporal and amplitude analysis of the change in diameter over time (distension waveform) is a suitable alternative for analysis of the pressure waveform. In preliminary studies, we noticed a temporary minor increase in the carotid artery distension waveform just before the start of systole, i.e., a discontinuity in the end-diastolic decaying part of the waveform. The aim of the present study was to analyze in detail the timing aspects of the end-diastolic distension waveform in relation to cardiac action. Specifically, we will demonstrate that the start of isovolumic ventricular contraction is persistently reflected as an inflection point in the pressure waveform as recorded in the aortic root (TP_{IC}), as well as in the carotid distension waveform (TD_{IC}) as it travels down the arterial tree. The time relationship between heart action and aortic pressure waveform was measured in a group of patients subjected to aortic valve replacement. The presence and precision of the inflection point in the carotid artery distension waveform in relation to the foot of systole was tested in a group of young, presumably healthy volunteers.

2.2 Methods

Subject and patient population

To demonstrate the relationship between isovolumic contraction and the presystolic timing events in the pressure waveform, left ventricular and aortic pressures were measured simultaneously in patients after replacement of the aortic valve by an artificial one. A subset of six patients (age 59 to 73 y; mean 68.3) was selected from a dataset of 32 patients on the basis of a normal pressure gradient across the artificial aortic valve. Patients with a pressure gradient >10 mm Hg were excluded because it was anticipated that elevated outflow resistance would modify cardiovascular hemodynamics, possibly obscuring the end-diastolic pressure perturbation. Because the main objective of the present study was to establish the intrasubject timing relationship of cardiac events, no further specification of the patients group is needed. Carotid artery distension waveforms were obtained from 10 presumably healthy male (age 19 to 30 y; mean 20.8) and 11 presumed healthy female (age 20 to 30 y;

The onset of ventricular isovolumic contraction as reflected in the carotid artery mean 21.9) volunteers. None of the subjects had a history of cardiovascular disease, diabetes or hypercholesterolemia, nor established hypertension. None of the subjects was on medication affecting the cardiovascular system. The studies were approved by the medical ethical committee of Maastricht University and the Academic Hospital Maastricht. Informed consent was obtained from all volunteers and patients before enrollment in the study.

Measurement of the carotid distension wave

Recordings were made in supine position using an ultrasound scanner (7.5 MHz linear array; HDI-9, ATL, Bellevue, WA, USA). In B-mode, a longitudinal section of the common carotid artery was localized, whereas an M-line at 2 to 3 cm proximal of the tip of the flow divider was selected. From this M-line, the ultrasound radiofrequency data were captured and stored on hard disk. Markers were placed manually on the radiofrequency signals of the first acquired echo line to indicate the anterior and posterior artery walls, and a software package was used to extract arterial wall velocity using correlation methods [17, 20]. The distension waveform was obtained via integration of wall velocity over time, i.e., conversion to displacement, and taking the difference between the time-dependent displacements of both walls. The correlation windows used had a length of 10 ms and were overlapping by 5 ms, resulting in a sample frequency of the distension curve of 200 Hz. The positions of the correlation windows were intermittently updated using the calculated motion (tracking windows) to ensure that the signal windows remained aligned with the moving wall reflections. The distension waveforms in the carotid artery were recorded three to five times, each recording covering four to seven consecutive heart cycles. Each distension waveform was filtered using a rectangular moving average filter with a window length of 15 ms (3 data points), without introducing a phase delay with respect to the unfiltered distension waveform. The resulting distension curve was interpolated using a cubic spline method (MatLab, The MathWorks, Inc., Natick, MA, USA), to end with a sample interval of 1 ms.

Detection of assumed onset ventricular contraction

Because the slope of the distension waveform becomes less negative at the inflection point (Figure 1, TD_{IC}), this time-point can be extracted by detecting a local maximum in the second derivative of the distension waveform preceding the largest maximum (systolic acceleration) between the R-top of the ECG and the occurrence of the systolic peak. The second derivative was obtained by passing the interpolated distension wave through a cascade of two first-order recursive high-pass filters with an effective cutoff frequency of 60 Hz. The

second high-pass filter was applied in reversed order to accomplish a zero phase shift in the second derivative.

Detection of foot systole of the TD_{IC}

Two ways were considered to identify the systolic foot. One was based on maximum acceleration in the distension wave, being the first large peak in the second derivative, and will be referred to as FS_{SD} , i.e., foot systole using the second derivative. Although this is a mathematical representation of a change in distension rather than being related to a specific physiologic event, it is easy to detect in the carotid distension wave and it has high accuracy and precision [21]. The other method was based on the intersection of a regression line through the upslope of a wave and a horizontal line through the preceding diastolic value (the local minimum of the distension wave). This method is referred to as the FS_{IT} , foot systole obtained by means of the intersecting tangent method [21].

Measurement and analysis of the left ventricular and aortic pressures immediately after replacement of a stenotic aortic valve by an artificial valve in 32 patients, the pressures in the left ventricle and the aorta were measured simultaneously with high-fidelity pressure transducers mounted on the tip of a catheter (CFL512, Leycom, The Netherlands, catheter CA71103PN, acquisition sampling frequency 250 Hz). Patients with a pressure drop across the artificial valve >10 mm Hg in peak systole (25 subjects) and patients without an identifiable TP_{IC} (1 subject) were excluded from data analysis, resulting in a subset of six patients. The intersecting tangent method was applied to the left ventricular pressure registration to extract the start of left ventricular contraction (referred to as FS_{IT-IV}).

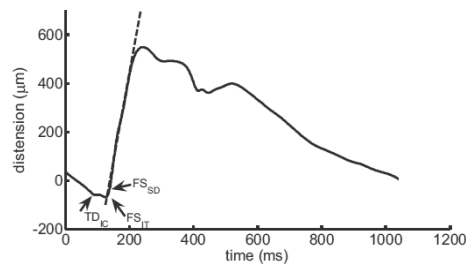


Figure 1. Carotid artery distension waveform of a healthy subject. TD_{IC} represents the onset of isovolumic contraction of the ventricles, FS_{IT} represents foot systole as determined by the intersecting tangent method and FS_{SD} represents foot systole as determined by means of the second derivative (Figure 2).

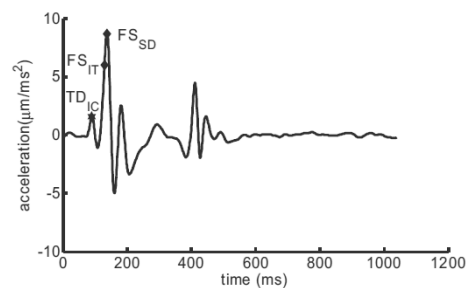


Figure 2. Second derivative of a distension waveform as recorded in the carotid artery of a healthy subject (Figure 1). TD_{IC} signals the onset of the perturbation in distension preceding the systolic foot. FS_{SD} and FS_{IT} represent foot systole as determined by means of the second derivative and the intersecting tangent method, respectively (Figure 1).

The onset of ventricular isovolumic contraction as reflected in the carotid artery

On the other hand, the second derivative method was used to extract TP_{IC} from the aortic pressure waveform. We used the time point where left ventricular pressure exceeds aortic pressure to indicate the opening of the aortic valve.

Statistical analysis

The patient dataset contained between one to three subsequent registrations per patient. Each registration contained seven to 35 heart cycles. For each patient, the intrasubject mean and standard deviation of TP_{IC} , FS_{IT-IV} and the differences between FS_{IT-IV} and TP_{IC} and between TP_{IC} and aortic valve opening, were calculated. The dataset of the normal subjects contained between three to five subsequent registrations per subject. Each registration contained four to seven consecutive cardiac cycles. For each cardiac cycle, the points of interest (TD_{IC} , FS_{IT} , FS_{SD}) were extracted as described above. For each point of interest, the median per registration was calculated and averaged per subject (subject mean). The intrasubject standard deviation was based on the deviation of the results per registration of the subject mean. The intersubject mean and standard deviation were calculated over the subject means. Bland-Altman plots [22] were used to evaluate the distribution of the registration results vs. the subject means.

2.3 Results

Figures 1 and 2 illustrate the methods used to extract the position of the systolic foot from the carotid artery distension waveform (Figure 1) and its second derivative (Figure 2) as a function of time as recorded in a presumably healthy subject. In both figures, the time points for foot systole obtained by means of the second derivative (FS_{SD}) and by means of the intersecting tangent method (FS_{IT}) are indicated. TD_{IC} reflects the onset of the isovolumic contraction, causing a discontinuity in the end-diastolic portion of the distension waveform. This observation is supported by Table 1, showing the intrasubject mean and standard deviation for the patient group. The positions of the systolic foot in the left ventricle pressure waveform (FS_{IT-IV}), the time point of the inflection in the aortic root pressure (TP_{IC}) and aortic valve opening are referenced to the R-top of the ECG (Figure 3). The detected inflection point (TP_{IC}) directly follows the onset of isovolumic

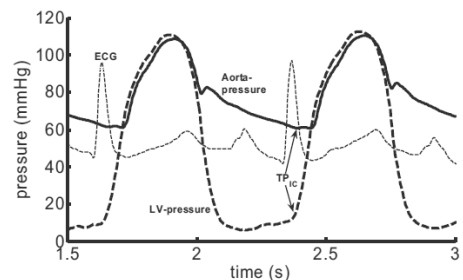


Figure 3. The simultaneous recording of ECG, left ventricular (dashed line) and aortic (solid line) pressure supports the notion that the inflection point in the end-diastolic aortic pressure follows the onset of the isovolumic contraction.

contraction (intersubject delay 7.8 ± 4.9 ms). The observed time delay between TP_{IC} and the foot of the aortic pressure wave is consistent with the duration of isovolumic contraction (intrasubject difference 5.4 ± 5.7 ms).

The time point in the carotid artery distension waveform associated with isovolumic contraction (TD_{IC}) has an intrasubject precision of 4.6 ms for a group mean \pm SD of 73.3 ± 9.6 ms (Figure 4). Incidentally, the program detected a false TD_{IC} (6 beats of a total 406 beats, all in one subject), explaining the outliers in the Bland-Altman plot. The deviations from the subject mean are independent of the mean. Similarly, the systolic foot based on the second derivative FS_{SD} could be detected with a

precision of 3.1ms for a group mean \pm SD of 113.1 ± 9.3 ms (Figure 5).

For this time point, the software extraction procedure functioned properly and the width of the distribution is fully explained by physiologic variations. Consequently, the precision of the FS_{SD} is better than that of the TD_{IC} .

The distribution of the time relationship between FS_{SD} and TD_{IC} is shown in Figure 6. The intrasubject standard deviation of the time delay $FS_{SD} - TD_{IC}$ is 4.6 ms for a group mean and standard deviation of 40.0 ± 9.4 ms. The precision of the time difference (4.6 ms) indicates that the observed perturbations in FS_{SD} (3.1 ms) and TD_{IC} (4.6 ms) are highly correlated.

Table 2 summarizes the intrasubject and intersubject statistics (mean and standard deviation) for TD_{IC} , FS_{IT} and FS_{SD} , as well as the time interval between TD_{IC} and FS_{SD} .

Table 1 Characteristics of the patient group

	Patient 1	Patient 2	Patient 3	Patient 4	Patient 5	Patient 6	Mean	SD
Age (y)	59	73	68	75	69	66	68.3	5.6
No. of beats	15	41	38	24	31	42	31.8	10.7
TP_{IC}	42.4 ± 4.5	28.7 ± 5.9	24.5 ± 2.8	32.6 ± 2.5	65.9 ± 8.7	41.0 ± 8.7	39.2	14.8
FS_{IT-iv}	33.1 ± 3.2	26.4 ± 2.0	17.4 ± 4.2	29.8 ± 2.6	50.7 ± 6.1	-5.8 ± 10	25.3	18.7
Aortic valve opening	111.1 ± 3.6	61.8 ± 3.8	80.7 ± 5.2	82.5 ± 3.7	104.4 ± 9.4	43.6 ± 8.4	80.7	25.4
$TP_{IC} - FS_{IT-iv}$	9.3 ± 5.2	2.2 ± 4.9	7.1 ± 4.8	2.8 ± 3.2	15.2 ± 11.1	9.9 ± 3.3	7.8	4.9
Valve opening- TP_{IC}	68.6 ± 6.5	33.2 ± 5.2	56.2 ± 5.8	49.8 ± 7.5	38.4 ± 12.0	39.5 ± 3.4	47.6	13.2
A = Valve opening- FS_{IT-iv}	77.4 ± 4.6	35.4 ± 3.3	63.3 ± 3.2	52.7 ± 2.3	53.7 ± 6.1	49.4 ± 4.0	55.3	14.1
B = $FS_{aorta} - TP_{IC}$	71.7 ± 7.6	31.2 ± 4.7	52.5 ± 5.7	57.8 ± 3.5	44.9 ± 10.5	41.2 ± 3.7	49.9	14.1
A-B	5.7	4.2	10.8	-5.1	8.8	8.2	5.4	5.7

The start of isovolumic contraction is determined by the intersecting tangent method (FS_{IT-iv}) applied to the left ventricular pressure recording of 6 patients subjected to aortic valve replacement (all data mean \pm SD ms). A few milliseconds later ($TP_{IC} - FS_{IT-iv}$), a minor perturbation can be noted in the aortic pressure recording. The duration of isovolumic contraction (Valve opening- FS_{IT-iv}) varies considerably from patient to patient, which is reflected in the time delay between TP_{IC} and the systolic foot of the aorta pressure (FS_{aorta}), determined with the second derivative method.

The onset of ventricular isovolumic contraction as reflected in the carotid artery

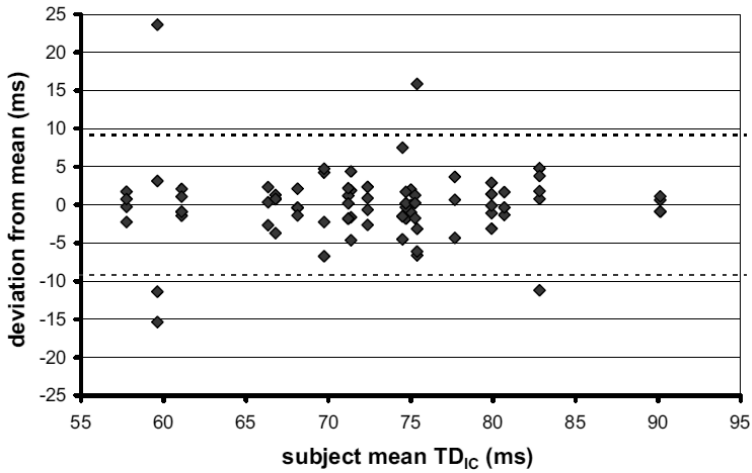


Figure 4. The intrasubject onset of left ventricular contraction as derived from the carotid artery distension waveform (TD_{IC}) has a standard deviation of 4.6 ms. The 2SD level (dotted lines) is relatively small with respect to the group mean (73.3 ms). Only one person shows a large spread.

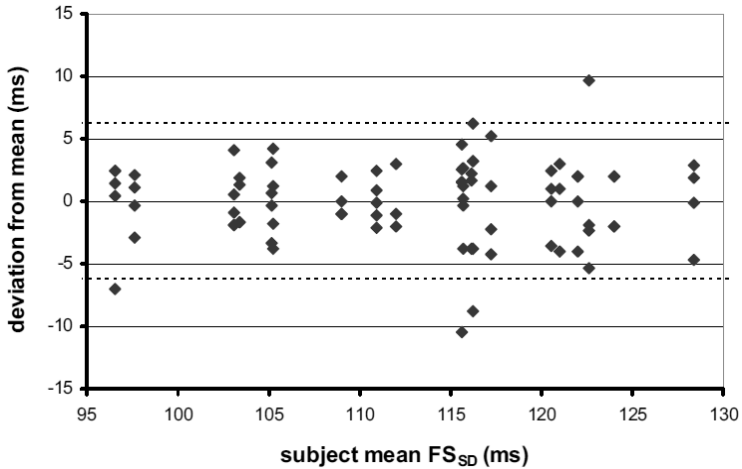


Figure 5. The intrasubject foot systole, determined with the second derivative (FS_{SD}) from the carotid artery distension waveform, has a uniform distribution and a standard deviation of 3.1 ms. The 2SD level (dotted lines) is relatively low compared with the group mean (113.1 ± 9.3 ms).

2.4 Discussion

The inflection point in the end-diastolic part of both the aortic pressure waveform (TP_{IC}) and the carotid artery distension waveform (TD_{IC}) has a consistent time relationship with the foot of the systolic part of these waveforms. For the distension waveform, the delay between both time points can be established with an intrasubject variation of <5 ms for a mean value of 40 ms. The pressure tracings from the left ventricle and the aortic root, in conjunction with the ECG, suggest that the inflection in the waveforms is caused by the onset of isovolumic contraction.

The root of the aorta is surrounded by atria, which could affect aortic pressure. An increase in atrial pressure during atrial contraction would cause an increase in aortic pressure gradient, whereas relaxation of the atria has a reversed effect. The results from the patient group show that the inflection point TP_{IC} occurs after the onset of ventricular contraction, excluding atrial contraction as the origin of the inflection point. Because atrial relaxation occurring during ventricular contraction can only explain a decrease in aortic pressure, it can be discarded as a source of the pressure perturbation.

Another possible source for the inflection point in the aortic pressure waveform is the behavior of the aortic valve during isovolumic contraction. The increase in left ventricular pressure during this phase of the cardiac cycle causes the elastic valve to bulge into the aorta. This displacement should increase with increasing left ventricular pressure, but the aortic pressure tracing (Figure 3) shows only a short disruption.

The backflow of blood from the coronary arteries into the aorta is a more likely explanation. During contraction, blood is almost instantly squeezed out of the myocardial vascular bed forward into the coronary sinus and backward into the coronary arteries, the latter causing a small pulse pressure wave to travel toward the aorta or, at least, a sharp decline in coronary blood flow [23, 24]. However, because the pressure–flow relationship is strongly modulated by the spatial alignment of the transducers and the frequency characteristics of the recording systems, direct quantitative evaluation of the timing relationship from figures remains difficult [25]. The short and fixed time delay between the foot of left ventricular pressure and the inflection point in the aortic pressure waveform (7.8 ms; Table 1) is consistent with the transit time of the pressure wave backwards through the coronary circulation, whereas the short duration of the perturbation

The onset of ventricular isovolumic contraction as reflected in the carotid artery excludes a direct interaction between ventricular contraction and the aortic pressure waveform.

Patient group vs. subject group

The time interval between TP_{IC} and aortic valve opening in the patient group and the time interval between TD_{IC} and foot systole (FS_{SD}) in the volunteers are comparable (Tables 1 and 2). This supports the notion that the aortic pressure perturbation as a result of ventricular contraction (TP_{IC}) maintains its time position relative to the systolic pulse wave as it travels along the arterial tree. Unfortunately, we were unable to combine distension measurements with the pressure measurements in the operating room.

The patient group was much older (59 to 73 y) than the volunteer group (19 to 30 y). Therefore, it can be expected that both groups differ in cardiac performance and elastic properties of the central arteries. The contractility of the heart decreases, and the diastolic pressure generally increases, with increasing age, causing prolongation of the isovolumic contraction [5]. This is supported by the observed duration of the isovolumic contraction estimated from the aortic pressure waveform (patient group: 50 ms), which is longer than that derived from the carotid artery distension waveform (normal subject group: 40 ms). The age aspects do not modify the observations that (1) within the patient group, the end-diastolic timing pattern of aortic pressure matches the timing sequence of the left ventricular pressure during isovolumic contraction and (2) the end-diastolic pressure pattern in the patient group matches the end-diastolic segment of the distension waveform in the group of young subjects. Possible differences in vascular elastic characteristics between both groups might affect the amplitude and frequency content of the waveforms considered but do not change the end-diastolic timing pattern.

Persistency of TP_{IC} and TD_{IC}

Of the patients with a pressure drop over the replaced aortic valve >10 mm Hg, only one patient lacked a recognizable TP_{IC} , which shows that the presystolic inflection point occurs persistently in the aortic pressure waveform. In all but one volunteer, we succeeded to extract automatically the onset of the end-diastolic pressure perturbation in the carotid artery distension waveform. This does not imply that, in this volunteer, the inflection point is hard to detect; an improper gain setting of the ultrasound system or a motion artifact might well explain the detection problem.

Precision

The patient group has an intrasubject precision of 5 ms for the time delay between the onset of isovolumic contraction and either the end-diastolic inflection point in the aortic pressure waveform or the opening of the aortic valve. The time delays reported in Table 1 exhibit a large subject-to-subject variation related to the clinical history and the condition of the patients. However, within a subject, they are consistent for a large number of consecutive heartbeats, inferring that the time delays derived from the distension tracing can be used to quantify cardiac performance in the future.

The volunteer study shows a high precision in the determination of FS_{SD} (Figure 5) and FS_{IT} . The difference between both methods in determining the onset of the systolic wave (second derivative, intersecting tangent) is substantially smaller than the intrasubject standard deviation (Table 2) and in agreement with earlier observations [21, 26]. The intrasubject standard deviation of TD_{IC} (4.6 ms) is in the order of the sample interval of the wall track algorithm of the ultrasound system, whereas the group exhibits a variation of 9.6 ms (Table 2). The absolute value of TD_{IC} includes the electrical activation of the ventricle, isovolumic contraction and the transit time of the pressure wave to the site of recording. The duration of the isovolumic contraction follows from the time delay between the inflection point and the systolic foot of the distension waveform. The precision of the relevant time interval $FS_{SD} - TD_{IC}$ (4.6 ms) hardly deviates from the precision of either FS_{SD} or TD_{IC} , indicating that beat-to-beat fluctuations in both are concurrent. The statistical characteristics of $FS_{IT} - TD_{IC}$ are similar (data not shown).

Influence of measurement method and data processing

The unknown position of the pressure transducer in the aorta in combination with pulse wave velocity could cause an overestimation of the time between the start of left ventricular contraction and the occurrence of TD_{IC} . A position error of 5 mm introduces a time error of 1 ms for a pulse wave velocity of 5 m/s, which is small compared with the observed precision of 5 ms per registration containing about five beats. Probably, the largest error source is the sample interval of 4 ms of the pressure acquisition system.

The wall position tracking method provides an unbiased estimate for wall displacement and, hence, for the distension waveform [20], provided that the echo signals comply with the dynamic range of the data acquisition system. The filters used to smooth the distension waveform and to calculate the second derivative are designed to have a zero phase shift, thus introducing no bias in

The onset of ventricular isovolumic contraction as reflected in the carotid artery the time estimate. The jitter in the timing of the R-top of the ECG, with respect to the acquisition of the echo signals, has a uniform distribution over a sample interval of 1 ms for an echo pulse repetition frequency of 1 kHz, and is negligible compared with the sample interval of the distension waveform (5 ms). Part of the observed precision is associated with the signal window length (presently set at 10 ms) to obtain a good precision of the displacement estimate [27]. A shorter window length can be employed if the ultrasound system can operate in echo mode at a pulse repetition frequency higher than 1 kHz. However, the best method to improve the precision is averaging over a number of repeated registrations.

2.5 Conclusion

This study demonstrates that it is possible to derive the duration of the isovolumic contraction from the carotid artery distension waveform as recorded noninvasively with current ultrasound techniques. The observed precision (5 ms) can be improved by using an ultrasound system with a higher pulse repetition frequency when acquiring distension waveforms.

2.6 References

1. Hasegawa M, Rodbard D, Kinoshita Y: **Timing of the carotid arterial sounds in normal adult men: measurement of left ventricular ejection, pre-ejection period and pulse transmission time.** *Cardiology* 1991, **78**(2):138-149.
2. Lantelme P, Khettab F, Custaud MA, Rial MO, Joanny C, Gharib C, Milon H: **Spontaneous baroreflex sensitivity: toward an ideal index of cardiovascular risk in hypertension?** *J Hypertens* 2002, **20**(5):935-944.
3. Millasseau SC, Kelly RP, Ritter JM, Chowienczyk PJ: **Determination of age-related increases in large artery stiffness by digital pulse contour analysis.** *Clin Sci (Lond)* 2002, **103**(4):371-377.
4. O'Rourke MF, Gallagher DE: **Pulse wave analysis.** *J Hypertens Suppl* 1996, **14**(5):S147-157.
5. Rhodes J, Udelson JE, Marx GR, Schmid CH, Konstam MA, Hijazi ZM, Bova SA, Fulton DR: **A new noninvasive method for the estimation of peak dP/dt.** *Circulation* 1993, **88**(6):2693-2699.
6. Tei C, Ling LH, Hodge DO, Bailey KR, Oh JK, Rodeheffer RJ, Tajik AJ, Seward JB: **New index of combined systolic and diastolic myocardial performance: a simple and reproducible measure of cardiac function--a study in normals and dilated cardiomyopathy.** *J Cardiol* 1995, **26**(6):357-366.
7. Tekten T, Onbasili AO, Ceyhan C, Unal S, Discigil B: **Novel approach to measure myocardial performance index: pulsed-wave tissue Doppler echocardiography.** *Echocardiography* 2003, **20**(6):503-510.

8. Yumoto Y, Satoh S, Fujita Y, Koga T, Kinukawa N, Nakano H: **Noninvasive measurement of isovolumetric contraction time during hypoxemia and acidemia: Fetal lamb validation as an index of cardiac contractility.** *Early Hum Dev* 2005, **81**(7):635-642.
9. Kelly R, Hayward C, Avolio A, O'Rourke M: **Noninvasive determination of age-related changes in the human arterial pulse.** *Circulation* 1989, **80**(6):1652-1659.
10. Pannier BM, Avolio AP, Hoeks A, Mancia G, Takazawa K: **Methods and devices for measuring arterial compliance in humans.** *Am J Hypertens* 2002, **15**(8):743-753.
11. Nichols W, O'Rourke M: **McDonald's Blood Flow in Arteries.** London: Edward Arnold; 1998.
12. Millasseau SC, Patel SJ, Redwood SR, Ritter JM, Chowienczyk PJ: **Pressure wave reflection assessed from the peripheral pulse: is a transfer function necessary?** *Hypertension* 2003, **41**(5):1016-1020.
13. O'Rourke MF: **Mechanical principles. Arterial stiffness and wave reflection.** *Pathol Biol (Paris)* 1999, **47**(6):623-633.
14. Pauca AL, O'Rourke MF, Kon ND: **Prospective evaluation of a method for estimating ascending aortic pressure from the radial artery pressure waveform.** *Hypertension* 2001, **38**(4):932-937.
15. Segers P, Carlier S, Pasquet A, Rabben SI, Hellevik LR, Remme E, De Backer T, De Sutter J, Thomas JD, Verdonck P: **Individualizing the aorto-radial pressure transfer function: feasibility of a model-based approach.** *Am J Physiol Heart Circ Physiol* 2000, **279**(2):H542-549.
16. Meinders JM, Hoeks AP: **Simultaneous assessment of diameter and pressure waveforms in the carotid artery.** *Ultrasound Med Biol* 2004, **30**(2):147-154.
17. Brands PJ, Hoeks AP, Willigers J, Willekes C, Reneman RS: **An integrated system for the non-invasive assessment of vessel wall and hemodynamic properties of large arteries by means of ultrasound.** *Eur J Ultrasound* 1999, **9**(3):257-266.
18. Powalowski T, Pensko B: **A noninvasive ultrasonic method for the elasticity evaluation of the carotid arteries and its application in the diagnosis of the cerebro-vascular system.** *Arch Acoust* 1988, **13**:109-126.
19. Van Bortel LM, Balkestein EJ, van der Heijden-Spek JJ, Vanmolkot FH, Staessen JA, Kragten JA, Vredeveld JW, Safar ME, Struijker Boudier HA, Hoeks AP: **Non-invasive assessment of local arterial pulse pressure: comparison of applanation tonometry and echo-tracking.** *J Hypertens* 2001, **19**(6):1037-1044.
20. Brands PJ, Hoeks AP, Ledoux LA, Reneman RS: **A radio frequency domain complex cross-correlation model to estimate blood flow velocity and tissue motion by means of ultrasound.** *Ultrasound Med Biol* 1997, **23**(6):911-920.
21. Chiu YC, Arand PW, Shroff SG, Feldman T, Carroll JD: **Determination of pulse wave velocities with computerized algorithms.** *Am Heart J* 1991, **121**(5):1460-1470.

The onset of ventricular isovolumic contraction as reflected in the carotid artery

22. Bland JM, Altman DG: **Statistical methods for assessing agreement between two methods of clinical measurement.** *Lancet* 1986, **1**(8476):307-310.
23. Davies JE, Whinnett ZI, Francis DP, Manisty CH, Aguado-Sierra J, Willson K, Foale RA, Malik IS, Hughes AD, Parker KH *et al*: **Evidence of a dominant backward-propagating "suction" wave responsible for diastolic coronary filling in humans, attenuated in left ventricular hypertrophy.** *Circulation* 2006, **113**(14):1768-1778.
24. Spaan JA (ed.): **Coronary blood flow. Mechanics, distribution and control.** Dordrecht, Germany: Kluwers Academic Publishers; 1991.
25. Hoeks AP, Willigers JM, Reneman RS: **Effects of assessment and processing techniques on the shape of arterial pressure-distension loops.** *J Vasc Res* 2000, **37**(6):494-500.
26. Millasseau SC, Stewart AD, Patel SJ, Redwood SR, Chowienczyk PJ: **Evaluation of carotid-femoral pulse wave velocity: influence of timing algorithm and heart rate.** *Hypertension* 2005, **45**(2):222-226.
27. Hoeks AP, Arts TG, Brands PJ, Reneman RS: **Comparison of the performance of the RF cross correlation and Doppler autocorrelation technique to estimate the mean velocity of simulated ultrasound signals.** *Ultrasound Med Biol* 1993, **19**(9):727-740.

Chapter 3

Coronary-aortic interaction during ventricular isovolumic contraction

Marc J. van Houwelingen, Daphne Merkus, Maaïke te Lintel Hekkert, Geert van Dijk, Arnold P.G. Hoeks, Dirk J. Duncker. **Coronary-aortic interaction during ventricular isovolumic contraction** Med. Biol. Eng. Comput. 2011 (in press).

Abstract

Objective: In earlier work we suggested that the start of the isovolumic contraction period could be identified in arterial pressure waveforms as the start of a temporary pre-systolic pressure perturbation (AIC_{start} , start of the Arterially detected Isovolumic Contraction), and presented the coronary retrograde volume flow in combination with a backwards traveling pressure wave as its most likely origin. In the present study we tested this hypothesis by means of a coronary artery occlusion protocol.

Results: In six Yorkshire X Landrace swine we simultaneously occluded the left anterior descending (LAD) and left circumflex (LCx) artery for 5 s followed by a 20 s reperfusion period before repeating this sequence at least 2 more times. A similar procedure was used to occlude only the right coronary artery (RCA) and finally all three main coronary arteries simultaneously. None of the occlusion protocols caused a decrease in the arterial pressure perturbation in the aorta during occlusion ($p>0.20$) nor an increase due to reactive hyperemia ($p>0.22$), despite a higher deceleration of coronary volume flow ($p=0.03$) or increased coronary conductance ($p=0.04$).

Conclusion: The results show that the pre-systolic aortic pressure perturbation does not originate from the coronary arteries.

3.1 Introduction

The arterial blood pressure waveform and its propagation characteristics contain a vast amount of information on various aspects of cardiovascular structure and function [1, 2], including arterial stiffness [3, 4], mechanical function of the heart [5, 6] and the severity of shock [7, 8].

Despite intense examination of the aortic pressure curve, small details are prone to be overlooked or erroneously discarded as noise. In a previous study we reported the presence of an arterial blood pressure perturbation preceding aortic valve opening in the common carotid artery in a group of healthy subjects as well as in the central aorta in a group of patients following aortic valve replacement [9]. The onset of this perturbation not only correlated in time with the preceding R-top of the ECG, but was also shown to coincide with the onset of the ventricular isovolumic contraction.

The exact cause of the perturbation was not determined in that study, but we hypothesized that the arterial pressure perturbation originated from the coronary arteries. During contraction, blood is almost instantly squeezed out of the myocardial vascular bed forward into the coronary sinus and backward into the coronary arteries. The latter causes a sharp decline in coronary blood volume flow [5, 10] or even a retrograde coronary volume flow, as well as a small pressure wave, traveling backwards towards the aorta [11, 12]. Both retrograde coronary volume flow and coronary pressure waves could contribute to the arterial pressure perturbation occurring prior to aortic valve opening.

In light of these considerations, we set out in the present study to test the hypothesis that coronary retrograde volume flow in combination with a backwards traveling coronary pressure wave during ventricular isovolumic contraction are the origin of the arterial pre-systolic pressure perturbation. For this purpose we assessed the pressure perturbation in the aorta in anesthetized swine before, during and after coronary artery occlusion. Specifically, we hypothesized that if the arterial pressure perturbation originates from the coronary artery circulation it should be abolished by the coronary artery occlusion. Conversely, during coronary reactive hyperemia following the release of occlusion the arterial pressure perturbation should be augmented.

3.2 Materials and Methods

Experiments were performed in six 3-4 month-old female Yorkshire X Landrace swine (44 ± 12 kg, mean \pm SD) in accordance with the Guide for the Care and Use of Laboratory animals (NIH Publication No. 85-23, revised 1996) and with approval of the Erasmus MC Animal Care Committee.

3.2.1 Instrumentation

Animals were sedated with intramuscular injection of Xylazine (2.25 mg/kg) and Tiletamine (5 mg/kg) plus Zolazepam (5 mg/kg) [13], anesthetized with a bolus of intravenous pentobarbital (15 mg/kg), intubated and ventilated with a tidal volume of 10 ml/kg. Ventilation was adjusted to keep blood gas concentrations within their physiological ranges. Anesthesia was maintained by a continuous pentobarbital infusion (6-12 mg/kg/h IV) [14].

A high fidelity lumen pressure sensor catheter (SPC 780C, Millar Instruments, Houston, Texas, USA) was inserted via the right carotid artery and advanced to measure aortic pressure approximately 2 cm distal to the aortic valve. Balloon occluders (FTS 3 mm) were positioned around the left anterior descending (LAD), left circumflex (LCx) and right (RCA) coronary arteries. Coronary volume flow probes (3mm, Transonic, Ithaca, New York, USA), to monitor coronary blood volume flow, were placed around the proximal LAD and RCA distal to the occluders. An electromagnetic aortic volume flow probe (Skalar, Delft, The Netherlands) was placed around the aorta just distal to the coronary arteries to monitor aortic blood volume flow.

3.2.2 Signal recording

ECG, aortic pressure and aortic and coronary artery volume flow signals were fed into a data acquisition board (National Instruments, Austin, Texas, USA, sample frequency 2000 Hz) and stored for offline processing. ECG and pressure transducer signal were amplified using a custom made amplifier system (EMI, Rotterdam, The Netherlands). Matlab (Natick, Massachusetts, USA) was used for storage and automated post processing of the recorded signals.

3.2.3 Protocol

After 30 minutes of stabilization, a triplicate 25 s sham measurement of ECG, aortic pressure and LAD and RCA volume flows were obtained. Subsequently, the LAD and LCx were simultaneously occluded three times for 5 s with a minimum interval of 20 s to allow restoration of coronary artery blood volume flow to baseline [15]. This procedure was followed by three 5 s occlusions of the

RCA separated by 20 s. Finally all three coronary arteries were simultaneously occluded three times, using the same 5 s occlusion and 20 s reperfusion intervals.

3.2.4 Data analysis

Measurement equipment introduced a $>10\text{ms}$ delay in the ECG compared to the aortic pressure and coronary volume flow signals. The delay was compensated for during post processing prior to extracting hemodynamic features. All signals were low pass filtered with a cut-off frequency of 80 Hz to remove noise. The onset of each heart cycle was identified using the Q-top of the ECG. From the aortic pressure recording, the maximum systolic (SBP), minimum diastolic (DBP) and mean blood pressure (MBP) values were determined. The onset of the arterial pressure perturbation, termed $\text{AIC}_{\text{start}}$ (start of the Arterially detected Isovolumic Contraction, Fig. 1) was identified as the position of the maximum of the second derivative of the aortic blood pressure (d^2P/dt^2_{max}) preceding the aortic valve opening [16]. To quantify the pressure perturbation in the aortic pressure following $\text{AIC}_{\text{start}}$, the pressure perturbation area (PPA) enclosed by the aortic pressure and a tangent was calculated. The tangent started at $\text{AIC}_{\text{start}}$ and ran through the point where it touched the aortic pressure curve again (Fig. 1). The results from the occlusion and reactive hyperemia data were normalized to the five cycle pre-occlusion PPA average.

Mean coronary artery blood volume flows (CBF) in the LAD and RCA were calculated and divided by MBP to calculate LAD and RCA vascular conductance changes. At the onset of ventricular contraction coronary artery volume flow decreases sharply. The rate of decrease, i.e. slope of the CBF

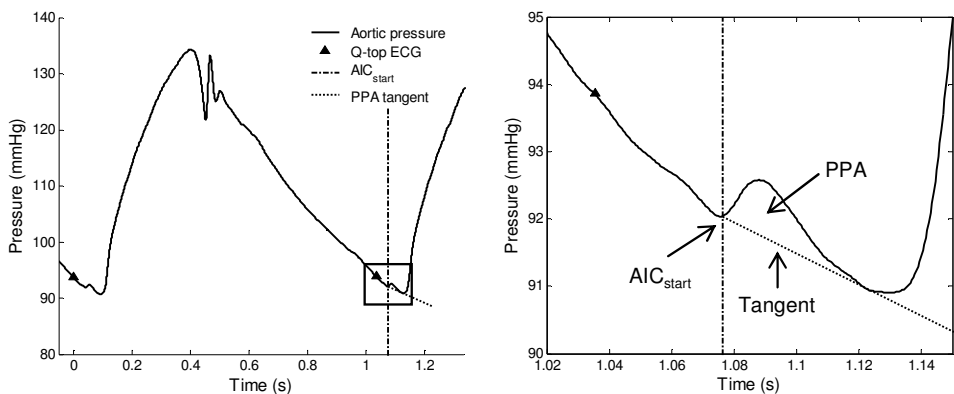


Figure 1. Example of an aortic pressure curve with the pressure perturbation enlarged on the right. $\text{AIC}_{\text{start}}$ (start of the Arterially detected Isovolumic Contraction) is indicated by the dash-dot vertical line and the preceding Q-top of the ECG by a triangle. The enlargement shows the touching tangent (dotted line) and the area between the pressure perturbation and this tangent (PPA)

signal, can be used in conjunction with coronary artery pressure for wave intensity analysis [17] to quantify the intensity of the backwards traveling pressure wave during early ventricular contraction. However, coronary artery pressure was not measured in the present study and hence not available. Consequently, the early systolic coronary artery volume flow slope was used as an indicator for wave intensity behavior during early ventricular contraction, assuming that the slope of coronary artery pressure does not change significantly during reactive hyperemia compared to pre-occlusion slope.

The results of 5 cardiac cycles preceding the onset of occlusion, 5 cycles immediately after the onset of occlusion and 5 cycles following the cessation of occlusion were stored in Excel (Microsoft, Seattle, Washington, USA). The cardiac cycles occurring during the transition from open to fully occluded coronary arteries were excluded from the analysis (typically one to two cycles). Similarly, the cardiac cycles after the release of the occlusion and prior to maximum reactive hyperemia were also excluded from the analysis (typically one to two cycles).

3.2.5 Statistics

All group data are summarized as mean \pm SD. A paired Student's t-test was used to test for statistical significance of the changes from baseline to occlusion and from baseline to reperfusion. A P-value below 0.05 was considered statistically significant. Statistical analysis of the coronary artery volume flow and aortic pressure data was performed using Excel (Microsoft, Seattle, Washington, USA).

3.3 Results

The applied protocols of 5 s occlusion followed by 20 s reperfusion did not significantly influence heart rate (HR), SBP, MBP and DBP (Table 1).

3.3.1 Effect of occlusion

Contrary to our hypothesis, no changes in PPA occurred during any of the occlusion combinations (all $P > 0.20$, Fig. 2 and Fig. 3). Furthermore, neither LAD+LCx nor RCA occlusion protocols influenced coronary artery volume flow, vascular conductance or early systolic volume flow slope in the non-occluded coronary arteries (Table 1).

Coronary-aortic interaction during ventricular isovolumic contraction

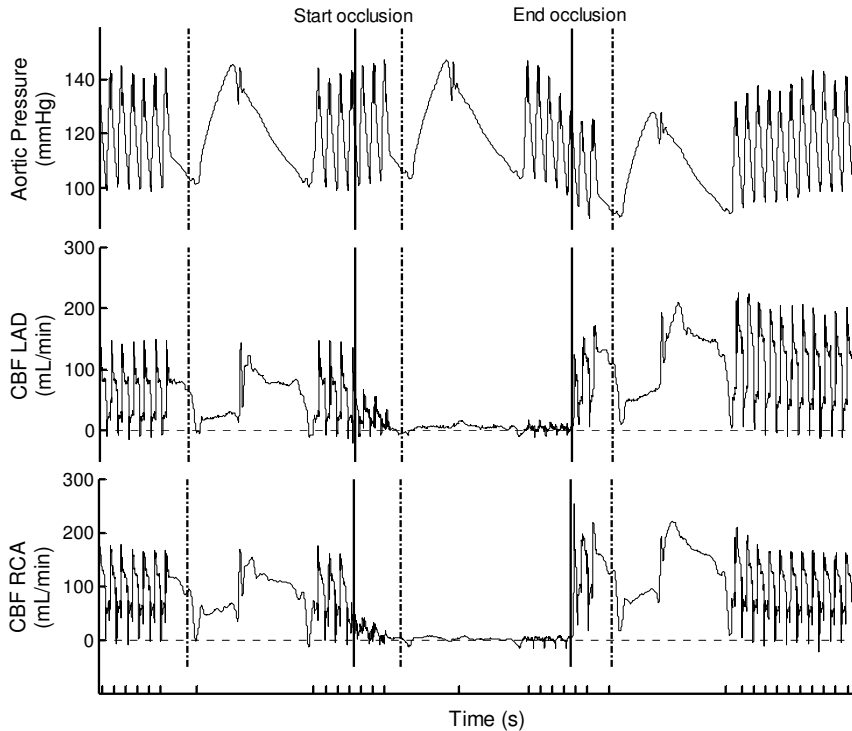


Figure 2. Shown are the aortic pressure and coronary artery flow (CBF) in the Left Anterior Descending (LAD) and Right Common Artery (RCA) during 3 vessel occlusion, with each period in a sequence expanded one beat to show details. The start and end of occlusion are indicated with a solid vertical line. The vertical dashed lines indicate the Q-top of the ECG for the expanded beats. The ticks on the time axis have a 1 second interval.

3.3.2 Effect of reactive hyperemia

Coronary vasodilatation and reactive hyperemia occurred in the LAD and RCA after release of coronary artery occlusion (Table 1). Compared to baseline values, mean CBF in the LAD and RCA increased by $79 \pm 27\%$ and $72 \pm 19\%$, respectively. The steepness of the early systolic volume flow slope in both LAD and RCA increased (i.e. the slope became more negative) under influence of reactive hyperemia, although it reached levels of statistical significance only following LAD+LCx occlusion ($P = 0.03$, Table 1). PPA was not enhanced by reactive hyperemia following any of the occlusion combinations (all $P > 0.22$, Fig. 4).

Table 1 Hemodynamic data.

		Protocol step		
		BL	CAO	H
Heart Rate (bpm)	sham	86 ± 41	86 ± 41	86 ± 42
	LAD+LCx	90 ± 43	90 ± 43	90 ± 43
	RCA	90 ± 49	90 ± 49	90 ± 49
	LAD+LCx+RCA	98 ± 57	98 ± 57	97 ± 57
Maximum Systolic Blood Pressure (mmHg)	sham	118 ± 23	120 ± 25	119 ± 23
	LAD+LCx	122 ± 27	126 ± 28	121 ± 24
	RCA	111 ± 20	114 ± 20	113 ± 19
	LAD+LCx+RCA	114 ± 25	116 ± 26	111 ± 20
Mean Blood Pressure (mmHg)	sham	100 ± 22	101 ± 23	101 ± 21
	LAD+LCx	104 ± 25	106 ± 26	102 ± 23
	RCA	93 ± 18	95 ± 19	95 ± 18
	LAD+LCx+RCA	97 ± 23	98 ± 24	94 ± 20
Minimum Diastolic Blood Pressure (mmHg)	sham	83 ± 20	83 ± 21	84 ± 20
	LAD+LCx	86 ± 24	88 ± 24	85 ± 22
	RCA	76 ± 17	77 ± 17	78 ± 16
	LAD+LCx+RCA	80 ± 21	82 ± 21	78 ± 18
mean CBF_{LAD} (mL/min)	sham	52 ± 16	51 ± 17	52 ± 15
	LAD+LCx	57 ± 24	--	105 ± 53 *
	RCA	64 ± 5	66 ± 6	64 ± 6
	LAD+LCx+RCA	61 ± 26	--	103 ± 39 **
mean CBF_{RCA} (mL/min)	sham	57 ± 44	59 ± 47	57 ± 45
	LAD+LCx	34 ± 16	34 ± 16	33 ± 15
	RCA	68 ± 45	--	127 ± 82 †
	LAD+LCx+RCA	70 ± 45	--	114 ± 74 †
Conductance_{LAD} (mL/min/mmHg)	sham	0.54 ± 0.24	0.53 ± 0.24	0.54 ± 0.24
	LAD+LCx	0.61 ± 0.34	--	1.11 ± 0.68 *
	RCA	0.71 ± 0.25	0.72 ± 0.26	0.71 ± 0.26
	LAD+LCx+RCA	0.67 ± 0.39	--	1.17 ± 0.64 *
Conductance_{RCA} (mL/min/mmHg)	sham	0.57 ± 0.37	0.57 ± 0.39	0.56 ± 0.38
	LAD+LCx	0.35 ± 0.06	0.35 ± 0.05	0.35 ± 0.06
	RCA	0.70 ± 0.40	--	1.30 ± 0.74 *
	LAD+LCx+RCA	0.68 ± 0.37	--	1.17 ± 0.64 †
LAD early systole flow slope (10 ³ mL/min ²)	sham	-69.5 ± 51.1	-71.2 ± 51.4	-67.5 ± 52.1
	LAD+LCx	-79.5 ± 37.9	--	-93.7 ± 43.6 *
	RCA	-80.6 ± 45.4	-81.7 ± 47.4	-77.6 ± 44.7
	LAD+LCx+RCA	-83.3 ± 51.2	--	-97.7 ± 49.8 †
RCA early systole flow slope (10 ³ mL/min ²)	sham	-57.2 ± 10.1	-60.9 ± 8.6	-52.2 ± 21.0
	LAD+LCx	-47.4 ± 18.8	-46.4 ± 16.7	-50.6 ± 5.5
	RCA	-66.3 ± 29.6	--	-81.6 ± 40.5
	LAD+LCx+RCA	-79.8 ± 49.7	--	-97.6 ± 47.6

Values are mean ± SD. mean CBF = mean Coronary artery Blood volume Flow, LAD = Left Anterior Descending, LCx = Left Circumflex, RCA = Right Coronary Artery. BL = baseline, CAO = coronary artery occlusion, H = hyperemia. ** $p < 0.01$ compared to the pre-occlusion value. * $p < 0.05$ indicates a significant difference compared to the pre-occlusion value. † $p = 0.15$.

Coronary-aortic interaction during ventricular isovolumic contraction

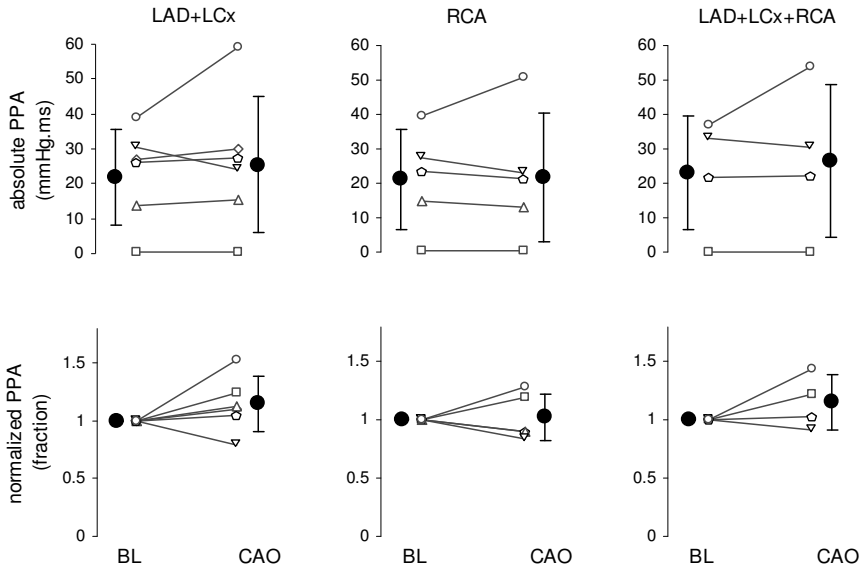


Figure 3. Pressure Perturbation Area (PPA) at baseline (BL) and coronary artery occlusion (CAO). Shown are individual animals (open symbols) and mean \pm SD (solid circles).

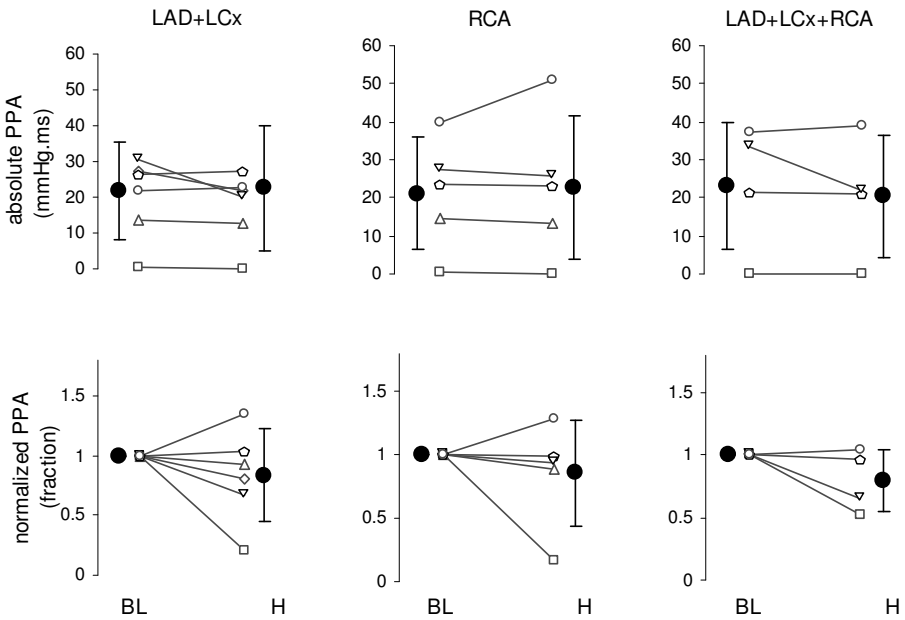


Figure 4. Pressure Perturbation Area (PPA) at baseline (BL) and hyperemia (H). Shown are individual animals (open symbols) and mean \pm SD (solid circles).

3.4 Discussion

In earlier work we hypothesized that the arterial pressure perturbation in the aorta preceding aortic valve opening originated from the coronary circulation during contraction. More specifically, we considered retrograde coronary artery blood volume flow in combination with a pressure wave traveling backwards in the coronary arteries towards the aorta during early systole as cause of the perturbation [16]. Retrograde coronary artery volume flow was first reported by Porter in 1896, and occurs during early ventricular systole [5, 10]. Wave intensity analysis, applied to the waves traveling in the coronary arteries, showed a backwards traveling pressure wave during ventricular isovolumic contraction [5, 6, 11, 12]. Although not explicitly reported by Davies et al. [11], the presented coronary artery pressure curves contained a clear pressure perturbation with similar timing properties as the investigated backwards compression wave, leading to our hypothesis [16]. However, in the present study we found no evidence to support our hypothesis, since the aortic pressure perturbation was not affected by coronary artery occlusion or subsequent hyperemia (respectively Fig. 3 and Fig. 4), indicating that the arterial pressure perturbation does not originate from the coronary arteries.

3.4.1 Effect of occlusion

Separate or combined occlusion of the LAD, LCx and RCA resulted in either a partial or full block of the interaction between the coronary arteries and the aorta. As coronary artery flow is blocked, early systolic retrograde volume flow and the backwards traveling pressure wave cannot enter the aorta. If the coronaries are the origin of the arterial pressure perturbation in the aorta that occurs just before aortic valve opening, occluding one or more coronary arteries is expected to decrease the magnitude of the perturbation or to abolish it entirely. Especially the LAD and LCx coronary arteries were expected to dominate the arterial pressure perturbation as the pressure generated in the left ventricle is higher than in the right ventricle resulting in a higher backwards traveling pressure wave in the LAD and LCx as compared to the RCA [18]. Further, the combined LAD+LCx volume flow is higher than RCA volume flow [19]. Therefore the largest changes in the pressure perturbation area PPA were expected to occur during LAD+LCx occlusion and the three vessel occlusion. In fact, with a complete three vessel occlusion the aortic pressure perturbation should be absent. In contrast to our initial hypothesis, we did not observe any decrease in pressure perturbation during any of the three occlusion protocols.

3.4.2 Effect of reactive hyperemia

During reactive hyperemia, maximum coronary artery volume flow increased by as much as 140% (individual data not shown), which is lower than the 200% increase after a 5 second occlusion reported by Duncker et al. in awake dogs [15]. The difference can be the result of either species differences or the use of pentobarbital as an anesthetic agent in the present study which decreases heart rate [20]. Because the heart rates in our animals (90 beats per minute) were indeed much lower than the heart rates reported by Duncker et al. (115 beats per minute, [15]), the oxygen debt build up during occlusion is lower, explaining the lower magnitude of reactive hyperemia [10]. In our animals the effect of reactive hyperemia on the intensity waves traveling through the coronary arteries could not be calculated, as coronary artery pressure was not measured [21]. However, Sun et al. [22] showed that an approximate doubling of coronary blood volume flow (and a marked decrease in the slope of early systolic blood volume flow) produced by intracoronary adenosine was not accompanied by an marked decrease in the slope of the coronary pressure upstroke. Thus, our results can be interpreted to suggest that the steeper rate of decrease in coronary artery volume flow during early systole was indicative of an increased backwards compression wave. If the arterial pressure perturbation in the aorta indeed originated from the coronary arteries, the increase in wave intensity was expected to increase PPA. However, contrary to our hypothesis PPA values during reactive hyperemia did not show an increase compared to baseline values. These observations are in agreement with the study by Sun et al. [22], in which the magnitude of the aortic pressure perturbation remained apparently unaltered, despite an eight-fold increase in peak backward compression wave intensity during vasodilatation. Similarly, they observed that paired pacing increased peak backwards compression wave intensity, without notably affecting the aortic pressure perturbation. It should be acknowledged that the separation of forward and backward waves is not straightforward as it depends on the determined coronary wave speed [21]. However, since Siebes et al. showed that the energy of forward and backward waves minimally varies with wave speed over a wide range of values [6], possible errors in the amplitude of the backwards compression wave as reported by Sun et al. [22] were assumed to be negligible.

It could be argued that loss of coronary artery retrograde volume flow during hyperemia [10, 15], may have opposed the backward-wave induced increases in PPA values, but this is unlikely for several reasons. First, a contribution of retrograde volume flow to PPA is not very likely as LAD retrograde volume flow in the present study under baseline conditions lasted only 44 ± 14 ms with an

amplitude of -34 ± 37 ml/min (resulting in a retrograde volume of 15 ± 16 μ l). This low value of retrograde volume flow would produce a pressure perturbation of 19×10^{-6} mm Hg, which is negligible compared to the aortic pressure change induced by the stroke volume (27 ± 11 ml under baseline conditions). Furthermore, retrograde volume flow did not occur in two of the six animals although these two animals did show a clear pressure perturbation. Second, and most important, we observed that simultaneous occlusion of all three coronary arteries (which blocked both coronary retrograde volume flow and coronary backward compression waves) had no effect on PPA.

Taken together, the observation that PPA did not change during either occlusion or reactive hyperemia demonstrates that the coronary arteries are not the source of the aortic pressure perturbation.

3.4.3 Methodological considerations

The quantification of the pressure perturbation is sensitive to the shape of the aortic pressure curve which may depend on factors like heart rate, isovolumic contraction period, vascular stiffness and systemic vascular resistance. Over the course of all three occlusion protocols variability was low within each animal (4.4 mmHg.ms over five consecutive heart cycles at baseline), most likely due to the stable heart rates and blood. In contrast, we observed a large variability in the absolute values of PPA over the entire animal group (22.3 ± 13.7 mmHg.ms over five consecutive heart cycles at baseline). For one animal, PPA was a factor 10 smaller compared to the PPA values of the other animals. The heart rate of this particular animal was high (167 beats per minute), thereby shortening ventricular pressure rise time [23]. This might have contributed to a shift of the arterial systolic pressure upslope towards the pressure perturbation. This shift leaves little room between the aortic pressure curve and its touching tangent, thereby decreasing the calculated PPA.

3.5 Conclusion

Although we previously have shown that the arterial pressure perturbation does originate from the contraction of the heart [16], the present study shows that it cannot be explained by coronary artery backflow or a backwards traveling coronary artery pressure wave induced by ventricular contraction. Therefore, the simultaneous occurrence of the backwards traveling pressure wave observed in the coronary arteries and the arterial pressure perturbation in the aorta is coincidental [11, 12, 22], but may reflect a common origin of these two phenomena.

3.6 References

1. O'Rourke MF, Gallagher DE: **Pulse wave analysis**. *J Hypertens Suppl* 1996, **14**(5):S147-157.
2. Avolio A, Westerhof BE, Siebes M, Tyberg JV: **Arterial hemodynamics and wave analysis in the frequency and time domains: an evaluation of the paradigms**. *Med Biol Eng Comput* 2009, **47**(2):107-110.
3. Millasseau SC, Ritter JM, Takazawa K, Chowienczyk PJ: **Contour analysis of the photoplethysmographic pulse measured at the finger**. *J Hypertens* 2006, **24**(8):1449-1456.
4. Cockcroft JR, Wilkinson IB: **Arterial stiffness and pulse contour analysis: an age old concept revisited**. *Clin Sci (Lond)* 2002, **103**(4):379-380.
5. Bender SB, van Houwelingen MJ, Merkus D, Duncker DJ, Laughlin MH: **Quantitative analysis of exercise-induced enhancement of early- and late-systolic retrograde coronary blood flow**. *J Appl Physiol*, **108**(3):507-514.
6. Siebes M, Kolyva C, Verhoeff BJ, Piek JJ, Spaan JA: **Potential and limitations of wave intensity analysis in coronary arteries**. *Med Biol Eng Comput* 2009, **47**(2):233-239.
7. Feissel M, Badie J, Merlani PG, Faller JP, Bendjelid K: **Pre-ejection period variations predict the fluid responsiveness of septic ventilated patients**. *Crit Care Med* 2005, **33**(11):2534-2539.
8. Pinsky MR: **Probing the limits of arterial pulse contour analysis to predict preload responsiveness**. *Anesth Analg* 2003, **96**(5):1245-1247.
9. Reesink KD, Hermeling E, Hoeberigs MC, Reneman RS, Hoeks AP: **Carotid artery pulse wave time characteristics to quantify ventriculoarterial responses to orthostatic challenge**. *J Appl Physiol* 2007, **102**(6):2128-2134.
10. Spaan JA (ed.): **Coronary blood flow. Mechanics, distribution and control**. Dordrecht, Germany: Kluwers Academic Publishers; 1991.
11. Davies JE, Whinnett ZI, Francis DP, Manisty CH, Aguado-Sierra J, Willson K, Foale RA, Malik IS, Hughes AD, Parker KH *et al*: **Evidence of a dominant backward-propagating "suction" wave responsible for diastolic coronary filling in humans, attenuated in left ventricular hypertrophy**. *Circulation* 2006, **113**(14):1768-1778.
12. Sun YH, Anderson TJ, Parker KH, Tyberg JV: **Wave-intensity analysis: a new approach to coronary hemodynamics**. *J Appl Physiol* 2000, **89**(4):1636-1644.
13. Ko JC, Williams BL, Smith VL, McGrath CJ, Jacobson JD: **Comparison of Telazol, Telazol-ketamine, Telazol-xylazine, and Telazol-ketamine-xylazine as chemical restraint and anesthetic induction combination in swine**. *Lab Anim Sci* 1993, **43**(5):476-480.
14. Sorop O, Merkus D, de Beer VJ, Houweling B, Pistea A, McFalls EO, Boomsma F, van Beusekom HM, van der Giessen WJ, VanBavel E *et al*: **Functional and structural adaptations of coronary microvessels**

- distal to a chronic coronary artery stenosis.** *Circ Res* 2008, **102**(7):795-803.
15. Duncker DJ, van Zon NS, Pavsek TJ, Herrlinger SK, Bache RJ: **Endogenous adenosine mediates coronary vasodilation during exercise after K(ATP)+ channel blockade.** *J Clin Invest* 1995, **95**(1):285-295.
 16. van Houwelingen MJ, Barenbrug PJ, Hoeberigs MC, Reneman RS, Hoeks AP: **The onset of ventricular isovolumic contraction as reflected in the carotid artery distension waveform.** *Ultrasound Med Biol* 2007, **33**(3):371-378.
 17. Parker KH, Jones CJ: **Forward and backward running waves in the arteries: analysis using the method of characteristics.** *J Biomech Eng* 1990, **112**(3):322-326.
 18. Hadjiloizou N, Davies JE, Malik IS, Aguado-Sierra J, Willson K, Foale RA, Parker KH, Hughes AD, Francis DP, Mayet J: **Differences in cardiac microcirculatory wave patterns between the proximal left mainstem and proximal right coronary artery.** *Am J Physiol Heart Circ Physiol* 2008, **295**(3):H1198-H1205.
 19. Pitt A, Friesinger GC, Ross RS: **Measurement of blood flow in the right and left coronary artery beds in humans and dogs using the ¹³³Xenon technique.** *Cardiovasc Res* 1969, **3**(1):100-106.
 20. Baum D, Halter JB, Taborsky GJ, Jr., Porte D, Jr.: **Pentobarbital effects on plasma catecholamines: temperature, heart rate, and blood pressure.** *Am J Physiol* 1985, **248**(1 Pt 1):E95-100.
 21. Parker KH: **An introduction to wave intensity analysis.** *Med Biol Eng Comput* 2009, **47**(2):175-188.
 22. Sun YH, Anderson TJ, Parker KH, Tyberg JV: **Effects of left ventricular contractility and coronary vascular resistance on coronary dynamics.** *Am J Physiol Heart Circ Physiol* 2004, **286**(4):H1590-1595.
 23. Hayward CS, Avolio AP, O'Rourke MF: **Arterial pulse wave velocity and heart rate.** *Hypertension* 2002, **40**(6):e8-9; author reply e8-9.

Chapter 4

Initiation of ventricular contraction as reflected in the arterial tree

Marc J. van Houwelingen, Daphne Merkus, Maaïke te Lintel Hekkert, Geert van Dijk, Arnold P.G. Hoeks, Dirk J. Duncker. **Initiation of ventricular contraction as reflected in the arterial tree** (in preparation).

Abstract

Prior to aortic valve opening, aortic pressure is perturbed by ventricular contraction. In earlier work we showed that the onset of this pressure perturbation coincided with the onset of the left ventricular (LV) isovolumic contraction (and hence will be referred to as start of the Arterially detected Isovolumic Contraction, AIC_{start}). In the present study we test the hypothesis that the pressure perturbation indeed has a cardiac origin and narrow down its cause. In 12 Yorkshire X Landrace swine wave intensity analysis revealed the cardiac origin of the aortic pressure perturbation, where AIC_{start} was followed by a positive intensity wave ($0.3 \times 10^5 \pm 0.3 \times 10^5 \text{ W}/(\text{m}^2 \text{ s}^2)$). Timing analysis of left ventricular pressure waveform showed that AIC_{start} was preceded by the onset of LV pressure rise ($12.1 \pm 6.2 \text{ ms}$, $p < 0.01$) and a left ventricular pressure perturbation ($3.8 \pm 1.8 \text{ ms}$, $p < 0.001$), which is a novel finding in this study. In 15 Yorkshire X Landrace swine, myocardial motion analysis showed a significantly higher segment shortening velocity during the first part of the LV pressure perturbation. Therefore, both the LV and aortic pressure perturbation are most likely caused by the early myocardial wall thickening in combination with the deceleration of longitudinal shortening, which also causes mitral valve closure. Consequently, AIC_{start} is useful in the determination of the isovolumic contraction period, a well known marker used in the quantification of cardiac dysfunction.

4.1 Introduction

The arterial pressure waveform contains information on the vascular system as well as the heart and has therefore been scrutinized extensively to obtain information on the cardiovascular hemodynamic status. We have recently shown that a specific perturbation of the arterial pressure waveform, just before the systolic phase, appeared to originate from cardiac contraction [1]. More specifically, we showed in a cardiac surgery patient group [1] that the onset of this pressure perturbation coincided with the onset of left ventricular (LV) contraction. Therefore, in the current study the onset of the arterial pre-systolic pressure perturbation will be referred to as the start of the Arterially detected Isovolumic Contraction Period (AIC_{start}).

In order to fully utilize AIC_{start} for the arterial determination of clinical parameters like the left ventricular isovolumic contraction period, it is important to determine the origin of the pressure perturbation. Initially, we hypothesized that this pressure perturbation originated from the coronary arteries [1]. We recently disproved this hypothesis by showing that simultaneous occlusion of all three main arteries did not affect the aortic pressure perturbation [2]. Alternatively, a mechanical interaction between the LV and the aortic root could cause the pressure perturbation. The aim of the present study was therefore to investigate whether a direct mechanical link between the heart and the aorta is the cause of the aortic pressure perturbation.

4.2 Methods

A total of 27 swine entered the study. Studies were performed in accordance with the Guide for the Care and Use of Laboratory animals (NIH Publication No. 85-23, revised 1996) and with approval of the Erasmus MC Animal Care Committee. In the first part of the study we examined whether the aortic pressure perturbation indeed originated from the heart and determined its exact onset with respect to the systolic timing intervals. The second part of this study tested the hypothesis that the pressure perturbation originated from the cardiac contraction. Both study parts were performed in separate groups of animals, which were subsequently used for other experimental studies.

4.2.1 Instrumentation

Part 1

Twelve 3-4 month-old female Yorkshire X Landrace swine (39 ± 11 kg; mean \pm SD) were sedated with intramuscular injections of Xylazine (2.25 mg/kg) and

Tiletamine plus Zolazepam (5 mg/kg) [3], anesthetized with a bolus of pentobarbital sodium (15 mg/kg IV), intubated and ventilated with an FiO₂ of 30%. Adjustments to tidal volume and ventilation frequency were made to keep blood gasses within the physiological range. Anesthesia was maintained by continuous pentobarbital sodium infusion (flow rate 6-12 mg/(kg.h) IV) [4].

After connecting ECG leads, a high fidelity double lumen pressure sensor catheter (30 mm inter-sensor distance, Millar Instruments, Houston, Texas, USA) was advanced via the right carotid artery into the LV, ensuring that the second sensor tip resided in the aorta. This enabled simultaneous monitoring and recording of both LV and aortic pressure. After sternotomy, an electromagnetic aortic volume flow probe (Skalar, Delft, The Netherlands) was placed around the aorta just distal to the coronary arteries to monitor aortic blood volume flow. After a stabilization period of ~30 minutes, LV and aortic pressure, aortic volume flow and ECG were recorded simultaneously for 3 minutes.

Part 2.

Fifteen 4 month-old female Yorkshire X Landrace swine (50 ± 3 kg) were sedated with ketamine (20 mg/kg IM) and midazolam (1 mg/kg IM), anesthetized with pentobarbital sodium (15 mg/kg IV) and intubated for ventilation with a FiO₂ of 30%. Anesthesia was maintained by 12 mg/(kg.h) IV pentobarbital sodium.

Animals were instrumented with a high fidelity single pressure sensor catheter (Millar Instruments, Houston, Texas, USA) inserted into the carotid artery and advanced into the LV. A fluid-filled catheter was inserted in the left femoral artery and advanced to the intrathoracic descending aorta to measure aortic blood pressure. After sternotomy, two pairs of ultrasonic crystals (Triton Technology INC., San Diego, CA, USA) were placed ~10 mm apart for myocardial segment length assessment during the isovolumic contraction period [5]. One pair was placed in the left circumflex artery (LCx) region near the base of the heart while the other was placed in the left anterior descending artery (LAD) region near the apex of the heart [6, 7]. Each pair was implanted in the midmyocardial layer parallel to the fiber direction. After a stabilization period of ~30 minutes, LV and aortic pressure and myocardial segment length data were recorded simultaneously for at least 10 cardiac cycles.

4.2.2 Data Analysis

To examine the interaction between the LV contraction and aortic pressure, data were digitally recorded using a data acquisition board (part 1: sample rate 2000Hz, National Instruments, Austin, Texas, USA; part 2: sample rate 375Hz, DATAQ instruments, Akron, Ohio, USA). Prior to storage, pressure signals were amplified using an amplifier system (Experimentele Medische Instrumentatie, Erasmus MC, Rotterdam, The Netherlands). Matlab (Natick, Massachusetts, USA) was used for signal conversion to their proper units and for automated post processing of the recorded signals. After low pass filtering of the recorded signals (80Hz, zero phase shift), hemodynamic and myocardial segment length features were determined.

In part 1, we used Wave Intensity Analysis (WIA) [8] to determine whether the heart is indeed the origin of the aortic pressure perturbation. Positive intensity values prove that the wave under investigation originates upstream of the sensors (forward wave) whereas negative values indicate a downstream origin (backward wave), enabling discrimination of the site of origin of the aortic pressure perturbation. For the WIA analysis blood volume flow was converted to blood velocity by dividing volume flow by the lumen area of the flow probe [9-11]. This procedure might underestimate wave intensity and energy as we neglect the area of the aortic wall, but will not influence the sign of the outcome and hence our results. Pressure and velocity curves were temporally aligned by fitting a linear curve through the early systolic phase of the pressure-velocity loop and minimizing the squared error between the pressure-velocity loop and the fitted curve [12]. Subsequently, the wave intensity was calculated from the first derivatives of the pressure and velocity curve. For WIA, pressure, velocity and wave intensity waveforms were ensemble averaged over corresponding intervals of 5 consecutive heart cycles. From the wave intensity ensembles the location of the first positive peak following AIC_{start} , its preceding zero-crossing and energy of the curve from AIC_{start} to aortic valve opening were determined. Pressure wave velocity was determined by dividing the average early systolic slope of the ensemble average pressure-velocity loops by blood density, which was assumed to be constant [8, 12].

In addition to WIA, specific temporal characteristics of the signals were derived. The onset of the heart cycle was identified using the Q-top of the ECG and served as a time reference for all extracted features. From the aortic pressure recording systolic, mean and diastolic blood pressure values were determined. Further, the foot of the aortic pressure pulse was determined by means of an intersecting tangent method [13]. The AIC_{start} (figure 1) was identified as the

position of the maximum of the second derivative of the aortic pressure preceding the aortic valve opening [1]. Similarly to the identification of AIC_{start} , the second derivative of the LV pressure was used to investigate the behavior of LV pressure during the isovolumic contraction period. If an LV pressure perturbation is present, its onset will be detectable as a peak in its second derivative ($P_{LV} \max d^2P/dt^2$), similar to AIC_{start} . Onset of LV pressure was determined with the intersecting tangent method [13]. Aortic valve opening was identified as the onset of the steep upslope in aortic volume flow following ventricular contraction.

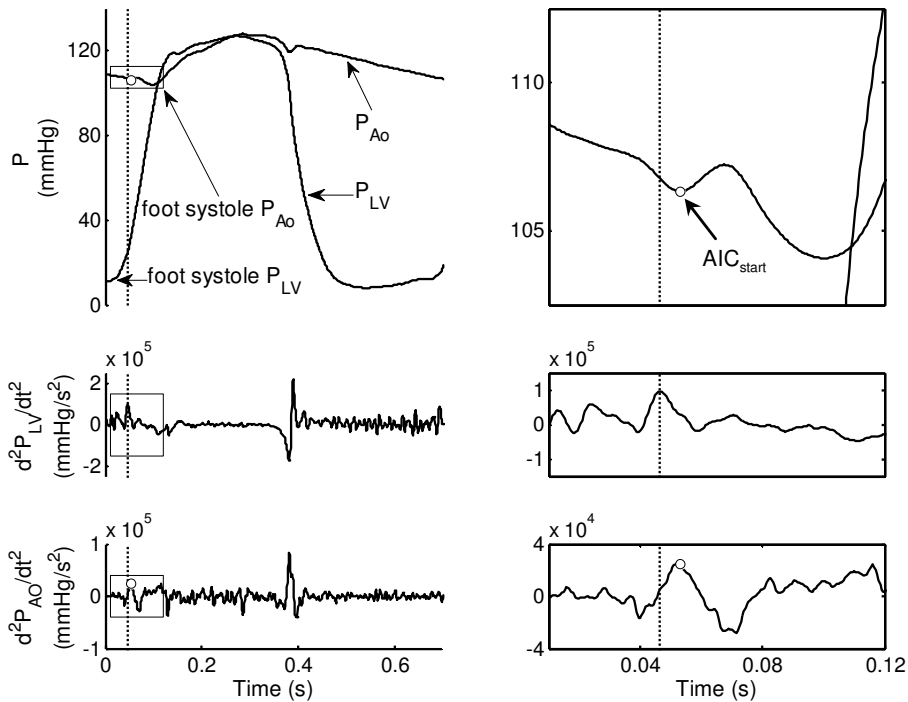


Figure 1. Aortic and LV pressure (respectively P_{Ao} and P_{LV} , top panels) together with the second derivative of both the LV pressure (middle panels) and aortic pressure (bottom panels). Enlargement of the areas enclosed by a rectangle are shown on the right for each respective curve. The circle indicates the onset of the aortic pressure perturbation AIC_{start} (open circle). The vertical dotted line indicates the onset of the LV pressure perturbation. The Q-top of the ECG (time reference) occurs at 0 seconds.

In part 2 the onset of the LV pressure perturbation early in the isovolumic contraction period was identified as the maximum peak in the second derivative of the LV pressure waveform prior to aortic valve opening. The cessation of the pressure perturbation was manually indicated per beat as the first large peak in the second derivative following the onset of the perturbation and preceding the

aortic valve opening. To enable comparison of myocardial segment lengths across animals, the recorded myocardial segment lengths were normalized to 10 mm. Three consecutive intervals, equal in duration, were defined prior (interval 1), and during (interval 2 and 3) the LV perturbation, where the total duration of the LV perturbation equaled the sum of interval 2 and 3. The slope of each interval was determined by fitting a linear curve over the data points within that interval. The segment shortening velocity before the onset of the LV pressure perturbation (interval 1) was compared to the shortening velocities of the intervals during the pressure perturbation occurrence (interval 2 and 3) allowing to assess whether the considered myocardial segment was contracting or expanding. The decrease in segment length that occurred during interval 2 and 3 was divided by diastolic segment length to determine fractional shortening that occurs during the left ventricular pressure perturbation.

4.2.3 Statistics

Statistical analysis of the LV and aortic pressure, aortic volume flow data and WIA data, as well as myocardial segment length data was performed using Excel (Microsoft, Seattle, Washington, USA) and Sigmastat (SPSS Inc., Chicago, Illinois, USA). All data are presented as mean \pm standard deviation (SD). A repeated measures ANOVA test followed by a post hoc Student-Newman-Keuls test was used to compare the extracted features, where appropriate. P-values lower than 0.05 were considered statistically significant.

4.3 Results

Heart rate, and LV and aortic blood pressures are presented in Table 1.

Table 1 hemodynamic variables part 1 and 2

Parameter		Part 1 (n = 12)	Part 2 (n = 15)
Heart rate	(beats per minute)	70 \pm 15	92 \pm 13
Left Ventricle	Maximum systolic blood pressure (mmHg)	112 \pm 19	101 \pm 10
	Maximum dP/dt (mmHg/s)	1441 \pm 217	138 \pm
Aorta	Maximum systolic blood pressure (mmHg)	109 \pm 22	101 \pm 10
	Mean blood pressure (mmHg)	92 \pm 23	85 \pm 10
	Minimum diastolic blood pressure (mmHg)	75 \pm 24	72 \pm 10
WIA _{aorta}	Peak Net Wave Intensity _{systole} ($\times 10^5$ W/m ² /s ²)	16.4 \pm 8.6	-
	Peak Net Wave Intensity _{pressure perturbation} ($\times 10^5$ W/m ² /s ²)	0.3 \pm 0.3	-
	Net Energy _{pressure perturbation} ($\times 10^3$ J/m ² /s ²)	0.22 \pm 0.30	-

Part 1

Systolic peak wave intensity equaled $16.4 \times 10^5 \pm 8.6 \times 10^5 \text{ W}/(\text{m}^2 \cdot \text{s}^2)$, which is similar to values reported in literature [9, 14] (Table 1, figure 2). Wave intensity analysis further revealed the persistent onset of a net positive wave intensity coinciding with the onset of $\text{AIC}_{\text{start}}$ (peak intensity $0.3 \times 10^5 \pm 0.3 \times 10^5 \text{ W}/(\text{m}^2 \cdot \text{s}^2)$, Table 1, figure 2, first positive peak following $\text{AIC}_{\text{start}}$), showing that the pressure perturbation following $\text{AIC}_{\text{start}}$ indeed originated from the heart. The onset of this initial positive wave occurred $2.3 \pm 2.7 \text{ ms}$ earlier than $\text{AIC}_{\text{start}}$ ($p=0.02$, figure 3), which is small compared to the duration of the pre-ejection period ($85.2 \pm 17.6 \text{ ms}$). Total energy of the intensity waveform occurring from $\text{AIC}_{\text{start}}$ to valve opening was positive ($0.22 \times 10^3 \pm 0.30 \times 10^3 \text{ J}/(\text{m}^2 \cdot \text{s}^2)$, Table 1), indicating that forward waves dominate the aortic pressure curve during the isovolumic contraction period and, hence, the cardiac origin of the arterial pressure perturbation.

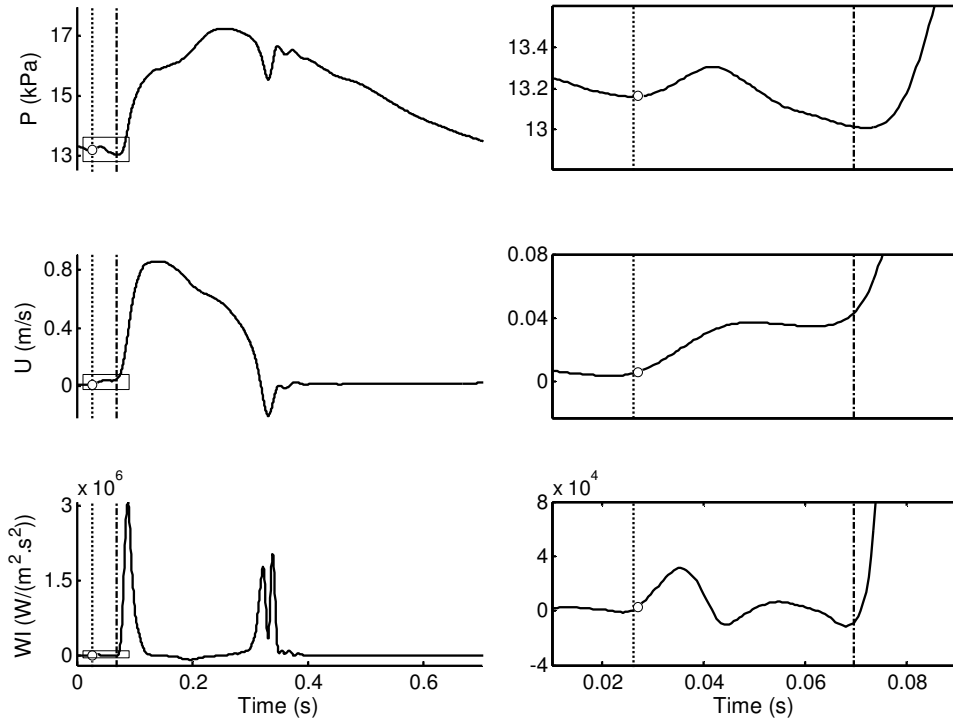


Figure 2. Representative aortic pressure, flow velocity and wave intensity curves over one heart cycle (left panels, respectively from top to bottom). Please note the units of pressure being kPa/s, used in the calculation of the wave intensity. Enlargement of the areas enclosed by a rectangle are shown on the right of each respective curve. In the bottom panels the net wave intensity curve is represented as a solid line. In all panels the circle indicates the onset of $\text{AIC}_{\text{start}}$ and the dotted vertical line indicates the onset of the positive intensity wave. The Q-top of the ECG (time reference) occurs at 0 seconds.

The aortic pressure perturbation occurred significantly later than the LV foot systole (12.1 ± 6.2 ms, $p < 0.001$). A persistent local peak in the second derivative of the LV pressure preceding AIC_{start} was identified as the onset of a LV pressure perturbation (see Figure 1 for a typical example). The LV pressure perturbation onset was preceded by the onset of LV foot systole (difference 8.9 ± 6.1 ms, $p < 0.003$). Both LV and aortic pressure perturbations were consistently present in all swine (onset LV pressure perturbation: 37.2 ± 11.0 ms, intra-animal SD 3.5ms; onset aortic pressure perturbation: 41.0 ± 10.1 ms, intra-animal SD 2.9 ms). The onset of the early systolic LV pressure perturbation occurred significantly earlier than AIC_{start} (3.8 ± 1.8 ms, $p < 0.001$), pointing to a ventricular origin of the aortic pressure perturbation. The short delay between the two could well be explained by the distance between the LV and aortic pressure transducers. Using the P-U loop method a pressure wave velocity of 3.3 ± 1.1 m/s was found. Multiplying pressure wave velocity with the found delay (3.8ms) reveals a pulse wave travel distance of 13 ± 4 mm which approximates the inter-sensor distance of 30mm. However, one should realize that part of the trajectory is surrounded by stiff material (the contracting myocardium and the aortic root) with a considerable higher pulse wave velocity, leading to an underestimation of pulse wave travel distance.

Figure 3 summarizes the temporal relations between the features extracted from the LV and aortic pressure curves, their second derivatives, and the aortic volume flow.

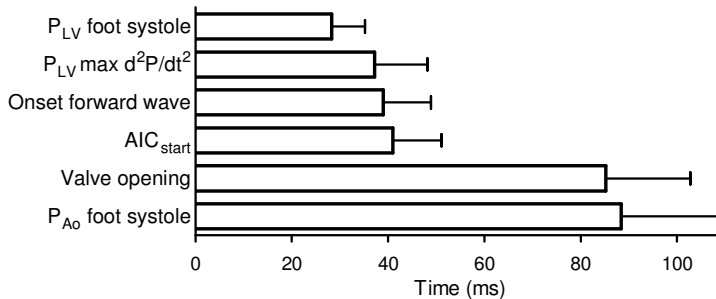


Figure 3. Temporal relation between the Q-top of the ECG (at 0 seconds) and from top to bottom the occurrence of the LV foot systole (P_{LV} foot systole), onset of LV pressure perturbation (P_{LV} max d^2P/dt^2), onset of the forward intensity wave just prior to AIC_{start} , the onset of the aortic pressure perturbation (AIC_{start}), the aortic valve opening and the aortic foot systole (P_{Ao} foot systole) in 10 animals. † $p < 0.003$ compared to P_{LV} max d^2P/dt^2 , ‡ $p < 0.001$ compared to AIC_{start} , * $p = 0.05$ compared to AIC_{start} . Data are mean \pm SD.

Part 2

To further investigate the origin of the LV and aortic pressure perturbations, myocardial segment lengths in the LCx region (near the base) and LAD region (near the apex) were recorded to determine whether changes in myocardial

contraction occur concurrently with the LV pressure perturbation (see figure 4 for a typical example). After onset of the LV pressure perturbation, the average shortening velocity of both base and apex myocardial segment length significantly increased, i.e. the slope of the myocardial segment length became more steep (slopes interval 2 compared to interval 1: LCx: -24.6 ± 14.8 mm/s compared to -7.1 ± 7.3 mm/s, $p < 0.002$; LAD: -7.2 ± 8.1 mm/s compared to -0.9 ± 8.5 mm/s, $p = 0.03$). During the second part of the LV pressure perturbation (interval 3) the shortening velocity decreased in the LCx and was reversed to lengthening in the LAD (LCx: -2.9 ± 4.9 mm/s, $p < 0.001$, LAD: 5.8 ± 10.4 mm/s, $p < 0.001$, compared to their interval 2 value). Myocardial segment length shortening during the entire ventricular pressure perturbation equaled 25 ± 17 % in the LCx region and 3 ± 9 % in the LAD region of the total systolic segment shortening.

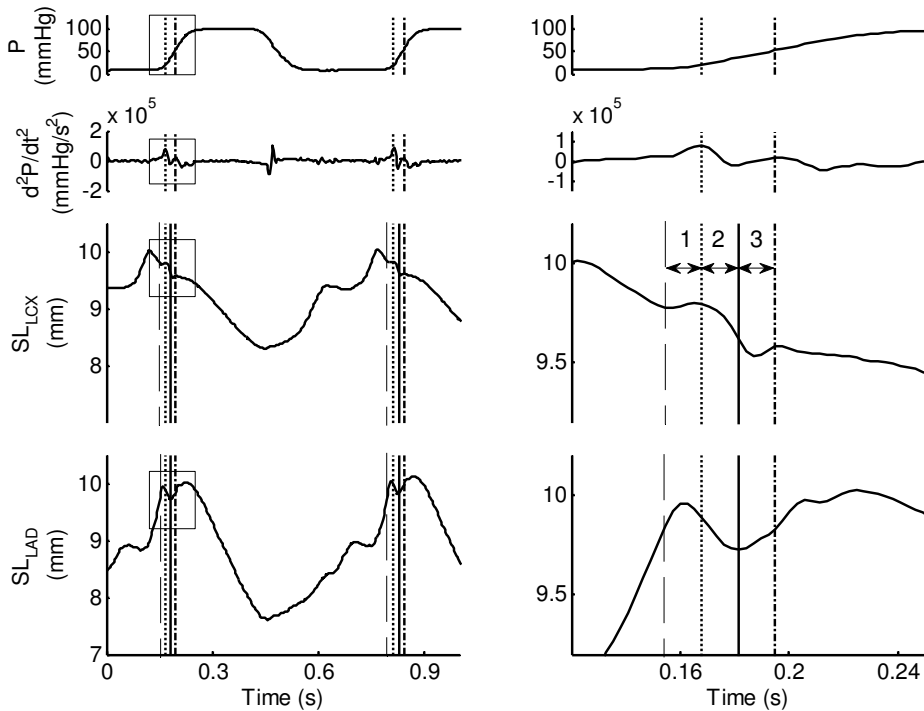


Figure 4. Representative LV pressure, its second derivative and LCx and LAD myocardial segment length (SL) curves over one heart cycle (left panels, respectively from top to bottom). Enlargement of the areas enclosed by a rectangle are shown on the right for each respective curve. The dotted vertical line indicates the onset of the LV pressure perturbation; the dash-dotted line indicates the approximated end of the LV pressure perturbation. The dashed vertical line in the bottom panels indicates the start of analysis interval 1. The solid vertical line in the bottom panels indicates the separation point between analysis interval 2 and 3. Intervals 1, 2 and 3 are equal in duration.

4.4 Discussion

In the present study we elucidate the origin of the aortic pressure perturbation by means of wave intensity analysis and found that the perturbation indeed originates from the heart. Moreover, the novel finding of an LV pressure perturbation coinciding with the aortic pressure perturbation and which onset precedes the onset of the aortic pressure perturbation confirms the myocardial origin. The analysis of myocardial segment length data shows that the origin of the LV and aortic pressure perturbation can be traced back to the initial LV contraction.

Cardiac contraction has been extensively investigated for a better understanding of the cardiac action using sonomicrometer techniques [15, 16], MRI tagging techniques [17, 18], cineradiography techniques [19] or ultrasound techniques [20, 21]. However, the mechanical interaction between myocardium and the aorta and its effects on the aortic pressure are usually not considered. The current work describes an aortic pressure perturbation caused by the interaction between the LV and aorta during the isovolumic contraction. This pressure perturbation was noticed earlier in the carotid distension wave [1] and was linked to the subsequent arterial systolic phase. At that time, the coronary arteries were suggested as a likely source; however by means of an occlusion protocol involving the 3 main coronary arteries we showed that they are in fact not the origin of the aortic pressure perturbation [2].

4.4.1 Cardiac origin.

In the present work we used wave intensity analysis to demonstrate that the aortic pressure perturbation indeed originates from the heart. The positive intensity wave following AIC_{start} suggested an origin upstream from the measurement site in the proximal aorta, i.e., the heart. The cardiac origin, combined with the proof that the coronary arteries are not the origin of the aortic pressure perturbation, leads to the conclusion that the aortic pressure perturbation is caused by a mechanical interaction between cardiac motion, as consequence of contraction, and the aorta. This is corroborated by our novel finding of the consistent occurrence of a pressure perturbation in the LV occurring just before the onset of AIC_{start} . The onset of the ventricular perturbation preceding AIC_{start} excludes a backward transmission of the aortic pressure perturbation through the closed aortic valve into the LV cavity. The latter option is also counterintuitive due to the stress exerted on the aortic valve during isovolumic contraction of the ventricle. Possible sources of the LV and aortic pressure perturbation include the mechanical coupling of the ventricle and aorta and the decelerating mitral inflow.

The timing of the features as found in our data shows that the LV and aortic pressure perturbation occur during the early phase of LV systole, immediately after LV foot systole. During that phase of cardiac contraction, basal endocardial fiber shortening causes an initial clockwise twisting, radial thickening and longitudinal shortening of the myocardial tissue [15, 19, 22, 23]. Ashikaga et al. [19] showed that an increase in subendocardial radial strain, indicating myocardial wall thickening, initiated at approximately 30% of the isovolumic contraction period, which they defined as the interval between the R-top of the ECG and aortic valve opening. Moreover, in their figure 1 [19], a clear pressure perturbation in both the aortic and LV pressure can be observed, also occurring at approximately 30% of the isovolumic contraction period. This corresponds to the timing properties of the onset of the LV pressure perturbation as we observed in our animals, which occurred at 44 ± 13 % of the pre-ejection period (interval Q-top ECG – aortic valve opening). Moreover, during the LV pressure perturbation in our animals a shortening of the LCx and LAD segment length indicated the presence of myocardial contraction during the pressure perturbation interval. Therefore, LV wall thickening caused by the subendocardial contraction could well contribute to the generation of the LV pressure perturbation.

Next to the increase in radial strain which indicated a thickening of the myocardial wall, the myocardium also shortens in a longitudinal direction [15, 19, 23]. Interestingly, in an early paper on heart sounds Reinhold et al. reported a perturbation in the aortic electrokymogram similar to the pressure perturbation investigated in the current study, and suggested the brisk downward movement of the base of the heart initiated by the isovolumic contraction of the heart as an explanation [24]. To our knowledge, this observation was not further related to cardiac motion. It is, however, not the brisk downward movement but the deceleration of this movement against the intracavitary blood volume that contributes to the LV and aortic pressure perturbations, which initiates at mitral valve closure [19, 25]. This is supported by the delayed mitral valve closure compared to the onset of LV pressure rise [26, 27], similar to the delay between the onset of LV pressure rise and onset of the LV pressure perturbation. For the duration of the basal deceleration a force is exerted on the LV intracavity blood volume as well as on the aortic valve. This would explain the occurrence of both the LV and aortic pressure perturbation, as well as their phasic nature. It could be argued that the deceleration of the myocardial base is not only mediated by the mitral valve closure, but also by the myocardial transmural heterogeneity of contraction [19, 22]. The latter would reduce the force generated by the basal

deceleration as a result of mitral valve closure, and hence the amplitude of the LV and aortic pressure perturbations.

The short delay between the onset of the LV and aortic pressure perturbation suggests that the LV pressure perturbation is transmitted through the flexible aortic valve and its surrounding tissue. The deceleration of the myocardial base against the LV intra-cavity blood volume, which likely causes the LV pressure perturbation, also likely causes an upward movement of the aortic valve leaflets contributing to the aortic pressure perturbation. Additionally, Sengupta et al. [28] showed that during the isovolumic contraction period blood is accelerated towards the LV outflow tract. It will decelerate by the opposition of the closed valves, where the mitral valve is restricted in movement by the chordae tendineae and papillary muscles while the aorta is only restrained by the opposing aortic pressure. Hence the flexible aortic valve is again a likely candidate for a transmission site from the LV to the aorta contributing to the aortic pressure perturbation. Indeed, Thubrikar et al. [29] showed an outwards movement of the aortic valve during the isovolumic contraction. Moreover, Lansac et al. [30] showed that at the onset of the isovolumic contraction the aorta started to expand at its base and commissural level, whereas expansion of the aorta at the level of sinotubular junction and ascending aorta was delayed to the second half of the isovolumic contraction. This is in line with the shape of the observed aortic volume flow waveform, which shows a small volume flow perturbation at the time of the aortic pressure perturbation (resulting in a positive energy of the aortic intensity waveform during the isovolumic contraction). Altogether, it is likely that the aortic pressure perturbation indeed originates from effect of the deceleration of the myocardial base and intra-cavity blood flow being transmitted through the aortic valve.

It could be argued that the deceleration of the inflow of blood from the left atrium into the ventricle caused by the very first part of ventricular contraction could perturb LV pressure (similar to the ticking sound after closing a water faucet). This is, however, unlikely as the aortic pressure perturbation starts early in the ventricular contraction and can last as long as the isovolumic contraction period itself. Indeed, Laniado et al. showed that the mitral valve is still open at zero inflow [26]. Hence an abrupt deceleration of blood from the left atrium is an unlikely source for the aortic pressure perturbation.

4.4.2 Clinical implications

The lengthening of the isovolumic contraction period has shown to be indicative of reduced ventricular function [31-33], and therefore the arterially detected

isovolumic contraction period could prove to be useful in clinical practice. Mitral valve closure is assumed to occur at atrial-ventricular pressure cross-over. Therefore, this pressure cross-over is usually considered as the start of the isovolumic contraction period [34]. As a substitute the systolic foot of the left ventricular pressure waveform is frequently used [27]. However, mitral valve closure occurs later than the onset of the LV pressure rise during systole [26, 35], possibly resulting in an overestimation of the isovolumic contraction period. To prevent overestimation, ultrasound techniques have been used to assess true mitral valve closure [36]. The present study suggests that the mechanisms involved in mitral valve closure [20, 28] and myocardial wall thickening [19] are the most likely source of the left ventricular and aortic pressure perturbations. Henceforth, the observation indicates that the onset of the aortic pressure perturbation can indeed be used to determine directly the onset of the isovolumic contraction and the duration of the isovolumic contraction period without the need for additional signals like the ECG or more invasive measurements, e.g. the LV pressure. Additionally, the onset of the pressure perturbation can also be assessed further down the arterial tree using ultrasound [1], enabling the non-invasive assessment of the isovolumic contraction period and contributing to a patient friendly quantification of LV function. Reesink et al. [37] already showed the feasibility of the quantification of ventriculo-arterial interaction by means of carotid ultrasound and pulse wave analysis during an orthostatic challenge in healthy volunteers. The observed relationship between the arterially determined isovolumic contraction period and orthostatic challenge points towards several useful clinical applications, e.g., in the field of shock.

4.5 Conclusion

The late diastolic aortic pressure perturbation and the novel finding of an early perturbation in the LV pressure are most likely caused by the early phase of the ventricular myocardial contraction. The resulting wall thickening of the heart in combination with the deceleration of longitudinal shortening and intra-cavity blood flow perturb LV pressure and most likely exert a mechanical force on the aortic foot and valve, thereby causing the aortic pressure perturbation. Since the latter coincides with the onset of the LV isovolumic contraction, the pressure perturbation measured in the aorta or even further distally in the carotid artery can be used as a marker for the onset of the isovolumic contraction. This is advantageous in a clinical setting where cardiac timing properties have shown to be useful but difficult to determine.

4.6 References

1. van Houwelingen MJ, Barenbrug PJ, Hoeberigs MC, Reneman RS, Hoeks AP: **The onset of ventricular isovolumic contraction as reflected in the carotid artery distension waveform.** *Ultrasound Med Biol* 2007, **33**(3):371-378.
2. van Houwelingen MJ, Merkus D, te Lintel Hekkert M, van Dijk G, Hoeks APG, Duncker DJ: **Coronary-aortic interaction during ventricular isovolemic contraction.** *Med Biol Eng Comput (in press)* 2011.
3. Ko JC, Williams BL, Smith VL, McGrath CJ, Jacobson JD: **Comparison of Telazol, Telazol-ketamine, Telazol-xylazine, and Telazol-ketamine-xylazine as chemical restraint and anesthetic induction combination in swine.** *Lab Anim Sci* 1993, **43**(5):476-480.
4. Sorop O, Merkus D, de Beer VJ, Houweling B, Pistea A, McFalls EO, Boomsma F, van Beusekom HM, van der Giessen WJ, VanBavel E *et al*: **Functional and structural adaptations of coronary microvessels distal to a chronic coronary artery stenosis.** *Circ Res* 2008, **102**(7):795-803.
5. Te Lintel Hekkert M, Dube GP, Regar E, de Boer M, Vranckx P, van der Giessen WJ, Serruys PW, Duncker DJ: **Preoxygenated hemoglobin-based oxygen carrier HBOC-201 annihilates myocardial ischemia during brief coronary artery occlusion in pigs.** *Am J Physiol Heart Circ Physiol* 2010, **298**(3):H1103-1113.
6. de Zeeuw S, Lameris TW, Duncker DJ, Hasan D, Boomsma F, van den Meiracker AH, Verdouw PD: **Cardioprotection in pigs by exogenous norepinephrine but not by cerebral ischemia-induced release of endogenous norepinephrine.** *Stroke* 2001, **32**(3):767-774.
7. de Zeeuw S, Trines SA, Krams R, Verdouw PD, Duncker DJ: **Cardiovascular profile of the calcium sensitizer EMD 57033 in open-chest anaesthetized pigs with regionally stunned myocardium.** *Br J Pharmacol* 2000, **129**(7):1413-1422.
8. Parker KH: **An introduction to wave intensity analysis.** *Med Biol Eng Comput* 2009, **47**(2):175-188.
9. Penny DJ, Mynard JP, Smolich JJ: **Aortic wave intensity analysis of ventricular-vascular interaction during incremental dobutamine infusion in adult sheep.** *Am J Physiol Heart Circ Physiol* 2008, **294**(1):H481-489.
10. Sun Y, Belenkie I, Wang JJ, Tyberg JV: **Assessment of right ventricular diastolic suction in dogs with the use of wave intensity analysis.** *Am J Physiol Heart Circ Physiol* 2006, **291**(6):H3114-3121.
11. Bender SB, van Houwelingen MJ, Merkus D, Duncker DJ, Laughlin MH: **Quantitative analysis of exercise-induced enhancement of early- and late-systolic retrograde coronary blood flow.** *J Appl Physiol* 2010, **108**(3):507-514.
12. Khir AW, Swalen MJ, Feng J, Parker KH: **Simultaneous determination of wave speed and arrival time of reflected waves**

- using the pressure-velocity loop. *Med Biol Eng Comput* 2007, **45**(12):1201-1210.
13. Chiu YC, Arand PW, Shroff SG, Feldman T, Carroll JD: **Determination of pulse wave velocities with computerized algorithms.** *Am Heart J* 1991, **121**(5):1460-1470.
 14. van den Wijngaard JP, Siebes M, Westerhof BE: **Comparison of arterial waves derived by classical wave separation and wave intensity analysis in a model of aortic coarctation.** *Med Biol Eng Comput* 2009, **47**(2):211-220.
 15. Edvardsen T, Urheim S, Skulstad H, Steine K, Ihlen H, Smiseth OA: **Quantification of left ventricular systolic function by tissue Doppler echocardiography: added value of measuring pre- and postejction velocities in ischemic myocardium.** *Circulation* 2002, **105**(17):2071-2077.
 16. Sengupta PP, Khandheria BK, Korinek J, Wang J, Jahangir A, Seward JB, Belohlavek M: **Apex-to-base dispersion in regional timing of left ventricular shortening and lengthening.** *J Am Coll Cardiol* 2006, **47**(1):163-172.
 17. Buckberg GD, Mahajan A, Jung B, Markl M, Hennig J, Ballester-Rodes M: **MRI myocardial motion and fiber tracking: a confirmation of knowledge from different imaging modalities.** *Eur J Cardiothorac Surg* 2006, **29 Suppl 1**:S165-177.
 18. Prinzen FW, Hunter WC, Wyman BT, McVeigh ER: **Mapping of regional myocardial strain and work during ventricular pacing: experimental study using magnetic resonance imaging tagging.** *J Am Coll Cardiol* 1999, **33**(6):1735-1742.
 19. Ashikaga H, van der Spoel TI, Coppola BA, Omens JH: **Transmural myocardial mechanics during isovolumic contraction.** *JACC Cardiovasc Imaging* 2009, **2**(2):202-211.
 20. Sengupta PP, Khandheria BK, Korinek J, Jahangir A, Yoshifuku S, Milosevic I, Belohlavek M: **Left ventricular isovolumic flow sequence during sinus and paced rhythms: new insights from use of high-resolution Doppler and ultrasonic digital particle imaging velocimetry.** *J Am Coll Cardiol* 2007, **49**(8):899-908.
 21. Vogel M, Cheung MM, Li J, Kristiansen SB, Schmidt MR, White PA, Sorensen K, Redington AN: **Noninvasive assessment of left ventricular force-frequency relationships using tissue Doppler-derived isovolumic acceleration: validation in an animal model.** *Circulation* 2003, **107**(12):1647-1652.
 22. Sengupta PP, Tajik AJ, Chandrasekaran K, Khandheria BK: **Twist mechanics of the left ventricle: principles and application.** *JACC Cardiovasc Imaging* 2008, **1**(3):366-376.
 23. Veyrat C, Larrazet F, Pellerin D: **Renewed interest in preejectional isovolumic phase: new applications of tissue Doppler indexes: implications to ventricular dyssynchrony.** *Am J Cardiol* 2005, **96**(7):1022-1030.
 24. Reinhold J, Rudhe U: **Relation of the first and second heart sounds to events in the cardiac cycle.** *Br Heart J* 1957, **19**(4):473-485.

25. Remme EW, Lyseggen E, Helle-Valle T, Opdahl A, Pettersen E, Vartdal T, Ragnarsson A, Ljosland M, Ihlen H, Edvardsen T *et al*: **Mechanisms of preejection and postejection velocity spikes in left ventricular myocardium: interaction between wall deformation and valve events.** *Circulation* 2008, **118**(4):373-380.
26. Laniado S, Yellin E, Kotler M, Levy L, Stadler J, Terdiman R: **A study of the dynamic relations between the mitral valve echogram and phasic mitral flow.** *Circulation* 1975, **51**(1):104-113.
27. Tsakiris AG, Gordon DA, Padiyar R, Frechette D: **Relation of mitral valve opening and closure to left atrial and ventricular pressures in the intact dog.** *Am J Physiol* 1978, **234**(2):H146-151.
28. Sengupta PP: **Exploring left ventricular isovolumic shortening and stretch mechanics: "The heart has its reasons..."** *JACC Cardiovasc Imaging* 2009, **2**(2):212-215.
29. Thubrikar M, Piepgrass WC, Shaner TW, Nolan SP: **The design of the normal aortic valve.** *Am J Physiol* 1981, **241**(6):H795-801.
30. Lansac E, Lim HS, Shomura Y, Lim KH, Rice NT, Goetz W, Acar C, Duran CM: **A four-dimensional study of the aortic root dynamics.** *Eur J Cardiothorac Surg* 2002, **22**(4):497-503.
31. Bruch C, Schmermund A, Marin D, Katz M, Bartel T, Schaar J, Erbel R: **Tei-index in patients with mild-to-moderate congestive heart failure.** *Eur Heart J* 2000, **21**(22):1888-1895.
32. Tei C, Ling LH, Hodge DO, Bailey KR, Oh JK, Rodeheffer RJ, Tajik AJ, Seward JB: **New index of combined systolic and diastolic myocardial performance: a simple and reproducible measure of cardiac function--a study in normals and dilated cardiomyopathy.** *J Cardiol* 1995, **26**(6):357-366.
33. Weissler AM, Harris WS, Schoenfeld CD: **Systolic time intervals in heart failure in man.** *Circulation* 1968, **37**(2):149-159.
34. Boron WF, Boulpaep EL: **Medical Physiology**, 2 edn. Philadelphia: Elsevier Saunders; 2005.
35. Goetz WA, Lansac E, Lim HS, Weber PA, Duran CM: **Left ventricular endocardial longitudinal and transverse changes during isovolumic contraction and relaxation: a challenge.** *Am J Physiol Heart Circ Physiol* 2005, **289**(1):H196-201.
36. Rubenstein JJ, Pohost GM, Dinsmore RE, Harthorne JW: **The echocardiographic determination of mitral valve opening and closure. Correlation with hemodynamic studies in man.** *Circulation* 1975, **51**(1):98-103.
37. Reesink KD, Hermeling E, Hoeberigs MC, Reneman RS, Hoeks AP: **Carotid artery pulse wave time characteristics to quantify ventriculoarterial responses to orthostatic challenge.** *J Appl Physiol* 2007, **102**(6):2128-2134.

Chapter 5

Arterial determination of the left ventricular isovolumic contraction period in the assessment of hemorrhagic shock severity

Marc J. van Houwelingen, Daphne Merkus, Jan Hofland, Robert Tenbrinck, Maaïke te Lintel Hekkert, Geert van Dijk, Arnold P.G. Hoeks, Dirk J. Duncker. **Arterial determination of the left ventricular isovolumic contraction period in the assessment of hemorrhagic shock severity** (in preparation).

Abstract

Recently, the ventilatory variation in pre-ejection period (Δ PEP) was found to predict the fluid-responsiveness of patients in shock. We hypothesized that the ventilation induced variation in the arterially determined isovolumic contraction period (Δ AIC) would be a more sensitive predictor than a remotely assessed Δ PEP, as it is not confounded by the electromechanical delay of the heart nor pulse travel time to the measurement site. To test this hypothesis we investigated the response of Δ AIC and Δ PEP to a graded hemorrhage protocol. The results were compared to the responses of pulse pressure variation (Δ PP) and stroke volume variation (Δ SV), which both have a high predictive value in the prediction of fluid responsiveness. A graded hemorrhage protocol followed by resuscitation using nor-epinephrine and autologous blood transfusion was instituted in 7 anesthetized Yorkshire X Landrace swine. Δ AIC correlated well with Δ PP ($r = 0.86$, $p < 0.001$), Δ SV ($r = 0.85$, $p < 0.001$) and Δ PEP ($r = 0.86$, $p < 0.001$). The coefficient of variation of Δ AIC (0.54) was found to be significantly lower than that of Δ PEP (0.91). Moreover, Δ AIC correlated well SV ($r = -0.62$, $p < 0.001$). Δ AIC can therefore be used to assess the level of hemorrhagic shock in a swine model and is likely to be a more sensitive predictor of fluid responsiveness than Δ PEP.

5.1 Introduction

A reduction in effective circulating blood volume, either by hemorrhage or vasodilatation that results in a decrease in left ventricular preload and hence stroke volume (SV) and cardiac output (CO) and induces systemic hypotension is a situation termed shock [1]. Patients in shock are typically treated with vasoactive agents and fluids to increase cardiac output and restore systemic arterial pressure. A patient with hemorrhagic shock requires administration of IV fluids, whereas a septic patient may not benefit from a large amount of IV fluids and may even experience adverse effects [2-7]. To predict whether patients will be fluid responsive and to determine the optimal quantity of fluids to be infused, several hemodynamic variables have been proposed, including central venous pressure, pulmonary wedge pressure and pulse pressure variation [8-12].

Positive pressure ventilation induces variations in preload which cause variations in stroke volume [12, 13], and hence in pulse pressure [14, 15]. The amplitude of the variation in stroke volume or pulse pressure reflects the part of the non-linear Frank-Starling preload-stroke volume curve that the heart is operating on. Thus, operating on the steep sloped part as a consequence of a low average preload, a small change in preload translates into a large change in stroke volume indicating an IV fluid responsive patient. Conversely, at normal preload values operating on the shallow sloped part a similar change in preload only results in a small variation in stroke volume [15]. In the latter case, a patient is less likely to benefit from IV fluid administration. Consequently, it is not surprising that variations in ventricular preload produced by positive pressure ventilation have been shown to predict fluid responsiveness better than static variables such as central venous pressure or pulmonary wedge pressure [14, 15]. Indeed, the relative variations in stroke volume and pulse pressure over the ventilatory cycle have been shown to be highly predictive of a patient's fluid-responsiveness [12-14].

A limitation of the ventilation-induced variations in pulse pressure as an index of filling status is that it requires an invasive blood pressure measurement. Since the variations in preload produced by ventilation also produce variations in systolic timing intervals [16-18], one could consider pressure waveform timing characteristics, instead of pressure amplitude properties, as a less invasive or even noninvasive assessment of fluid responsiveness [16, 17, 19, 20]. Based on the observation that the pre-ejection period (PEP) depends mainly on preload [21], Bendjelid et al. [16] proposed its relative variation produced by positive pressure ventilation (Δ PEP) as a predictor of fluid-responsiveness. In

septic patients, these authors showed that the Δ PEP, as measured at the level of the radial artery, was indeed able to predict whether a particular patient would respond to IV fluid infusion [16].

The PEP can be divided into two intervals (figure 1). The first interval, the electro-mechanical delay (EMD) reflects the time between the Q-top of the ECG and the mitral valve closure. The second interval is the isovolumic contraction period. Recently we reported the presence of an aortic pressure perturbation prior to aortic valve opening [20], of which the onset corresponds with the onset of isovolumic contraction (figure 1). This arterially detected isovolumic contraction start (AIC_{start}) [20] can be used to separate the PEP into the EMD and isovolumic contraction period. The elapsed time between the Q-top of the ECG and AIC_{start} equals EMD whereas the time interval between AIC_{start} and the systolic foot of the arterial pressure pulse reflects the isovolumic contraction period and will be referred to as the arterially determined isovolumic contraction period (AIC). When PEP is determined based on arterial pressure measurements in a distal artery, a third time interval is added to PEP, representing the time required for a pressure pulse wave to travel from the heart to the remote measurement site.

We hypothesized that the ventilation-induced preload variation principally affects the isovolumic contraction period and has very little influence on the EMD and pulse wave travel time. The latter show less variation on a beat-to-beat basis and appear largely dependent on hemodynamic variables such as heart rate, mean arterial blood pressure and vascular stiffness and are influenced by sympathetic activity [22-24]. Consequently, we hypothesized that

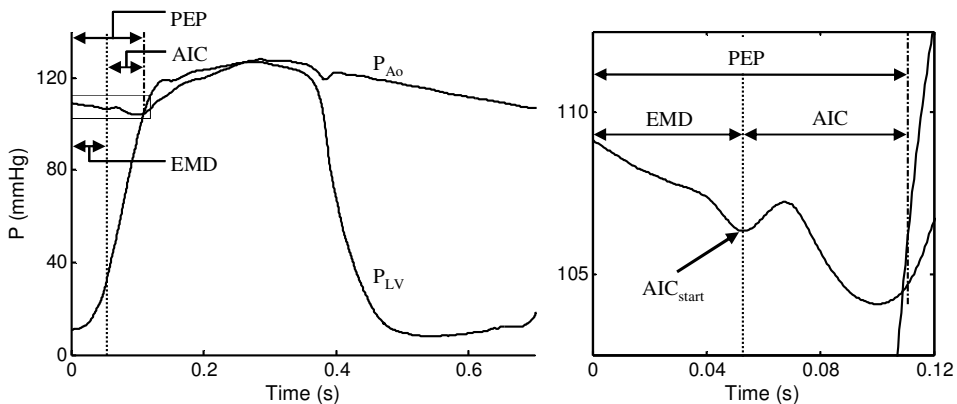


Figure 1. Representative aortic and left ventricular pressure (respectively P_{Ao} and P_{LV}). Enlargement of the area enclosed by a rectangle is shown on the right. The dotted vertical line indicates the onset of the aortic pressure perturbation AIC_{start} . The vertical dash-dotted line indicates the arterial systolic foot. The Q-top of the ECG occurs at 0 seconds. PEP: pre-ejection period, EMD: electro-mechanical delay, AIC: arterially determined isovolumic contraction period.

the relative ventilation induced variation in the isovolumic contraction period (ΔAIC) is a more sensitive predictor of fluid-responsiveness than ΔPEP as it is not confounded by EMD and pulse wave travel time.

To test this hypothesis, we performed a graded hemorrhage protocol in anesthetized swine. ΔAIC and ΔPEP were compared with the relative ventilatory variation in both pulse pressure (ΔPP) and stroke volume (ΔSV), which are clinically used parameters for the prediction of fluid-responsiveness.

5.2 Materials and methods

5.2.1 Animals

Studies were performed in seven 3-4 month-old female Yorkshire X Landrace swine (32 ± 5 kg; mean \pm SD) in accordance with the Guide for the Care and Use of Laboratory animals (NIH Publication No. 85-23, revised 1996) and with approval of the Erasmus MC Animal Care Committee.

5.2.2 Surgical procedures

Swine were sedated with an intramuscular injection of xylazine (2.25 mg/kg), tiletamine (5 mg/kg) and zolazepam (5 mg/kg) [25], and anesthetized with sevoflurane (1.8-2.4% end tidal concentration [26]), in combination with buprenorphine (4 μ g/kg/h IV) [27]. This combination suppresses respiratory effort during positive pressure ventilation, a prerequisite for adequate measurement of variables such as ΔPP , ΔSV and ΔPEP [28]. Subsequently, swine were intubated and mechanically ventilated with a target tidal volume of ~ 10 ml/kg bodyweight (range 10.9 ± 1.6 ml/kg) and with F_iO_2 set to 0.30. The target tidal volume was maintained during the execution of this study protocol, and ventilation frequency was adjusted to keep blood gases within their physiological range (P_{CO_2} 4.0-6.0 kPa, $S_aO_2 > 92\%$).

Following ECG lead connection, a high fidelity double lumen pressure sensor catheter (Millar Instruments, Houston, Texas, USA) was inserted into the right carotid artery and advanced into the left ventricle (LV) with the second sensor residing in the aorta. This enabled simultaneous monitoring and recording of both LV and aortic pressure. Following sternotomy, an electromagnetic aortic flow probe (Skalar, Delft, The Netherlands) was placed around the ascending aorta just distal to the coronary arteries to monitor aortic blood volume flow. Subsequently, the thorax was closed by pulling the sternum together to prevent evaporation of fluids. Sternotomy resulted in an increase in lung compliance from 20 ± 5 ml/mbar to 26 ± 5 ml/mbar ($p < 0.001$), which was not affected by

subsequent approximation of the chest walls (25 ± 5 ml/mbar; $p=0.01$ vs. closed chest at baseline).

5.2.3 Signal processing

ECG and pressure transducer signals were amplified using a wide-band (1000Hz) amplifier system (Experimetria, Budapest, Hungary) and fed along with the aortic flow, airway pressure and airway flow signals into a data acquisition board (National Instruments, Austin, Texas, USA, sample frequency 2000Hz) and stored for offline processing. Matlab (Natick, Massachusetts, USA) was used for signal conversion to their proper units prior to storage as well as for automated post processing of the recorded signals using custom made applications.

5.2.4 Experimental protocol

After ~30 min of stabilization, baseline measurements of ECG, LV and aortic pressure, aortic flow and airway pressure and flow were recorded simultaneously during a 3 min period (BL). Thereafter, a 3-step graded hemorrhage protocol was executed, using a blood extraction rate of 25 ml/min. The first hemorrhage step (H1) consisted of withdrawal of 5 ml of blood per kilogram bodyweight, followed by 15 min of stabilization, and recording of hemodynamic variables. Subsequently, the second hemorrhage step (H2) was performed, consisting of another 5 ml/kg blood (cumulative 10 ml/kg) withdrawal. This was also followed by 15 min of stabilization and recording of hemodynamics. The third hemorrhage step (H3) consisted of withdrawal of 10 ml/kg blood (cumulative 20 ml/kg), again followed by 15 min of stabilization (figure 2 top left panel). Since swine have a blood volume of ~67ml/kg [29], withdrawal of a total amount of 20ml/kg was expected to result in severe hemorrhagic shock. All extracted blood was saved with ~40 U.I./ml heparin to enable transfusion of autologous blood at a later stage in the experimental protocol. No fluids were added for volume compensation at any point during the experimental protocol.

After completion of the 3-step hemorrhage protocol, a continuous intra-venous infusion of nor-epinephrine (NE) was started and titrated to restore mean arterial pressure levels to baseline values (figure 2 top left panel), followed by 15 min of stabilization. Then, infusion of NE was stopped and swine underwent a 10 min transfusion with autologous blood (T), followed once again by 15 min of stabilization.

At the end of each 15 min stabilization period, only after cardiac output and mean aortic pressure had reached stable levels (on average after 25 minutes), ECG, LV and aortic blood pressure, aortic blood flow and airway pressure and flow were recorded simultaneously for 3 minutes, prior to proceeding to the next protocol step.

5.2.5 Data analysis

Delays between pressure and ECG introduced by the equipment were assessed using a peak to peak delay method and compensated for during post processing prior to low pass filtering (80 Hz, zero phase shift) and extraction of hemodynamic features. Prior to analysis, episodes of cardiac arrhythmias were excluded.

Onset of the cardiac cycle was identified using the Q-top of the ECG and used as a reference for all extracted timing features. It was further used for the determination of heart rate (HR). The aortic flow signal was used to measure stroke volume and cardiac output. Systemic vascular resistance was calculated as the ratio of mean aortic blood pressure and cardiac output. LV pressure was used to determine LV end diastolic pressure, as an index of preload, as well as the rate of rise of LV pressure at 30 mmHg ($LVdP/dt_{P30}$), as an afterload-insensitive index of contractility [30]. Aortic pressure was used to determine peak systolic (SAP), mean (MAP) and minimum diastolic (DAP) arterial blood pressure values. Pulse pressure (PP) was calculated as the difference between SAP and DAP. PEP was determined as the interval between the Q-top of the ECG and the foot of the aortic pressure pulse (figure 1); the latter was determined by means of an intersecting tangent method [31]. AIC was determined as the interval between AIC_{start} , identified as a peak in the second derivative of the aortic pressure preceding the onset of systole [20], and the foot of the aortic pressure pulse also used for the determination of PEP. As aortic pressure was measured just distal (~1cm) to the aortic valve, the electromechanical delay EMD was determined as the interval between the Q-top of the ECG and AIC_{start} (figure 1).

The relative ventilatory variation in PP and SV (respectively ΔPP and ΔSV) were determined using the maximum and minimum value of the feature during respectively inspiration and expiration in the following equation: $\Delta = 100 * (MAX - MIN) / ((MAX + MIN) / 2)$ [10, 15, 16]. Ventilatory variation in PEP, AIC and EMD were determined by taking their maximum and minimum within the same ventilatory cycle in which the minimum and maximum PP, respectively, were detected [16, 17]. Then, the relative ventilatory variation in PEP, AIC and EMD

were calculated similarly to ΔPP and ΔSV , yielding ΔPEP , ΔAIC and ΔEMD , respectively.

5.2.6 Statistical Analysis

Statistical analysis of all hemodynamic data was performed by using Excel (Seattle, Washington, USA) and SigmaStat (San Jose, California, USA) software. All data are presented as mean \pm SD. A repeated measures ANOVA test followed by a post-hoc Student-Newman-Keuls test was used to analyze the extracted features. Normality of data was tested using a Kolmogorov Smirnov test. Pearson's correlation was used to test correlations between variables. P-values < 0.05 were considered statistically significant. To compare variability of ΔAIC and ΔPEP , the coefficient of variation was determined by calculating the mean of the SD-mean ratios for each animal during hemorrhage and resuscitation.

5.3 Results

5.3.1 Effect of graded hemorrhage and resuscitation on hemodynamic variables

Figure 2 shows the hemodynamic responses to graded hemorrhage. Stepwise hemorrhage up to 20 ml/kg decreased preload, as reflected in the progressive decrease in LV end-diastolic pressure, resulting in progressive decreases in SV and arterial blood pressure. The latter was accompanied by a, probably

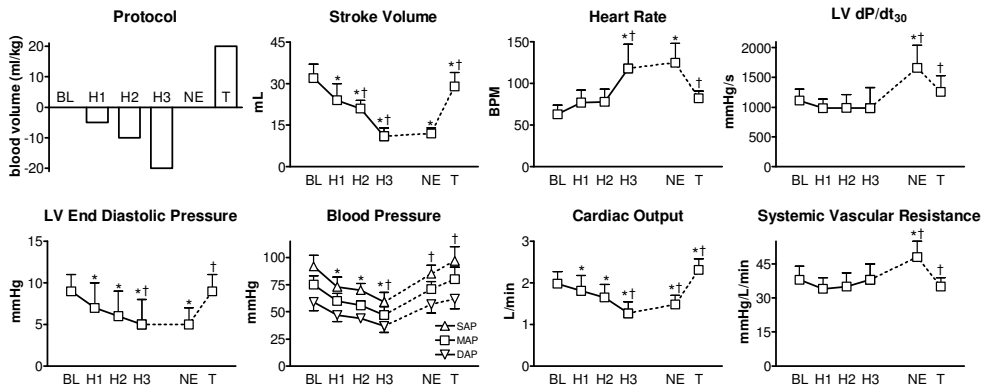


Figure 2. Hemodynamics during graded hemorrhagic shock and intervention. BL.; H1: hemorrhage - 5 ml/kg blood, H2: hemorrhage -10 ml/kg blood, H3: hemorrhage -20 ml/kg blood, NE: norepinephrine, T: transfusion of blood. * indicates a significant difference from baseline ($p < 0.05$). † indicates a significant difference from the previous protocol step ($p < 0.05$). In the Blood Pressure panel significance indicators refer to maximum systolic (SAP), mean (MAP) as well as minimum diastolic (DAP) arterial blood pressure, except for DAP at T.

baroreflex mediated, increase in heart rate. Nevertheless cardiac output decreased while $LVdP/dt_{P30}$ and systemic vascular resistance were not significantly affected by the graded hemorrhage.

Notwithstanding the severe shock produced by the stepwise hemorrhage, all animals survived the entire experimental protocol. Titration of nor-epinephrine infusion restored arterial blood pressure to baseline values by increasing systemic vascular resistance as cardiac output was not significantly affected (figure 2). The other hemodynamic variables were also minimally affected with the exception of an increase in $LVdP/dt_{P30}$ ($p < 0.05$). Washout of nor-epinephrine and transfusion of autologous blood resulted in restoration of all hemodynamic variables towards baseline values.

5.3.2 Effect graded hemorrhage and resuscitation on ΔAIC

ΔSV , ΔPP , ΔPEP and ΔAIC all increased with progressively graded hemorrhage (figure 3). Resuscitation with nor-epinephrine reduced ΔSV ($p < 0.001$), ΔAIC ($p < 0.001$) and ΔPEP ($p = 0.08$), but not ΔPP , compared to the last hemorrhage step although levels were not fully restored to baseline values. Autologous blood transfusion (20 ml/kg), during washout of nor-epinephrine, fully restored ΔSV , ΔPP , ΔPEP and $\Delta AICV$ to baseline values (all $p > 0.70$ vs. baseline, figure 3). During the entire hemorrhage and resuscitation protocol ΔPEP was significantly smaller than ΔSV , ΔPP and ΔAIC (all $p < 0.001$).

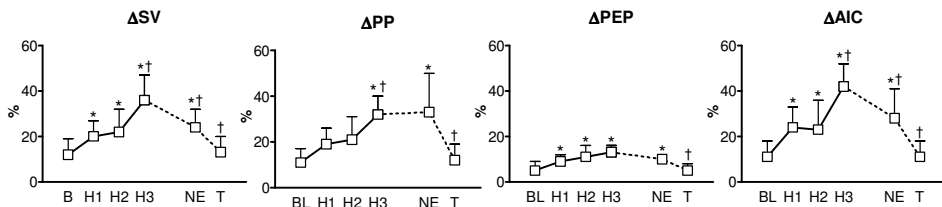


Figure 3. ΔSV , ΔPP , ΔPEP and ΔAIC during graded hemorrhagic shock and intervention. Relative ventilatory variation in stroke volume (ΔSV), pulse pressure (ΔPP), pre-ejection period (ΔPEP) and arterially determined isovolumic contraction period (ΔAIC). BL: baseline, H1: hemorrhage -5 ml/kg blood, H2: hemorrhage -10 ml/kg blood, H3: hemorrhage -20 ml/kg blood, NE: nor-epinephrine, T: transfusion of blood. * indicates a significant difference from baseline ($p < 0.05$). † indicates a significant difference from the previous protocol step ($p < 0.05$).

An excellent correlation was observed between ΔPP and ΔSV ($r = 0.97$, $p < 0.001$, figure 4). Very good correlations were also observed between ΔPEP and either ΔPP ($r = 0.90$, $p < 0.001$, figure 4) or ΔSV ($r = 0.88$, $p < 0.001$; not shown). A similar correlation was found between ΔAIC and both ΔPP ($r = 0.86$, $p < 0.001$, figure 4) and ΔSV ($r = 0.85$, $p < 0.001$; not shown), illustrating that both ΔPEP and ΔAIC can be used as substitutes for ΔPP and ΔSV . Despite the good correlation

between ΔAIC and ΔPEP ($r = 0.86$, $p < 0.001$, figure 4), the coefficient of variation of ΔPEP was substantially higher than that of ΔAIC (respectively 0.91 and 0.54, $p = 0.02$). The larger coefficient of variation of ΔPEP might in part be caused by ΔEMD , which failed to correlate significantly with ΔPEP ($r = 0.25$, $p = 0.12$). ΔEMD was also not correlated with either ΔPP ($r = 0.16$, $p = 0.33$) or ΔSV ($r = 0.19$, $p = 0.25$).

Stroke volume correlated well with ΔSV ($r = -0.62$, $p < 0.001$), ΔPP ($r = -0.66$, $p < 0.001$), ΔPEP ($r = -0.54$, $p < 0.001$) and ΔAIC ($r = -0.62$, $p < 0.001$). ΔEMD failed to correlate significantly with SV.

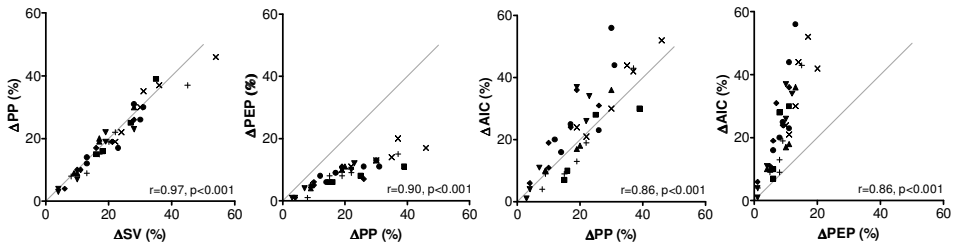


Figure 4. Correlation between ΔSV , ΔPP , ΔPEP and ΔAIC . Correlation of ventilation induced relative variation in pulse pressure (ΔPP) and stroke volume (ΔSV , left panel), ΔPP with relative ventilatory variation in pre-ejection period (ΔPEP , center left panel) and relative ventilatory variation in arterially determined isovolumic contraction period (ΔAIC , center right panel) and correlation between ΔPEP and ΔAIC (right panel). Each symbol represents data from a different animal. The line of identity is indicated in gray.

5.4 Discussion

The main purpose of the present study was to determine (i) whether a ventilation induced relative change in arterially determined isovolumic contraction period (ΔAIC) can be used to assess the level of hemorrhagic shock in a swine model and (ii) whether this ΔAIC is a more sensitive predictor of fluid-responsiveness than the ventilation-induced relative change in pre-ejection period (ΔPEP), which was suggested as a non-invasive substitute for ΔPP and ΔSV . The results show that ΔAIC increased with progressive hemorrhagic shock and decreased with subsequent resuscitation and restoration of circulating volume. Moreover, ΔAIC exhibited a good correlation with both ΔPP and ΔSV in swine during graded hemorrhage and following treatment. The correlation-coefficients between ΔAIC and ΔPP or ΔSV as compared to the correlation-coefficients between ΔPEP and ΔPP or ΔSV were virtually identical in our study. The correlation coefficients between stroke volume and ΔAIC , ΔPP , ΔSV or ΔPEP were also similar. Moreover, both ΔAIC and ΔPEP correlated well with changes in stroke volume. However, compared to ΔPEP , ΔAIC was more sensitive in reflecting blood loss during graded hemorrhage and the effect of

subsequent resuscitation as indicated by its lower coefficient of variation. The above results demonstrate that ΔAIC provides a good prediction of fluid responsiveness.

ΔSV is able to predict fluid responsiveness [32-34], but is difficult to obtain directly in a clinical setting [32, 33]. Consequently, either approximation of stroke volume using pulse contour analysis [32, 33, 35] or substitutes like ΔPP [10, 15] are typically used at the patient's bedside. In line with previous reports we also observed an excellent correlation between ΔSV and ΔPP [36, 37], which are both known to be good predictors of fluid responsiveness in mechanically ventilated patients [8, 12]. Furthermore, we found that ΔPEP correlated well with both ΔPP and ΔSV , which is in accordance with previous observations in coronary artery bypass graft surgery patients [16] and in a group of septic patients [17]. Interestingly, the ΔPEP over the ventilatory cycle at baseline (5%) was slightly larger in our study as compared to the cutoff value between responders and non-responders found by Feissel et al. (4%) [17], which could, at least in part, be explained by the ~20% higher tidal volume in combination with a relative low lung compliance in our animals as compared to septic shock patients [38, 39]. However, a more likely explanation is offered by the more distal measurement site used by Bendjelid et al. [16] and Feissel et al. [17]. Determination of the PEP in the radial artery will confound the average of the maximum and minimum PEP with an additional pulse wave travel time. For example, a pulse wave velocity of 10 m/s adds a pulse wave travel time of 60 ms to PEP for a radial artery measurement site at 60 cm from the heart. The ventilatory variation in pulse wave travel time compared to the total pulse wave travel time is likely small [40]; therefore the additional pulse wave travel time will reduce ΔPEP .

The PEP can be divided into the EMD and the isovolumic contraction period using the time at which the mitral valve closes. In our animal model we did not measure left atrial pressure, which is sometimes used in combination with LV pressure to determine mitral valve closure [41] and the resulting EMD. However, it has been shown that the pressure cross over from left atrial to LV pressure does not coincide with mitral valve closure [42, 43]. In previous work we showed that AIC_{start} , when measured close to the aortic valve, might be a better estimate for mitral valve closure occurrence and hence for EMD [44]. We found no correlation between ΔEMD and either ΔSV or ΔPP , suggesting that ΔEMD does not contribute to ΔPEP . Nevertheless, it could be argued that EMD is modulated by ventilation because AIC_{start} , which is used in the calculation of EMD, occurs later than the onset of LV pressure increase [44] and hence

depends on preload dependent contractile force [45] and the rate of rise of LV pressure [46] in the ventricle. Although we found a significant correlation between $LVdP/dt_{30}$ and AIC_{start} ($r = -0.36$, $p = 0.02$), the slope of the relation is very small which indicates that small changes in preload produced by ventilation are unlikely to cause noticeable ventilatory variations in EMD. This is confirmed by the lack of correlation between ΔEMD and ΔPEP . Moreover, the large coefficient of variation found for ΔPEP suggests that ΔEMD might even hamper ΔPEP .

The duration of isovolumic contraction changes with alterations in preload, as was shown some 40 years ago by Wallace et al. [47]. The present study shows that even small changes in preload induced by positive pressure ventilation can be detected in the duration of AIC. Moreover, we found a good correlation between ΔAIC and either ΔSV or ΔPP , which was as good as the correlations between ΔPEP and either ΔSV or ΔPP . However the coefficient of variation in ΔAIC is significantly lower than that of ΔPEP , which indicates that ΔAIC might be superior over ΔPEP . Indeed, ΔPEP is confounded by EMD (which changes minimally over the ventilatory cycle) and, if assessed peripherally, by pulse travel time, while ΔAIC is not. This allows comparison of ΔAIC independent of the measurement site, contrary to ΔPEP . Moreover, ΔAIC does not require an ECG, preventing errors due to possible measurement delays introduced by equipment characteristics and interfacing that could occur in the determination of PEP.

A high temporal resolution is required to detect reliably changes in both ΔPEP and ΔAIC . The radial pressure assessed by Bendjelid et al. had a temporal resolution of 10 ms [16], which is low compared to the absolute ventilatory variation in PEP that we found (~ 7 ms, data not shown), and likely explains their lower accuracy of the remotely assessed ΔPEP in the prediction of fluid responsiveness as compared to radial ΔPP [16]. Indeed, Feissel et al. [17], recording radial artery pressure with a temporal resolution of 2 ms, found the radial ΔPEP to be as accurate a predictor for fluid responsiveness as radial ΔPP . Using a temporal resolution of 0.5 ms, we found a good correlation between ΔPP and both ΔPEP and ΔAIC .

5.5 Conclusion

The present study shows that the relative ventilatory variation in the electro mechanical delay ΔEMD does not change under influence of progressive shock, whereas the relative ventilatory variation in the arterially determined isovolumic contraction period ΔAIC does. Nevertheless, ΔAIC and the relative ventilatory

variation in pre-ejection period Δ PEP correlated equally well with the gold standards for the prediction of fluid-responsiveness reported in mechanically ventilated patients, i.e. pulse pressure variation and stroke volume variation [12, 15, 32]. Additionally, both Δ AIC and Δ PEP correlated well with changes in stroke volume. Since Δ AIC has a lower coefficient of variation compared to that of Δ PEP and since Δ AIC is insensitive to pulse travel time, we conclude that Δ AIC is a better indicator of progressive hemorrhage and a more sensitive predictor of fluid responsiveness than Δ PEP. Moreover, the possibility to determine AIC non-invasively in a distal artery is likely to allow the integration of Δ AIC as an index of fluid status and predictor of fluid responsiveness in clinical practice.

5.6 References

1. Hardaway RM, 3rd: **Monitoring of the patient in a state of shock.** *Surg Gynecol Obstet* 1979, **148**(3):339-345.
2. Durairaj L, Schmidt GA: **Fluid therapy in resuscitated sepsis: less is more.** *Chest* 2008, **133**(1):252-263.
3. Magder S: **Fluid status and fluid responsiveness.** *Curr Opin Crit Care*, **16**(4):289-296.
4. Michard F, Reuter DA: **Assessing cardiac preload or fluid responsiveness? It depends on the question we want to answer.** *Intensive Care Med* 2003, **29**(8):1396; author reply 1397.
5. Pinsky MR: **Functional hemodynamic monitoring.** *Intensive Care Med* 2002, **28**(4):386-388.
6. Vincent JL, Sakr Y, Sprung CL, Ranieri VM, Reinhart K, Gerlach H, Moreno R, Carlet J, Le Gall JR, Payen D: **Sepsis in European intensive care units: results of the SOAP study.** *Crit Care Med* 2006, **34**(2):344-353.
7. Wiedemann HP, Wheeler AP, Bernard GR, Thompson BT, Hayden D, deBoisblanc B, Connors AF, Jr., Hite RD, Harabin AL: **Comparison of two fluid-management strategies in acute lung injury.** *N Engl J Med* 2006, **354**(24):2564-2575.
8. Benington S, Ferris P, Nirmalan M: **Emerging trends in minimally invasive haemodynamic monitoring and optimization of fluid therapy.** *Eur J Anaesthesiol* 2009, **26**(11):893-905.
9. Godje O, Peyerl M, Seebauer T, Lamm P, Mair H, Reichart B: **Central venous pressure, pulmonary capillary wedge pressure and intrathoracic blood volumes as preload indicators in cardiac surgery patients.** *Eur J Cardiothorac Surg* 1998, **13**(5):533-539; discussion 539-540.
10. Gunn SR, Pinsky MR: **Implications of arterial pressure variation in patients in the intensive care unit.** *Curr Opin Crit Care* 2001, **7**(3):212-217.

11. Michard F, Teboul JL: **Predicting fluid responsiveness in ICU patients: a critical analysis of the evidence.** *Chest* 2002, **121**(6):2000-2008.
12. Reuter DA, Felbinger TW, Schmidt C, Kilger E, Goedje O, Lamm P, Goetz AE: **Stroke volume variations for assessment of cardiac responsiveness to volume loading in mechanically ventilated patients after cardiac surgery.** *Intensive Care Med* 2002, **28**(4):392-398.
13. Wiesenack C, Fiegl C, Keyser A, Prasser C, Keyl C: **Assessment of fluid responsiveness in mechanically ventilated cardiac surgical patients.** *Eur J Anaesthesiol* 2005, **22**(9):658-665.
14. Marik PE, Cavallazzi R, Vasu T, Hirani A: **Dynamic changes in arterial waveform derived variables and fluid responsiveness in mechanically ventilated patients: a systematic review of the literature.** *Crit Care Med* 2009, **37**(9):2642-2647.
15. Michard F, Teboul JL: **Using heart-lung interactions to assess fluid responsiveness during mechanical ventilation.** *Crit Care* 2000, **4**(5):282-289.
16. Bendjelid K, Suter PM, Romand JA: **The respiratory change in pre-ejection period: a new method to predict fluid responsiveness.** *J Appl Physiol* 2004, **96**(1):337-342.
17. Feissel M, Badie J, Merlani PG, Faller JP, Bendjelid K: **Pre-ejection period variations predict the fluid responsiveness of septic ventilated patients.** *Crit Care Med* 2005, **33**(11):2534-2539.
18. Vistisen ST, Struijk JJ, Larsson A: **Automated pre-ejection period variation indexed to tidal volume predicts fluid responsiveness after cardiac surgery.** *Acta Anaesthesiol Scand* 2009, **53**(4):534-542.
19. Reesink KD, Hermeling E, Hoeberigs MC, Reneman RS, Hoeks AP: **Carotid artery pulse wave time characteristics to quantify ventriculoarterial responses to orthostatic challenge.** *J Appl Physiol* 2007, **102**(6):2128-2134.
20. van Houwelingen MJ, Barenbrug PJ, Hoeberigs MC, Reneman RS, Hoeks AP: **The onset of ventricular isovolumic contraction as reflected in the carotid artery distension waveform.** *Ultrasound Med Biol* 2007, **33**(3):371-378.
21. Weissler AM: **Current concepts in cardiology. Systolic-time intervals.** *N Engl J Med* 1977, **296**(6):321-324.
22. Cassidy SC, McGovern JJ, Chan DP, Allen HD: **Effects of commonly used adrenergic agonists on left ventricular function and systemic vascular resistance in young piglets.** *Am Heart J* 1997, **133**(2):174-183.
23. Imrich R, Eldadah BA, Benthoo O, Pechnik S, Sharabi Y, Holmes C, Grossman E, Goldstein DS: **Functional effects of cardiac sympathetic denervation in neurogenic orthostatic hypotension.** *Parkinsonism Relat Disord* 2009, **15**(2):122-127.
24. Kleber AG: **Crosstalk between theoretical and experimental studies for the understanding of cardiac electrical impulse propagation.** *J Electrocardiol* 2007, **40**(6 Suppl):S136-141.

25. Ko JC, Williams BL, Smith VL, McGrath CJ, Jacobson JD: **Comparison of Telazol, Telazol-ketamine, Telazol-xylazine, and Telazol-ketamine-xylazine as chemical restraint and anesthetic induction combination in swine.** *Lab Anim Sci* 1993, **43**(5):476-480.
26. Holmstrom A, Akeson J: **Cerebral blood flow at 0.5 and 1.0 minimal alveolar concentrations of desflurane or sevoflurane compared with isoflurane in normoventilated pigs.** *J Neurosurg Anesthesiol* 2003, **15**(2):90-97.
27. Rodriguez NA, Cooper DM, Risdahl JM: **Antinociceptive activity of and clinical experience with buprenorphine in swine.** *Contemp Top Lab Anim Sci* 2001, **40**(3):17-20.
28. Teboul JL, Monnet X: **Prediction of volume responsiveness in critically ill patients with spontaneous breathing activity.** *Curr Opin Crit Care* 2008, **14**(3):334-339.
29. Hannon JP, Bossone CA, Wade CE: **Normal physiological values for conscious pigs used in biomedical research.** *Lab Anim Sci* 1990, **40**(3):293-298.
30. van der Velden J, Merkus D, Klarenbeek BR, James AT, Boontje NM, Dekkers DH, Stienen GJ, Lamers JM, Duncker DJ: **Alterations in myofilament function contribute to left ventricular dysfunction in pigs early after myocardial infarction.** *Circ Res* 2004, **95**(11):e85-95.
31. Chiu YC, Arand PW, Shroff SG, Feldman T, Carroll JD: **Determination of pulse wave velocities with computerized algorithms.** *Am Heart J* 1991, **121**(5):1460-1470.
32. Biais M, Nouette-Gaulain K, Rouillet S, Quinart A, Revel P, Sztark F: **A comparison of stroke volume variation measured by Vigileo/FloTrac system and aortic Doppler echocardiography.** *Anesth Analg* 2009, **109**(2):466-469.
33. De Castro V, Goarin JP, Lhotel L, Mabrouk N, Perel A, Coriat P: **Comparison of stroke volume (SV) and stroke volume respiratory variation (SVV) measured by the axillary artery pulse-contour method and by aortic Doppler echocardiography in patients undergoing aortic surgery.** *Br J Anaesth* 2006, **97**(5):605-610.
34. Reuter DA, Kirchner A, Felbinger TW, Weis FC, Kilger E, Lamm P, Goetz AE: **Usefulness of left ventricular stroke volume variation to assess fluid responsiveness in patients with reduced cardiac function.** *Crit Care Med* 2003, **31**(5):1399-1404.
35. Lahner D, Kabon B, Marschalek C, Chiari A, Pestel G, Kaider A, Fleischmann E, Hetz H: **Evaluation of stroke volume variation obtained by arterial pulse contour analysis to predict fluid responsiveness intraoperatively.** *Br J Anaesth* 2009, **103**(3):346-351.
36. Berkenstadt H, Friedman Z, Preisman S, Keidan I, Livingstone D, Perel A: **Pulse pressure and stroke volume variations during severe haemorrhage in ventilated dogs.** *Br J Anaesth* 2005, **94**(6):721-726.
37. Reuter DA, Goresch T, Goepfert MS, Wildhirt SM, Kilger E, Goetz AE: **Effects of mid-line thoracotomy on the interaction between mechanical ventilation and cardiac filling during cardiac surgery.** *Br J Anaesth* 2004, **92**(6):808-813.

38. Krausz MM, Perel A, Eimerl D, Cotev S: **Cardiopulmonary effects of volume loading in patients in septic shock.** *Ann Surg* 1977, **185**(4):429-434.
39. Kuzkov VV, Kirov MY, Sovershaev MA, Kuklin VN, Suborov EV, Waerhaug K, Bjertnaes LJ: **Extravascular lung water determined with single transpulmonary thermodilution correlates with the severity of sepsis-induced acute lung injury.** *Crit Care Med* 2006, **34**(6):1647-1653.
40. Quinsac C, Heil M, Jackson A, Dark P: **Instantaneous versus average wave speed calculation in large mammals under acute hemorrhage.** *Conf Proc IEEE Eng Med Biol Soc* 2007, **2007**:971-972.
41. Lauboeck H: **The conditions of mitral valve closure.** *J Biomed Eng* 1980, **2**(2):93-96.
42. Goetz WA, Lansac E, Lim HS, Weber PA, Duran CM: **Left ventricular endocardial longitudinal and transverse changes during isovolumic contraction and relaxation: a challenge.** *Am J Physiol Heart Circ Physiol* 2005, **289**(1):H196-201.
43. Laniado S, Yellin E, Kotler M, Levy L, Stadler J, Terdiman R: **A study of the dynamic relations between the mitral valve echogram and phasic mitral flow.** *Circulation* 1975, **51**(1):104-113.
44. van Houwelingen MJ, Merkus D, te Lintel Hekkert M, van Dijk G, Hoeks APG, Duncker DJ: **Initiation of ventricular contraction as reflected in the arterial tree.** *Unpublished data.*
45. Starling E: **The Linacre Lecture on the Law of the Heart Given at Cambridge, 1915.** 1918.
46. Frank O: **Dynamik de Herzmuskels.** *Z Biol* 1895, **32**:370:447.
47. Wallace AG, Mitchell JH, Skinner NS, Sarnoff SJ: **Duration of the phases of left ventricular systole.** *Circ Res* 1963, **12**:611-619.

Chapter 6

General discussion and
conclusion

6.1 What's in a Wave?

In this thesis we presented and discussed a persistent pre-systolic pressure perturbation occurring in the aortic pressure waveform and carotid distension waveform (carotid diameter change caused by the arterial pressure waveform, chapter 2). We showed that this pre-systolic pressure perturbation originated from the cardiac contraction but not from the coronary arteries (chapter 3). Moreover, we observed that the aortic pressure perturbation was preceded by a left ventricular pressure perturbation. Detailed timing analysis of ventricular and aortic pressures, in combination with analysis of the left ventricular myocardial contraction, showed that the onset of the aortic pre-systolic pressure perturbation most likely relates to the mitral valve closure (chapter 4). Therefore the analysis of the arterial pre-systolic pressure perturbation suffices to determine the left ventricular isovolumic contraction period. The arterially determined duration of the isovolumic contraction period was successfully used in the detection of a developing hemorrhagic shock (chapter 5). Further research is warranted to test its validity as a substitute for left ventricular isovolumic contraction period when assessed in distal arteries, as well as its applicability in the field of circulatory shock.

In a paper on heart sounds by Reinhold et al. [1], the aortic pre-systolic pressure perturbation had also been briefly reported. Without further evidence, the authors suggested the downward motion of the ventricular base as the origin. Although several other studies as well as textbooks have shown the presence of a pre-systolic aortic pressure perturbation [2-4], its origin was never systematically investigated. Timing analysis of left ventricular and aortic pressure showed that the aortic pressure perturbation coincided with the onset of the left ventricular pressure rise, suggesting its clinical value in the determination of systolic timing intervals (chapter 2). In a follow up study on chapter 2, Reesink et al. [5] reported the successful noninvasive quantification of the ventriculoarterial responses to an orthostatic challenge using the carotid distension waveform assessed by ultrasound [5]. The latter study corroborates our suggestion that the pressure perturbation is useful in non-invasive assessment of cardiovascular performance.

To optimize the applicability of the arterial pre-systolic pressure perturbation in the assessment of cardiovascular performance, its origin needs to be known. Previously Reinhold et al. [1] suggested the downward motion of the ventricular base. Alternatively, in chapter 2 we proposed the compression of coronary vascular bed during cardiac contraction, causing a backflow of blood and a

small pressure wave to travel towards the aorta [6, 7]. The latter suggestion was tested in chapter 3 by occluding a combination of all three main coronary arteries. Occlusion and subsequent increased myocardial blood volume as a result of reactive hyperemia should have respectively decreased and increased the arterial pre-systolic pressure perturbation. However, the shape of the arterial pre-systolic pressure perturbation remained unaltered during either state, disproving compression of the coronary vascular bed as the origin of the pressure perturbation.

In chapter 2 we observed a persistent time delay between the onset of the pre-systolic pressure perturbation and the aortic systolic foot within normal healthy people and patients, indicating a cardiac origin. In chapter 4, we therefore used aortic wave intensity analysis to show the cardiac origin of the aortic pressure perturbation. The use of high fidelity pressure and flow sensors also enabled a more detailed analysis of timing and amplitude properties of the blood pressures, blood volume flow and myocardial segment length changes. This analysis showed that the onset of the aortic pressure perturbation in swine occurred significantly later than the onset of left ventricular pressure rise. The analysis further showed that the aortic pressure perturbation was preceded by a left ventricular pressure perturbation, which we propose to coincide with the mitral valve closure. The latter observation is supported by evidence that the mitral valve is not yet closed at the onset of left ventricular pressure rise but occurs after onset of left ventricular pressure rise [8, 9]. Moreover, the onset of changes in left ventricular radial strain shown by Ashikaga et al. [10] correspond with the onset of the left ventricular pressure perturbation during the pre-ejection period. It was further shown that at the same time the cardiac base decelerates as a consequence of mitral valve closure and twisting motion of the myocardium [10, 11]. Therefore, we concluded that the onset of the aortic pressure perturbation truly reflects the onset of the isovolumic contraction of the left ventricle (chapter 4).

In chapter 5 we pursued the applicability of the arterially determined isovolumic contraction period. Lengthening of the isovolumic contraction period has been shown to be indicative of a reduced ventricular function [12-14]. Similarly, the duration of the pre-ejection period, which can easily be obtained using the ECG and the (peripheral) arterial pressure waveform, has been used in the quantification of left ventricular performance [14-17]. The pre-ejection period encompasses the sum of the electro mechanical delay, the isovolumic contraction period and, depending on the arterial measurement site, pulse travel time. Preload, contractility and afterload mainly influence the isovolumic

contraction period and have a negligible influence on the electro mechanical delay of the ventricle [18]. Therefore, the isovolumic contraction period is usually considered the main contributor to a change in duration of the pre-ejection period as a result of a reduced ventricular function [5, 19].

Chan et al. [17] found that a head-up tilt induced decrease in preload results in an increase in pre-ejection period and proposed that this static variable could be used as a non-invasive indicator for blood loss in patients. However, hypovolemia does not only decrease preload, which increases the duration of the isovolumic contraction period and hence pre-ejection period. Excessive hypovolemia is accompanied by an increase in heart rate and a decrease in afterload, having a reducing effect on the isovolumic contraction period. Therefore, the behavior of the pre-ejection period in the face of hypovolemia is hard to predict.

Using ventilation induced variations in hemodynamic variables such as pulse pressure and stroke volume allows to assess the working point of the heart on its Franks-Starling curve and, hence, to predict whether a patient responds favorable to fluids [20, 21]. Additionally, using their relative rather than the absolute variation supports the determination of a subject-independent threshold value to discriminate between responders and non-responders. Consequently, the pulse pressure [20, 22] and stroke volume [21, 23] are used in a clinical setting as dynamic predictors of fluid responsiveness. As a less invasive predictor, Bendjelid et al. [24] proposed the relative ventilatory variation in pre-ejection period (ΔPEP) as a dynamic predictor of fluid responsiveness. Despite the spurious components contributing to the assessed pre-ejection period (electro mechanical delay and pulse travel time), it was shown that the ventilation induced relative variation in pre-ejection period (assessed in the radial artery, ΔPEP_{ra}) could be used as a non-invasive predictor of fluid responsiveness in both cardiac surgery and septic patients [24, 25].

The assessment of the isovolumic contraction period from the arterial pressure waveform (arterially determined isovolumic contraction period, AIC) allows for a more direct approach. During a graded hemorrhage protocol (chapter 5) and subsequent resuscitation both ΔPEP and the novel proposed ventilation induced relative variation in the isovolumic contraction period (ΔAIC) were determined from the aortic pressure waveform (referred to as ΔPEP_{Ao} and ΔAIC_{Ao} , respectively). Both parameters correlated well with markers shown to have a high predictive value for a patient's filling status and fluid responsiveness, i.e. pulse pressure variation and stroke volume variation

(chapter 5). Moreover, ΔAIC_{A_0} increased significantly more than ΔPEP_{A_0} in the face of a decreased circulating blood volume. Subsequent resuscitation decreased both variables towards baseline levels. In light of the lower coefficient of variation of ΔAIC_{A_0} compared to that of ΔPEP_{A_0} we concluded in chapter 5 that ΔAIC_{A_0} is a more sensitive indicator of a decrease in circulating volume and the effectiveness of subsequent resuscitation than ΔPEP_{A_0} .

6.2 Methodological considerations

The extraction of ventilation induced variations (in the order of a few milliseconds) requires a sensitive method to measure and analyze the arterial pressure waveform. In chapter 3 to 5 the blood pressure was recorded with an invasive high fidelity micro manometer tipped catheter, providing a high temporal and pressure amplitude resolution. Due to sterilization problems and high cost, these type of invasive blood pressure sensors are in a clinical setting frequently replaced by a fluid filled catheter with an external disposable pressure sensor. These type of sensors do, however, result in a reduced fidelity of the blood pressure recording as compared to micro manometer tipped catheters [26]. This possibly results in the degradation of the shape of the arterial pre-systolic pressure perturbation, hampering the extraction of the isovolumic contraction period. As an alternative, the applanation tonometer provides a method to record the blood pressure waveform noninvasively. This technique requires a stiff background to compress the artery under investigation [27] and a lean skin to avoid cushioning of the pulse pressure. It is therefore not suited for major arteries close to the heart. Additionally, an unsteady hand during manual applanation tonometry might introduce noise that could obscure the pre-systolic pressure perturbation [28]. Moreover, techniques that use peripheral recording sites frequently apply generalized transfer functions to reconstruct the central arterial blood pressure waveform [3, 29]. Consequently, using such transfer functions will suppress patient specific information in the pressure waveform [30] and likely distorts the patient specific shape of the arterial pre-systolic pressure perturbation.

Another matter of concern with respect to the detection of the pre-systolic pressure perturbation is its small magnitude compared to total pulse pressure. Moreover, it is likely that the pre-systolic pressure perturbation will be attenuated whilst traveling through the arterial tree, due to its higher frequency components [3]. However, we are primarily interested in the timing rather than the amplitude characteristics of the pressure perturbation, with the advantage that it allows the use of a substitute for the arterial pressure wave. As long as a monotone ascending relationship exists between the pressure wave and its

substitute, timing properties of the arterial pressure wave are preserved [31-33]. This prerequisite holds for the pressure-diameter relationship of the carotid artery, allowing the non-invasive extraction of timing properties of the carotid distension waveform. Indeed we demonstrated in chapter 2 that, despite its small magnitude, the pre-systolic perturbation could be identified in the carotid distension waveform assessed noninvasively with ultrasound techniques [5, 34]. Only techniques with a sufficiently high bandwidth, like ultrasound or high fidelity micro manometer tipped catheters, can estimate reliably the time interval between the onset of the pre-systolic pressure perturbation and the systolic foot (~45 ms, chapter 4). Moreover, a high temporal resolution will further facilitate the high precision discrimination of the onset of AIC, which changes cyclically with ventilation (~7 ms, chapter 5).

6.2.1 Variability of the arterially detected isovolumic contraction period

A high temporal resolution will allow the determination of the onset of the arterial pre-systolic pressure perturbation with high precision. In chapter 2 the intra-subject standard deviation found in the onset of the carotid distension perturbation (4.6 ms) was of the order of the temporal resolution of 5 ms. This indicates that the variability could be reduced by using more advanced signal processing and measurement techniques. Increasing the sample frequency increased phase precision, as suggested in chapter 2, The high fidelity pressure recording (transducer bandwidth 1kHz in combination with a sample frequency of 2kHz) used in chapter 4 showed a standard deviation of 2.9 ms which is well above the sample interval (0.5 ms). Therefore, the standard deviation of 2.9 ms (chapter 4) may be attributed to the biological variation in the onset of the arterial pre-systolic pressure perturbation, whereas part of the variation exceeding ~3 ms (chapter 2) may be caused by low frequency noise (e.g. unstable probe position) in combination with the lower sample frequency.

After removing high frequency noise Reesink et al. [5] applied a second order zero-phase-delay high-pass filter to the carotid distension data set as used in chapter 2 (subjects in the supine position) to obtain its second derivative up to the filter cut-off frequency (60 Hz). These filters were also used in chapter 2. A high cut-off frequency of the high-pass filter favors a higher temporal resolution but will make the detection process more susceptible to phase noise in the waveform, noise that may originate from an unstable breath hold or unstable probe position. Indeed, in chapter 5 it was shown that changes in intrapleural pressure affect the duration of the isovolumic contraction period determined from the aortic pressure waveform (AIC_{A_0}). Consequently, an unstable breath

hold would increase the standard deviation of AIC_{Ao} . The effects of an unstable breath hold can be attenuated by an additional second-order zero-phase-delay recursive high-pass filter. Reesink et al. [5] achieved with a high-pass filter with a cutoff frequency of 20 Hz applied to the second derivative of the distension waveform a lower standard deviation (4 ms) than we were able to in chapter 2 without this additional high pass filter (5 ms). Applying again a second order zero-phase-delay high-pass filter to the second derivative of the carotid distension wave suppressed almost all low-frequency components. It consequently decreased the standard deviation of the onset of the carotid distension perturbation from 4.6 ms to 3 ms ($p < 0.05$, F-test), similar to the standard deviation that we found in the aortic data set in chapter 4.

Remarkably, we found no ventilation induced variation in $AIC_{Ao-start}$ with respect to the Q-top of the ECG (chapter 5). To test the influence of ventilation on AIC_{start} in both the aorta and carotid artery ($AIC_{Ao-start}$ and $AIC_{ca-start}$, respectively), we used a data subset from chapter 3 ($n=6$), for which the standard deviation of the $AIC_{Ao-start}$ equaled 3.0 ms if ventilation phase was not considered. Using only the end expiration values of the $AIC_{Ao-start}$ reduced the standard deviation to 2.9 ms, indicating that in our protocol ventilation has only a minor effect on $AIC_{Ao-start}$. For the carotid artery blood pressure, which was recorded simultaneously with the aortic blood pressure, $AIC_{ca-start}$ standard deviation without and with compensation for ventilation was also similar to each other (3.4 ms and 3.3 ms, respectively), confirming the lack of influence of ventilation on $AIC_{Ao-start}$ as observed in chapter 5. Therefore, the difference between the standard deviation in $AIC_{start-ca}$ reported by Reesink et al. [5] and the value found in chapter 2 is likely to originate from the removal of the effect of an unstable probe position.

The higher intra-subject standard deviation of the isovolumic contraction period determined from the aortic blood waveform in the patient group after cardiac surgery (6.4 ms, $n=6$, chapter 2) may be explained by the ventilation these patients were on (chapter 5). However, it was found not to differ significantly (F-test) from the intra-subject standard deviation of the carotid determined isovolumic contraction period in normal volunteers (4.6 ms, $n=21$, chapter 2).

6.2.2 What's in a distal arterial wave?

The shape of the arterial pressure waveform changes while traveling through the arterial tree (see also chapter 1 and section 6.2). However, maintenance of the pulse shape contour is a prerequisite of proper timing analysis of the carotid

pressure waveform [5]. The pulse shape contour may be altered by changes in pulse wave velocity and reflections, as well as velocity dispersion. However, the distensibility coefficients of the aorta and carotid artery in humans are similar [35], implying an unaltered pulse wave velocity. Moreover, any impedance change at the aortic-carotid bifurcation [36] will likely change the amplitude of the transmitted arterial pulse wave but not the timing properties of the wave. However, a major confounder for the waveform shape will be wave velocity dispersion, i.e. the wave speed at higher (systolic) blood pressure will be higher than at lower (diastolic) blood pressure. The effect of velocity dispersion might be negligible for the timing characteristics of the late diastolic pressure perturbation because of the low variations in amplitude involved. Moreover, the length of the human aorto-carotid trajectory is limited to maximally 25 cm, restricting possible dispersion effects.

To determine the influence of a more distal measurement site on the timing and amplitude of the pre-systolic pressure perturbation, left ventricular, aortic and carotid pressure were recorded during the execution of the protocol described in chapter 5. A single cardiac cycle is presented in Figure 1 in which the middle and bottom panel show enlargements of the top panel.

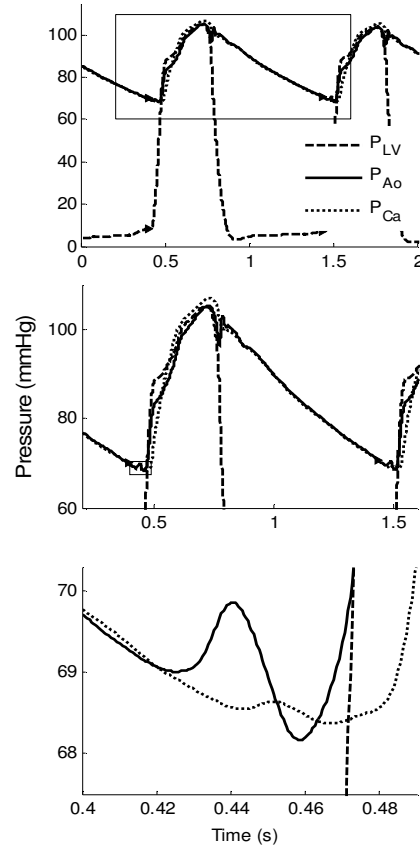


Figure 1. simultaneous recording of left ventricular (dashed line), aortic (solid line) and carotid (dotted line) pressure. The middle panel shows the enlargement of the rectangle in the top panel, the bottom panel shows the enlargement of the rectangle in the middle panel. The Q-top of the ECG occurs at $t = 0$ s. $AIC_{Ao-start}$ and $AIC_{Ca-start}$ indicate the onset of the pre-systolic pressure perturbation in respectively the aortic and carotid pressure waveform. AIC_{Ao} and AIC_{Ca} indicate the duration of the arterially determined isovolumic contraction period from the aortic and carotid pressure waveform respectively.

Although the pulse pressure in the carotid artery was slightly higher than the aortic pulse pressure (difference 2 ± 2 mmHg, $r=0.96$, $p=0.06$, over all animals

and protocol steps), the pre-systolic pressure perturbation had a lower amplitude in the carotid artery than in the aorta. The area under the pressure perturbation used in chapter 3 to quantify the magnitude of the pressure perturbation demonstrated a decrease in the pressure perturbation area of 12 ± 3 mmHg.ms in the aortic pressure wave to 5 ± 2 mmHg.ms in the carotid pressure wave ($p=0.003$). This attenuation is most likely caused by the impedance transition from the aortic to the carotid measurement site, that attenuates higher frequency components more than the low frequency components of the arterial pressure waveform [3].

Due to the limited pulse wave travel time, the onset of the carotid pre-systolic pressure perturbation occurs 14.9 ± 1.0 ms later than the onset of the aortic pre-systolic pressure perturbation ($r=0.99$, $p<0.001$, over all animals and protocol steps). Similarly, the onset of the arterial systolic foot arrived 14.0 ± 1.6 ms later in the carotid artery as compared to the aorta ($r=0.97$, $p<0.001$, over all animals and protocol steps). As the pulse wave travel time of AIC_{start} and the onset of the arterial systolic foot are similar, the difference between the duration of the isovolumic contraction period determined using either the aortic (AIC_{Ao}) or carotid (AIC_{ca}) pressure waveform was small and not significant (-0.8 ± 1.6 ms, $p=0.27$, over all animals and protocol steps). AIC_{Ao} correlated well with AIC_{ca} ($r=0.95$, $p<0.001$). Given the short distance and the low number of branching points between the aorta and carotid artery, the observations described above cannot readily be translated to more peripherally located measurement sites.

Pre-systolic pressure perturbation in more distal arteries

As shown above, the pre-systolic arterial pressure perturbation is modulated by (changes in) vascular impedance as it travels down the arterial tree. Therefore, it cannot be excluded that in more distal arteries, like the radial or digital artery, the pressure perturbation is attenuated to such extent that it can no longer be discerned. These more distal arteries are of specific interest, as they allow for a less invasive or non-invasive assessment of the arterial pressure wave. Interestingly, finger arterial pressure wave recordings still contain a pre-systolic pressure perturbation (Figure 2) which is related to the aortic pre-systolic pressure perturbation described in this thesis. Because of the practical implications, this warrants further research.

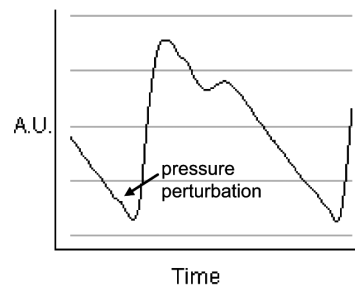


Figure 2. finger arterial tonometry pressure wave

6.3 Carotid pre-systolic pressure perturbation in hemorrhagic shock

The applicability of the pre-systolic pressure perturbation assessed in a more distal artery could be evaluated with the carotid arterial pressure recorded during the execution of the hemorrhagic shock and resuscitation protocol described in chapter 5. The ventilation induced variation in isovolumic contraction period determined from the carotid artery pressure waveform (ΔAIC_{ca}) was subsequently compared to its aortic determined equivalent and to the conventional measures, i.e. ventilation induced relative variation in pulse pressure (ΔPP) and stroke volume (ΔSV). In hemorrhagic shock, these conventional measures have a high predictive value for whether a patient will respond to intravenously administered fluids [17-20]. In chapter 5 we found a good correlation between the ventilation induced relative variation in isovolumic contraction period determined from the aortic pressure waveform (ΔAIC_{Ao}) and both the aortic ΔPP and ΔSV . The middle panel in Figure 3 shows the change in ΔAIC_{ca} under influence of blood withdrawal and intervention. For reference ΔAIC_{Ao} was added to the figure. No significant difference (Student t-test, $n=7$) was found between ΔAIC_{ca} and ΔAIC_{Ao} ($p=0.46$). Moreover, ΔAIC_{ca} correlated well with ΔAIC_{Ao} ($r=0.94$, $p=0.006$), ΔPP ($r=0.82$, $p<0.001$) and ΔSV ($r=0.79$, $p<0.001$).

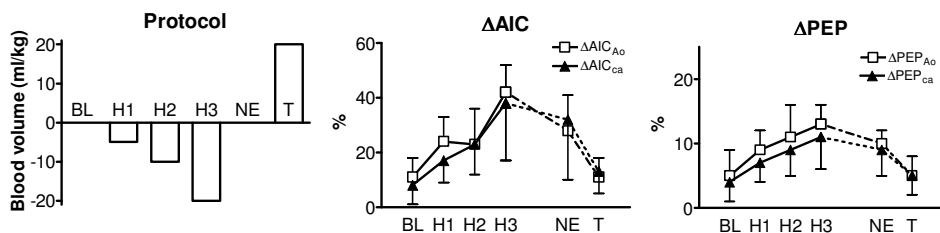


Figure 3. effect of hemorrhage and intervention (left panel) on ΔAIC_{ca} compared to ΔAIC_{Ao} (middle panel) and ΔPEP_{ca} compared to ΔPEP_{Ao} (right panel).

The right panel in Figure 3 shows the change in ventilation induced relative variation in pre-ejection period determined from the carotid pressure waveform (ΔPEP_{ca}) under influence of blood withdrawal and intervention. Again for reference, ventilation induced relative variation in pre-ejection period determined from the aortic pressure waveform (ΔPEP_{Ao}) was added to the figure. ΔPEP_{ca} was significantly lower than ΔPEP_{Ao} ($p=0.01$, Student t-test, $n=7$). Nevertheless, ΔPEP_{ca} correlated well with ΔPEP_{Ao} ($r=0.98$, $p<0.001$), ΔPP ($r=0.86$, $p<0.001$) and ΔSV ($r=0.85$, $p<0.001$).

The significant decrease in $\Delta\text{PEP}_{\text{ca}}$ due to its more distal measurement site confirms the dependence of ΔPEP on pulse travel time (as suggested in chapter 5) and hence its dependence on the length of the trajectory involved. Consequently, the determination of one single ΔPEP threshold for discrimination between responders and non-responders to fluid administration [25] is impossible, as pulse wave velocity is related to many factors like e.g. age [37, 38], gender [38], obesity [39], diabetes [40, 41] and hypertension [42, 43]. The large variation in pulse wave velocity between subjects causes a large variation in ΔPEP between subjects. Even in subjects with a similar pulse wave velocity, the distance from the heart to the measurement site should be the same within and across subjects to allow a fixed discrimination threshold to discern between responders and non-responders. The effects of a change in pulse wave velocity and distance from the heart to the measurement site on PEP and ΔPEP are summarized in Table 1.

	PEP	ΔPEP	AIC	ΔAIC
Average pulse wave velocity \uparrow	\downarrow	\uparrow	-	-
Average pulse wave velocity \downarrow	\uparrow	\downarrow	-	-
Distance heart-measurement site \uparrow	\uparrow	\uparrow	-	-
Distance heart-measurement site \downarrow	\downarrow	\downarrow	-	-

Table 1 the influence of a change in pulse wave velocity or distance from the heart to the measurement site on pre-ejection period (PEP), ventilation induced relative variation in PEP (ΔPEP), arterially detected isovolumic contraction period (AIC) and ventilation induced relative variation in AIC (ΔAIC). An increase, decrease and no change are respectively indicated as \uparrow , \downarrow and -.

It could be argued that sympathetic activity during hemorrhage may increase arterial stiffness, thereby shortening pulse travel time. A decreased pulse travel time would decrease the average of PEP over a ventilation cycle and hence increase the relative variation ΔPEP . However, there is a lack of change in delay between the aortic and carotid onset of the pre-systolic pressure perturbation with decreasing circulating blood volume ($p=0.65$). This indicates that the pulse wave velocity over the ascending aorta-carotid artery trajectory in our animals remains constant under influence of hemorrhage. Indeed, Quinsac et al. [44] showed that neither graded hemorrhage nor subsequent auto donation of blood changes average pulse wave velocity, despite an estimated blood loss of 27%. Moreover, the ventilation induced relative variation in the onset of the carotid pre-systolic pressure perturbation $\text{AIC}_{\text{ca-start}}$, which consists of the left ventricular electromechanical delay and pulse travel time, did not correlate with the ventilation induced relative variation in pulse pressure (ΔPP) determined from the aortic pressure ($r=0.18$, $p=0.27$). Therefore, ventilation

induced changes in pulse wave velocity do not measurably augment ΔPEP under influence of hemorrhage. Table 1 summarizes the influence of a change in pulse wave velocity or distance from the heart to the measurement site on average AIC and ΔAIC .

6.4 Future Perspectives

Although the arterial pre-systolic pressure perturbation was discovered as early as 1957 [1], to our knowledge it was not further considered in the following five decades until the publication of chapter 2. Since then only two papers have been published on the perturbation, one concerning the (re)discovery (chapter 2 of this thesis) and one concerning its application in the quantification of the ventriculoarterial interaction [5]. In chapter 3 and 4 the origin of the arterial pre-systolic pressure perturbation was narrowed down. However, the contribution of the deceleration of the downwards movement of the cardiac base and the deceleration of intra-cavity blood flow against the aortic valve need to be investigated for a better understanding of the generation of the pre-systolic arterial pressure perturbation and hence future applications using this perturbation. For this purpose, some suggestions are forwarded in section 6.4.1. Although chapter 5 and the present chapter show a proof of concept of the applicability of ΔAIC in the detection of shock in a controlled model of hemorrhagic shock in swine, it requires substantial research prior to using it as a guide for fluid administration (section 6.4.2).

6.4.1 Origin pressure perturbation

In chapter 4 we suggested that the onset of the left ventricular pressure perturbation coincided with mitral valve closure. The onset of the left ventricular pressure perturbation was closely followed in time by the aortic pressure perturbation. The observed small delay between both pressure perturbations (3.8 ± 1.8 ms, $p < 0.001$) was explained by the pulse wave velocity in combination with the distance between the 2 pressure sensors, i.e. by the pulse travel time. Therefore, the aortic pre-systolic pressure perturbation in conjunction with the onset of the systolic aortic pressure increase could be used to determine the isovolumic contraction period. Proving the origin of the perturbation requires methods that change the hypothesized interaction between the origin on the left ventricular and aortic pressure. Such methods will be discussed below.

Prevention of outward movement aortic valve

In chapter 4 we hypothesized that the outward movement of the aortic valve leaflets contributes to the aortic pressure perturbation. This can be tested by

replacing the aortic valve with a heart valve prosthesis based on rigid leaflets (e.g. with tilting disks). In this type of heart valve prosthesis outwards movement of the valve does not occur. Provided that the aortic pressure perturbation indeed originates from the outwards movement of the aortic valve, the aortic pressure perturbation should not occur if such a heart valve prosthesis is in place. In chapter 2, flexible bio-prosthetic heart valves were used, and therefore did not exclude outward movement [45].

Prevention of deceleration of downwards movement cardiac base

The sudden deceleration of the initial downwards movement of the cardiac base during early systole was suggested as a possible source for the left ventricular and aortic pressure perturbation. This sudden deceleration is explained by the closure of the mitral valve [11], effectively leaving no room for the intra-ventricular volume to go to, hence, halting the downwards movement of the base. If downwards base motion and mitral valve closure are related, then an artificially created acute mitral valve regurgitation should reduce the deceleration of the base and hence the amplitude of the left ventricular early systolic pressure perturbation. Acute mitral valve regurgitation should also decrease the deceleration of blood against the aortic valve [46]. Consequently, the aortic pressure perturbation would be attenuated provided that the blood flow deceleration contributes to the aortic pre-systolic pressure perturbation. Acute and reversible mitral valve regurgitation could be instituted by shifting an open cage catheter in and out of the mitral valve annulus.

Alteration of blood flow direction in the ventricle

Ballester-Rodes et al. report a base to apex contraction sequence based on the myocardial band concept of Torrent-Guasp [47, 48]. This concept presents the heart as a single band of muscle tissue that is folded in a helical fashion explaining the twisting motion of the heart. They showed that, although electrical activation is initiated in the apex of the heart, ventricular mechanical contraction of the heart is initiated in the endocardial layers at the basal part of the ventricles [47]. It subsequently moves via the endocardial layer down to the apex, after which the epicardial layer starts to contract from the apex towards the base. As the left ventricular early systolic and aortic pre-systolic pressure perturbation occur during the initial phase of ventricular contraction, the cardiac deformation due to endocardial contraction would be responsible for the redirection of blood flow towards the aortic and mitral valve. Therefore, if the aortic pressure perturbation indeed originates from the deceleration of blood flow against the aortic valve, changing the contraction sequence should alter the direction of blood flow, decreasing the magnitude of the aortic pressure

perturbation. A reversed contraction sequence may be effectuated by cardiac pacing [49, 50].

6.4.2 Application of the arterial detected isovolumic contraction period in the field of circulatory shock

In this thesis we showed that the ventilation induced relative variation in the arterially determined isovolumic contraction period (ΔAIC) increased progressively with progressing severity of hemorrhagic shock. Moreover, we demonstrated a good correlation with the ventilation induced relative variation in pulse pressure (ΔPP) and stroke volume (ΔSV), which are clinically used predictors of fluid responsiveness in hypovolumic and septic shock patients [22]. Nevertheless, this is only the first step towards clinical use of ΔAIC in the field of shock. The usability of ΔAIC in the prediction of fluid responsiveness in septic shock patients still needs to be tested, and a threshold value to discriminate responders and non-responders to fluid administration should be determined. Moreover, it has been shown that several factors are related to the amplitude of ΔPP and ΔSV , like ventilation settings [51, 52] or the use of vasoactive agents [53], which are likely to affect ΔAIC too.

Hadian et al. [53] showed that the use of inotropic support or vasoconstrictors did not alter ΔPP , which is consistent with our findings in chapter 5. In contrast to ΔPP , ΔSV as well as ΔAIC did decrease in response to nor-epinephrine (chapter 5). Hadian et al. [53] additionally showed that nitroprusside increased ΔPP , which was attributed to an increase in intravenous compartment volume, resulting in a relative hypovolumic state. Next to the direct effect of inotropic and vasoactive agents on ΔAIC , changes in arterial compliance and resistance might influence the shape of the aortic pre-systolic pressure perturbation and hence hamper the detection of its onset either in the aorta or in more peripheral arteries. Consequently, it is essential to determine the exact effect of inotropic and vasoactive agents on AIC and ΔAIC .

Changes in ΔPP and ΔSV originate from the effect of changes in intrapleural pressure on cardiac pre-load. Therefore, the magnitude of ΔPP and ΔSV change in response to changes in intrapleural pressure following changes in ventilation settings [51, 52]. Additionally, it has been shown that when a patient shows respiratory effort, the predictive value to fluid responsiveness of both ΔPP and ΔSV decreases [54]. Therefore, a prerequisite of using dynamic markers of fluid responsiveness (like ΔPP , ΔSV) is that the patient is on stable mechanical ventilation with a suppressed respiratory drive. Similarly, ΔAIC is likely to be influenced by intrapleural pressure swings due to changes in

ventilation settings or patient respiratory effort. The interaction between the characteristics of intrapleural pressures and of these dynamic markers needs further consideration.

Using non-invasive methods to acquire specific amplitude information of the arterial pressure wave requires a known and fixed relationship between the local pressure amplitude and the measured pulse contour shape. Timing analysis of the arterial pressure wave only requires a monotone ascending relationship between the arterial pressure wave and the acquired signal. Timing analysis data, acquired from the non-invasively derived arterial pulse contour, are therefore directly related to the timing properties of the arterial pressure wave, whereas amplitude derived data might not. Invasive measurement of arterial pressure is not readily available in the early stages of a patient's care path (e.g. in the ambulance), whereas non-invasive methods to acquire the arterial pulse contour are. Timing analysis of these signals could therefore provide valuable information earlier and in addition to standard amplitude analysis.

The advantage of ΔAIC over the use of ΔPP and ΔSV is, as explained above, its potential for non-invasive determination. In a pre-hospital setting (e.g. at the scene of an accident), the invasive measured arterial blood pressure waveform is not available to monitor ΔPP and ΔSV . In such situations, ΔAIC determined with non-invasive techniques can be used to detect the onset and progression of shock and guide resuscitation. Early detection of shock allows for an early goal directed therapy, which has shown to reduce mortality of patients with septic shock [55, 56] thereby reducing length and cost of hospitalization [57].

6.5 References

1. Reinhold J, Rudhe U: **Relation of the first and second heart sounds to events in the cardiac cycle.** *Br Heart J* 1957, **19**(4):473-485.
2. Fung YC: **Biomechanics Circulation**, 2 edn: Springer; 1996.
3. Nichols W, O'Rourke M: **McDonald's Blood Flow in Arteries**, 3 edn: Edward Arnold; 1990.
4. Sokolow M, McIlroy M: **Clinical Cardiology**, 2 edn. Los Altos: Lange Medical Publications; 1979.
5. Reesink KD, Hermeling E, Hoeberigs MC, Reneman RS, Hoeks AP: **Carotid artery pulse wave time characteristics to quantify ventriculoarterial responses to orthostatic challenge.** *J Appl Physiol* 2007, **102**(6):2128-2134.
6. Davies JE, Whinnett ZI, Francis DP, Manisty CH, Aguado-Sierra J, Willson K, Foale RA, Malik IS, Hughes AD, Parker KH *et al*: **Evidence of a dominant backward-propagating "suction" wave responsible for diastolic coronary filling in humans, attenuated in left ventricular hypertrophy.** *Circulation* 2006, **113**(14):1768-1778.

7. Spaan J: **Coronary blood flow. Mechanics, distribution and control.** Dordrecht: Kluwer Academic Publishers; 1991.
8. Goetz WA, Lansac E, Lim HS, Weber PA, Duran CM: **Left ventricular endocardial longitudinal and transverse changes during isovolumic contraction and relaxation: a challenge.** *Am J Physiol Heart Circ Physiol* 2005, **289**(1):H196-201.
9. Laniado S, Yellin E, Kotler M, Levy L, Stadler J, Terdiman R: **A study of the dynamic relations between the mitral valve echogram and phasic mitral flow.** *Circulation* 1975, **51**(1):104-113.
10. Ashikaga H, van der Spoel TI, Coppola BA, Omens JH: **Transmural myocardial mechanics during isovolumic contraction.** *JACC Cardiovasc Imaging* 2009, **2**(2):202-211.
11. Remme EW, Lyseggen E, Helle-Valle T, Opdahl A, Pettersen E, Vartdal T, Ragnarsson A, Ljosland M, Ihlen H, Edvardsen T *et al*: **Mechanisms of preejection and postejecion velocity spikes in left ventricular myocardium: interaction between wall deformation and valve events.** *Circulation* 2008, **118**(4):373-380.
12. Bruch C, Schmermund A, Marin D, Katz M, Bartel T, Schaar J, Erbel R: **Tei-index in patients with mild-to-moderate congestive heart failure.** *Eur Heart J* 2000, **21**(22):1888-1895.
13. Tei C, Ling LH, Hodge DO, Bailey KR, Oh JK, Rodeheffer RJ, Tajik AJ, Seward JB: **New index of combined systolic and diastolic myocardial performance: a simple and reproducible measure of cardiac function--a study in normals and dilated cardiomyopathy.** *J Cardiol* 1995, **26**(6):357-366.
14. Weissler AM, Harris WS, Schoenfeld CD: **Systolic time intervals in heart failure in man.** *Circulation* 1968, **37**(2):149-159.
15. Vijayalakshmi P, Mohan M, Babu PB: **Effect of 60 degrees head-up tilt on systolic time intervals in hypertensive patients.** *Indian J Physiol Pharmacol* 2002, **46**(1):45-50.
16. Hasegawa M, Rodbard D, Kinoshita Y: **Timing of the carotid arterial sounds in normal adult men: measurement of left ventricular ejection, pre-ejection period and pulse transmission time.** *Cardiology* 1991, **78**(2):138-149.
17. Chan GS, Middleton PM, Celler BG, Wang L, Lovell NH: **Change in pulse transit time and pre-ejection period during head-up tilt-induced progressive central hypovolaemia.** *J Clin Monit Comput* 2007, **21**(5):283-293.
18. Martin CE, Shaver JA, Thompson ME, Reddy PS, Leonard JJ: **Direct correlation of external systolic time intervals with internal indices of left ventricular function in man.** *Circulation* 1971, **44**(3):419-431.
19. Gillebert TC, Van de Veire N, De Buyzere ML, De Sutter J: **Time intervals and global cardiac function. Use and limitations.** *Eur Heart J* 2004, **25**(24):2185-2186.
20. Michard F, Teboul JL: **Using heart-lung interactions to assess fluid responsiveness during mechanical ventilation.** *Crit Care* 2000, **4**(5):282-289.
21. Reuter DA, Felbinger TW, Schmidt C, Kilger E, Goedje O, Lamm P, Goetz AE: **Stroke volume variations for assessment of cardiac responsiveness to volume loading in mechanically ventilated patients after cardiac surgery.** *Intensive Care Med* 2002, **28**(4):392-398.
22. Marik PE, Cavallazzi R, Vasu T, Hirani A: **Dynamic changes in arterial waveform derived variables and fluid responsiveness in mechanically ventilated patients: a systematic review of the literature.** *Crit Care Med* 2009, **37**(9):2642-2647.

23. Wiesenack C, Fiegl C, Keyser A, Prasser C, Keyl C: **Assessment of fluid responsiveness in mechanically ventilated cardiac surgical patients.** *Eur J Anaesthesiol* 2005, **22**(9):658-665.
24. Bendjelid K, Suter PM, Romand JA: **The respiratory change in preejection period: a new method to predict fluid responsiveness.** *J Appl Physiol* 2004, **96**(1):337-342.
25. Feissel M, Badie J, Merlani PG, Faller JP, Bendjelid K: **Pre-ejection period variations predict the fluid responsiveness of septic ventilated patients.** *Crit Care Med* 2005, **33**(11):2534-2539.
26. Rothe CF, Kim KC: **Measuring systolic arterial blood pressure. Possible errors from extension tubes or disposable transducer domes.** *Crit Care Med* 1980, **8**(11):683-689.
27. Kelly R, Hayward C, Avolio A, O'Rourke M: **Noninvasive determination of age-related changes in the human arterial pulse.** *Circulation* 1989, **80**(6):1652-1659.
28. Pannier BM, Avolio AP, Hoeks A, Mancia G, Takazawa K: **Methods and devices for measuring arterial compliance in humans.** *Am J Hypertens* 2002, **15**(8):743-753.
29. Pauca AL, O'Rourke MF, Kon ND: **Prospective evaluation of a method for estimating ascending aortic pressure from the radial artery pressure waveform.** *Hypertension* 2001, **38**(4):932-937.
30. Segers P, Carlier S, Pasquet A, Rabben SI, Hellevik LR, Remme E, De Backer T, De Sutter J, Thomas JD, Verdonck P: **Individualizing the aorto-radial pressure transfer function: feasibility of a model-based approach.** *Am J Physiol Heart Circ Physiol* 2000, **279**(2):H542-549.
31. Meinders JM, Hoeks AP: **Simultaneous assessment of diameter and pressure waveforms in the carotid artery.** *Ultrasound Med Biol* 2004, **30**(2):147-154.
32. Powalowski T, Pensko B: **A noninvasive ultrasonic method for the elasticity evaluation of the carotid arteries and its application in the diagnosis of the cerebro-vascular system.** *Arch Acoust* 1988, **13**:109-126.
33. Van Bortel LM, Balkestein EJ, van der Heijden-Spek JJ, Vanmolkot FH, Staessen JA, Kragten JA, Vredeveld JW, Safar ME, Struijker Boudier HA, Hoeks AP: **Non-invasive assessment of local arterial pulse pressure: comparison of applanation tonometry and echo-tracking.** *J Hypertens* 2001, **19**(6):1037-1044.
34. van Houwelingen MJ, Barenbrug PJ, Hoeberigs MC, Reneman RS, Hoeks AP: **The onset of ventricular isovolumic contraction as reflected in the carotid artery distension waveform.** *Ultrasound Med Biol* 2007, **33**(3):371-378.
35. Studinger P, Lenard Z, Reneman R, Kollai M: **Measurement of aortic arch distension wave with the echo-track technique.** *Ultrasound Med Biol* 2000, **26**(8):1285-1291.
36. Mitchell GF, Lacourciere Y, Ouellet JP, Izzo JL, Jr., Neutel J, Kerwin LJ, Block AJ, Pfeffer MA: **Determinants of elevated pulse pressure in middle-aged and older subjects with uncomplicated systolic hypertension: the role of proximal aortic diameter and the aortic pressure-flow relationship.** *Circulation* 2003, **108**(13):1592-1598.
37. Lee HY, Oh BH: **Aging and arterial stiffness.** *Circ J*, **74**(11):2257-2262.
38. Tomiyama H, Yamashina A, Arai T, Hirose K, Koji Y, Chikamori T, Hori S, Yamamoto Y, Doba N, Hinohara S: **Influences of age and gender on results of noninvasive brachial-ankle pulse wave velocity measurement--a survey of 12517 subjects.** *Atherosclerosis* 2003, **166**(2):303-309.

39. Urbina EM, Kimball TR, Khoury PR, Daniels SR, Dolan LM: **Increased arterial stiffness is found in adolescents with obesity or obesity-related type 2 diabetes mellitus.** *J Hypertens*, **28**(8):1692-1698.
40. Airaksinen KE, Salmela PI, Linnaluoto MK, Ikaheimo MJ, Ahola K, Ryhanen LJ: **Diminished arterial elasticity in diabetes: association with fluorescent advanced glycosylation end products in collagen.** *Cardiovasc Res* 1993, **27**(6):942-945.
41. Stehouwer CD, Henry RM, Ferreira I: **Arterial stiffness in diabetes and the metabolic syndrome: a pathway to cardiovascular disease.** *Diabetologia* 2008, **51**(4):527-539.
42. Blacher J, Safar ME: **Large-artery stiffness, hypertension and cardiovascular risk in older patients.** *Nat Clin Pract Cardiovasc Med* 2005, **2**(9):450-455.
43. Greenwald SE: **Ageing of the conduit arteries.** *J Pathol* 2007, **211**(2):157-172.
44. Quinsac C, Heil M, Jackson A, Dark P: **Instantaneous versus average wave speed calculation in large mammals under acute hemorrhage.** *Conf Proc IEEE Eng Med Biol Soc* 2007, **2007**:971-972.
45. Iyengar AKS, Sugimoto H, Smith DB, Sacks MS: **Dynamic in vitro quantification of bioprosthetic heart valve leaflet motion using structured light projection.** *Ann Biomed Eng* 2001, **29**(11):963-973.
46. Sengupta PP: **Exploring left ventricular isovolumic shortening and stretch mechanics: "The heart has its reasons..."** *JACC Cardiovasc Imaging* 2009, **2**(2):212-215.
47. Ballester-Rodes M, Flotats A, Torrent-Guasp F, Carrio-Gasset I, Ballester-Alomar M, Carreras F, Ferreira A, Narula J: **The sequence of regional ventricular motion.** *Eur J Cardiothorac Surg* 2006, **29** Suppl 1:S139-144.
48. Kocica MJ, Corno AF, Lackovic V, Kanjuh VI: **The helical ventricular myocardial band of Torrent-Guasp.** *Semin Thorac Cardiovasc Surg Pediatr Card Surg Annu* 2007:52-60.
49. Miyazawa K, Arai T, Shirato K, Haneda T, Ikeda S: **Regional contraction patterns of the left ventricle during ventricular pacing.** *Tohoku J Exp Med* 1977, **122**(2):167-174.
50. Ahlberg SE, Grenz NA, Ewert DL, Iuzzo PA, Mulligan LJ: **Effect of pacing site on systolic mechanical restitution curves in the in vivo canine model.** *Cardiovasc Eng* 2007, **7**(3):89-96.
51. Oliveira RH, Azevedo LC, Park M, Schettino GP: **Influence of ventilatory settings on static and functional haemodynamic parameters during experimental hypovolaemia.** *Eur J Anaesthesiol* 2009, **26**(1):66-72.
52. Renner J, Cavus E, Meybohm P, Tonner P, Steinfath M, Scholz J, Lutter G, Bein B: **Stroke volume variation during hemorrhage and after fluid loading: impact of different tidal volumes.** *Acta Anaesthesiol Scand* 2007, **51**(5):538-544.
53. Hadian M, Severyn DA, Pinsky MR: **The effects of vasoactive drugs on pulse pressure and stroke volume variation in postoperative ventilated patients.** *J Crit Care*.
54. Teboul JL, Monnet X: **Prediction of volume responsiveness in critically ill patients with spontaneous breathing activity.** *Curr Opin Crit Care* 2008, **14**(3):334-339.
55. Jones AE, Focht A, Horton JM, Kline JA: **Prospective external validation of the clinical effectiveness of an emergency department-based early goal-directed therapy protocol for severe sepsis and septic shock.** *Chest* 2007, **132**(2):425-432.

56. Rivers E, Nguyen B, Havstad S, Ressler J, Muzzin A, Knoblich B, Peterson E, Tomlanovich M: **Early goal-directed therapy in the treatment of severe sepsis and septic shock.** *N Engl J Med* 2001, **345**(19):1368-1377.
57. Huang DT, Clermont G, Dremsizov TT, Angus DC: **Implementation of early goal-directed therapy for severe sepsis and septic shock: A decision analysis.** *Crit Care Med* 2007, **35**(9):2090-2100.

Summary

In western society, cardiovascular disease is one of the leading causes of death. An appropriate lifestyle and therapeutic interventions can delay the deterioration of cardiovascular disease. As a result, early detection of cardiovascular disease has received significant attention. Two of the oldest cardiovascular signals measured are blood pressure and ECG, which can provide information on cardiac and vascular function. Not only have these measures their application in the detection of cardiovascular disease, they are also useful in the detection of more acute failure of the cardiovascular system (for example during hemorrhagic shock).

Information on the cardiovascular status and possible malfunctioning of the circulation of blood is contained within the amplitude and timing characteristics of the arterial blood pressure waveform. Therefore, the blood pressure waveform has since its availability been part of daily clinical practice, where the shape itself and derived measures indicative of the cardiovascular (dys)function have become available in monitoring equipment to aid in the evaluation of a patient.

For more than half a century, timing properties of the cardiac contraction have been recognized as indicators of cardiac function. For example, the duration of the left ventricular contraction prior to ejection of blood (the isovolumic contraction period, IC) is well known to increase with cardiac dysfunction. Next to the isovolumic contraction period, the time required for ejection of blood is also used to determine whether the circulation of blood might be compromised. The ejection period can easily be determined from the arterial pressure waveform. In contrast, the isovolumic contraction period is more difficult to determine as it requires a combination of signals (like the invasive blood pressure waveform in two places) or cumbersome techniques like cardiac ultrasound. The latter requires a trained operator and provides only intermittent values. The advantage of analyzing timing properties rather than amplitude properties of the arterial pressure waveform is that it allows the use of non-invasive measurement techniques for which the relation between pressure and the derived signal is required to be only a monotone one.

In this thesis we presented a late diastolic arterial pressure perturbation found in the carotid distensibility wave (carotid diameter change caused by the arterial pressure waveform) in healthy subjects and in the aortic pressure waveform of cardiac surgery patients (chapter 2). The consistent occurrence of such a perturbation prior to the systolic upstroke of the arterial pressure waveform indicated a cardiac origin. Analysis of the simultaneous recorded aortic and left

ventricular pressure waveform in cardiac surgery patients showed that the onset of the pressure perturbation coincided with the onset of left ventricular contraction. It was therefore concluded that the interval between the onset of the aortic pressure perturbation and the onset of the aortic systolic pressure rise could be used as a substitute for the left ventricular isovolumic contraction period. Compression of the coronary vascular bed during the isovolumic contraction, generating a backwards traveling pressure and flow wave, was suggested to cause the aortic pressure perturbation.

In chapter 3 we set out to test this coronary origin hypothesis in a swine animal model. For that purpose we briefly occluded all three major coronary arteries. If coronary compression indeed would have caused the aortic pressure perturbation, simultaneous occlusion of all three major coronary arteries would principally have abolished the arterial pressure perturbation. However, occlusion did not affect the magnitude of the pressure perturbation. Moreover, compression of the increased myocardial blood volume due to reactive hyperemia following release of the occlusion should have increased the magnitude of the pressure perturbation according to this hypothesis. This was also not observed. Therefore, it was concluded in chapter 3 that compression of the coronary arteries does not cause the aortic pressure perturbation.

In chapter 4 we used wave intensity analysis to show that the pressure perturbation indeed originated from the heart. Detailed temporal analysis of both the aortic and left ventricular pressure waveform during the left ventricular systolic phase showed that the onset of the aortic pressure perturbation was preceded by the initiation of left ventricular pressure increase. The latter is frequently used as a substitute for mitral valve closure, the onset of the isovolumic contraction period. However, it is well known that mitral valve closure lags behind the onset of left ventricular pressure rise. The novel find of a left ventricular pressure perturbation, which onset occurs later than the onset of left ventricular pressure rise and precedes the aortic pressure perturbation by only a few milliseconds, suggested an origin that also causes the abrupt closure of the mitral valve. This left ventricular pressure perturbation is likely transmitted through the aortic valve and its surrounding tissue causing the aortic pressure perturbation. In chapter 4 we concluded that the onset of the aortic pressure perturbation indeed reflects the onset of the isovolumic contraction of the left ventricle and can therefore be used to determine the left ventricular isovolumic contraction period from the aortic pressure waveform (AIC, Arterially determined Isovolumic Contraction period).

In chapter 5 we induced a graded hemorrhagic shock in a swine animal model to test the applicability of the arterially determined isovolumic contraction period (AIC). During hemorrhagic shock, ventricular preload and consequently cardiac output, stroke volume and arterial pressure will drop with a decrease in circulating blood volume. Likewise, the left ventricular isovolumic contraction period will change as a consequence of a decreased preload and afterload. However, static measures related to preload (e.g. central venous pressure or pulmonary artery wedge pressure) have shown to be poor predictors of whether or not a patient will benefit from administration of fluids. It is well known that positive pressure ventilation can be used to determine how the heart will respond to an increased preload, induced by fluid administration. In chapter 5 it was shown that the ventilation induced variation in left ventricular preload induced cyclic variations in AIC, similar to the ventilation induced variations in stroke volume and pulse pressure (maximum - minimum arterial pressure). From the latter two it is known that the relative amplitude of the variation is a good predictor to whether or not a patient is fluid responsive. In our swine model of hemorrhagic shock we showed that the ventilation induced relative variation in AIC correlated well with the ventilation induced relative variation in stroke volume and pulse pressure. Therefore, we showed the value of the ventilation induced relative variation in AIC as an indicator for the progression of hemorrhagic shock and the effectiveness of subsequent resuscitation.

The pre-ejection period (the period from the onset of the Q-top of the ECG to the onset of the systolic upstroke in the arterial blood pressure waveform) is also modulated by positive pressure ventilation. It was recently shown that its ventilation induced relative variation was able to predict whether or not cardiac surgery and septic shock patients would benefit from fluids (when assessed from the radial artery pressure waveform). In chapter 5 the ventilation induced relative variation in AIC was compared to that of the pre-ejection period. This comparison showed that the ventilation induced relative variation in AIC was a better indicator for the progression of hemorrhagic shock and the effectiveness of subsequent resuscitation than the ventilation induced relative variation in the pre-ejection period.

In the general discussion the effect of a more distal measurement site (the carotid artery) was discussed (chapter 6). It was shown that AIC can reliably be determined from the carotid artery pressure waveform. Moreover, the ventilation induced relative variation in AIC determined from the carotid artery pressure waveform still correlated well with the ventilation induced relative variations in stroke volume and pulse pressure over the progression of hemorrhage and

subsequent resuscitation. It was further shown that the more distal measurement site did not affect the magnitude of the ventilation induced relative variation in AIC. In contrast, the magnitude of the ventilation induced relative variation of carotid artery assessed pre-ejection period decreased significantly. Therefore, a threshold value for the discrimination between responders and non-responders to fluid resuscitation can be determined for the ventilation induced relative variation in AIC, but not for the relative variation in pre-ejection period.

Samenvatting

In de westerse samenleving kunnen de meeste sterftegevallen toegeschreven worden aan hart- en vaatziekten. Een gezonde levensstijl en therapeutische behandeling kunnen de verergering van hart- en vaatziekten vertragen. Om deze reden zijn de mogelijkheden voor een vroege detectie van hart- en vaatziekten veelvuldig onderzocht. Zowel de bloeddruk als het ECG signaal bevat informatie over kwaliteit van functioneren van het hart en het vatenstelsel. Deze signalen worden niet alleen toegepast bij de detectie van ontwikkeling van hart- en vaatziekten, maar zijn ook nuttig in de onderkenning van het acute disfunctioneren van de circulatie (bijvoorbeeld de herkenning van de ontwikkeling van hypovolemische shock, een tekort aan bloed).

Informatie over kwaliteit van functioneren van het hart en het vatenstelsel kan geëxtraheerd worden uit de amplitude- en tijdseigenschappen van de arteriële bloeddruk golfvorm. Het is dus niet raar dat de arteriële bloeddruk golfvorm beschikbaar is in de kliniek, waar de vorm zelf en afgeleide meetwaardes helpen bij de evaluatie van een patiënt.

De duur van de verschillende fases van de contractie van het hart worden al meer dan een halve eeuw gebruikt als indicatoren voor het functioneren van het hart. Zo is van de duur van contractie van het linker ventrikel voorafgaand aan de ejectie van bloed (de isovolumetrische contractie periode, IC) bekend dat deze toeneemt als het hart minder goed functioneert. Daarnaast wordt ook de duur van ejectie van bloed gebruikt voor de detectie van een gecompromitteerde circulatie. De duur van ejectie is gemakkelijk te bepalen door middel van analyse van enkel de arteriële bloeddruk golfvorm, in tegenstelling tot de isovolumetrische contractie periode. Voor de laatste is een combinatie van signalen nodig zoals een invasieve meting van de bloeddruk golfvorm op 2 plaatsen. Middels ultrageluid kan de isovolumetrische contractie periode niet-invasief bepaald worden. Voor deze arbeidsintensieve methode is echter wel een speciale opleiding vereist. Daar komt bij dat deze methode niet geschikt is voor een continue bepaling van de tijdsintervallen. Het voordeel van de analyse van tijdseigenschappen in plaats van amplitude eigenschappen is dat het verschillende niet-invasieve meetmethodes toelaat. Voor tijdsanalyse is er namelijk enkel een monotone relatie vereist tussen de arteriële bloeddruk golfvorm en het niet-invasief gemeten signaal. Voor de amplitude analyse dient daarentegen de exacte relatie tussen de bloeddruk golfvorm en het gemeten signaal bekend te zijn.

In dit proefschrift presenteren we een kleine perturbatie aan het einde van de diastole fase van de arteriële bloeddruk golfvorm. Deze werd opgemerkt in de

niet-invasief bepaalde distensie golfvorm van de halsslagader (verandering van de doorsnede als gevolg van de arteriële bloeddruk) in gezonde vrijwilligers (hoofdstuk 2). Deze perturbatie bleek ook op te treden in de aorta bloeddruk golfvorm van patiënten na een hartoperatie (hoofdstuk 2). Het consistente optreden van een dergelijke perturbatie vlak voor de opgaande systolische flank van de arteriële bloeddruk golfvorm duidde op een oorsprong in het hart. Analyse van de bloeddruk golfvorm in het linker ventrikel en de aorta in de patiënten groep liet zien dat het begin van de drukperturbatie gelijk viel met het begin van de isovolumetrische contractie periode. Daaruit volgde de conclusie dat het tijdsinterval tussen het begin van de drukperturbatie en het begin van de opgaande systolische flank van de aorta bloeddruk golfvorm gebruikt kon worden als vervanging voor de isovolumetrische contractie periode van het linker ventrikel. In dit hoofdstuk werd gehypothetiseerd dat de drukperturbatie ontstond door bloed dat werd terug geperst in de aorta door de samendrukking van de coronaire vaten tijdens de contractie.

In hoofdstuk 3 hebben we de hypothese dat de drukperturbatie afkomstig was uit de coronaire vaten getest in een varkensmodel. In dit model hebben we de drie grote kransslagaders kort geoccludeerd. Als de drukperturbatie uit de coronaire vaten zou komen, zou een dergelijke occlusie er voor zorgen dat de perturbatie niet zou optreden. Echter, occlusie zorgde er niet voor een amplitudeverandering van de perturbatie. Compressie van het verhoogde volume in het coronaire vaatbed als gevolg van reactieve hyperemie (volgend op de opheffing van de occlusie) had volgens de coronaire oorsprong hypothese de amplitude van de drukperturbatie moeten vergroten. Dit was echter ook niet het geval. Derhalve werd er in hoofdstuk 3 geconcludeerd dat samendrukking van de coronaire vaten niet de oorzaak is van de drukperturbatie in de aorta bloeddruk golfvorm.

In hoofdstuk 4 hebben we wave intensity analysis gebruikt om aan te tonen dat de drukperturbatie echt van het hart afkomstig was. Uit een gedetailleerde tijdsanalyse van de aorta en linker ventrikel bloeddruk golfvorm tijdens de isovolumetrische contractie periode volgde dat de drukperturbatie in de aorta vooraf werd gegaan door het begin van de bloeddrukstijging in het linker ventrikel. Deze laatste wordt vaak gebruikt als vervanging voor de sluiting van de mitralisklep, wat het begin is van de isovolumetrische contractie periode. Echter, het is bekend dat de sluiting van de mitralisklep later plaats vindt dan het begin van deze bloeddrukstijging. De vondst van een drukperturbatie in de opgaande flank van de linker ventrikel bloeddruk, welke net voor de aorta drukperturbatie start, duidt op een mechanische oorsprong die ook de abrupte

sluiting van de mitralisklep veroorzaakt. Deze linker ventrikel drukperturbatie wordt waarschijnlijk voortgeplant via de aortaklep zelf en het omliggende weefsel, met als gevolg de aorta drukperturbatie. In hoofdstuk 4 concludeerden we dat het begin van de aorta drukperturbatie inderdaad het begin van de isovolumetrische contractie periode weergeeft, en dat het dus gebruikt kan worden om de isovolumetrische contractie periode uit enkel de aorta bloeddruk golfvorm te bepalen.

In hoofdstuk 5 hebben we in een varkensmodel een hemorrhagische shock (ernstig bloedverlies) geïnduceerd om de toepasbaarheid van de arterieel bepaalde isovolumetrische contractie periode (AIC) te testen. Hemorrhagische shock zorgt ervoor dat de vullingsdruk van het hart zakt, waardoor het hart minder bloed rondpompt en de arteriële bloeddruk zakt. Als gevolg van de veranderende vullingsdruk zal ook de isovolumetrische contractie periode veranderen. De langzame veranderingen in de hierboven genoemde waardes kunnen echter niet voorspellen of een patiënt baat heeft bij toediening van vloeistof. Uit onderzoek is bekend dat cyclische veranderingen in de bloeddruk golfvorm en slagvolume veroorzaakt door beademing gebruikt kunnen worden om te voorspellen hoe het hart reageert op een verhoging van de vullingsdruk als gevolg van het toedienen van vloeistof. In hoofdstuk 5 werd aangetoond dat beademing ook een de cyclische verandering in AIC veroorzaakt, vergelijkbaar met de cyclische veranderingen in slagvolume en arteriële polsdruk (bovendruk minus onderdruk). Van deze laatste twee is bekend dat de relatieve amplitude van de variatie kan voorspellen of een patiënt baat heeft bij toediening van vloeistof. In het varkensmodel hebben we aangetoond dat de cyclische variatie in AIC goed correleert met de cyclische veranderingen in de polsdruk en slagvolume. Deze goede correlatie toont het nut aan van de relatieve amplitude van de cyclische variatie in AIC als een indicator voor de verergering van hemorrhagische shock en voor de effectiviteit van behandeling.

De pre-ejectie periode (het interval tussen de Q-top van het ECG en het begin van de opgaande flank van de arteriële bloeddruk golfvorm tijdens systole) varieert ook cyclisch tijdens beademing. Er is recentelijk aangetoond dat de relatieve variatie in pre-ejectie periode (bepaald met de bloeddrukmeting aan de pols) gebruikt kan worden bij de voorspelling of een patiënt baat heeft bij vloeistof toediening. In hoofdstuk 5 hebben we de ventilatie geïnduceerde relatieve variatie in pre-ejectie periode vergeleken met die van AIC. Hieruit bleek dat de ventilatie geïnduceerde relatieve variatie in AIC een betere indicatie gaf van de verergering van hemorrhagische shock en de effectiviteit

van behandeling dan de ventilatie geïnduceerde relatieve variatie in pre-ejectie periode.

In hoofdstuk 6 hebben we het effect van een meetlocatie verder van het hart (de halsslagader) getest. In dit hoofdstuk werd aangetoond dat AIC nog steeds goed in de halsslagader te detecteren is. Ook correleerde de ventilatie geïnduceerde relatieve variatie in AIC, bepaald uit de bloeddruk golfvorm van de halsslagader, ook goed met de ventilatie geïnduceerde relatieve variatie in polsdruk en slagvolume tijdens de verergering van hemorrhagische shock en de behandeling hiervan. Verder veranderde de amplitude van de relatieve variatie van AIC niet als gevolg van een meetlocatie verder van het hart. Dit was wel het geval voor de ventilatie geïnduceerde relatieve variatie in pre-ejectie periode, welke significant afnam. Hieruit volgde dat de relatieve variatie in AIC beter geschikt is om een grens te bepalen voor het onderscheiden van patiënten die baat hebben bij vloeistoftoediening dan de relatieve variatie in pre-ejectie periode.

Dankwoord

Dit schrijvende betekent dat, ondanks dat het boekje bij de kleine leescommissie ligt, het werk nog niet af is. Gelukkig klinkt raar, maar zo zal ik er zeker op terug gaan kijken.

Laat ik allereerst beginnen met het niet geheel normale verloop van mijn studie. Ik noem het bewust een studie, omdat ik enorm veel heb geleerd. Arnold, al bij ons eerste gesprek werd het me meteen duidelijk dat ik nog een hele hoop kon leren op een hele hoop gebieden (daar ben jij op jouw manier erg goed in). En dat gevoel is me bijgebleven als een drijfveer voor onderzoek. Het jaar dat ik onder jouw begeleiding heb mogen werken, met helaas alleen het eerste half jaar Jan als copromotor, heeft zeker zijn donkere momenten gekend. Maar gelukkig ook hele plezierige en leerzame momenten. Ik ben je dan ook erg dankbaar voor het willen continueren van het promotorschap, toen ik de studie weer oppakte in Rotterdam. En zonder Jeroen, Evelien, Liselotte en Nazia, en alle andere collega's zou het natuurlijk nooit zo leuk zijn geweest als dat ik het heb ervaren!

Na mijn start bij Dräger heb ik dan ook regelmatig getwijfeld of ik er goed aan had gedaan om te stoppen bij het lab van Arnold. Zeker in de eerste periode miste ik het onderzoek erg, en was elke fles zuurstof er een teveel (pas toen begreep ik het nut van programmeren, namelijk automatiseren). Gelukkig kon ik met hulp van Adrie en Geert een doorstart maken met het onderzoek dat ik bij Arnold was gestart. Echter niet in Maastricht, maar in het Erasmus MC in Rotterdam. Adrie, jij was zeker een van de betere bazen die ik heb gehad. Geert, ik heb het altijd goed met je kunnen vinden, wat denk ik ook heeft geleid tot de uiterst plezierige samenwerking. Ik vraag me af wie er nu een grotere klusser is... Hoewel Adrie en Geert veel hebben betekend voor de voortzetting van het onderzoek, mag ik ook zeker niet Miriam, Bas en Rob vergeten. Zonder hun steun was het realiseren van dit proefschrift nooit mogelijk geweest. Miriam, vooral jou wil ik bedanken voor het tonen van interesse en de steun binnen Dräger. Voor de dagelijkse afleiding binnen Dräger heb ik ook nog een aantal mensen te bedanken. John, zonder jou zou het geheel in het lab maar een saaie bedoening zijn geweest. Vooral de "tussendoortjes" voor de cadeaucommissie waren erg ontspannend. René, om herhaling te voorkomen, je komt bij het paranimfen stuk aan de beurt! Eugéne moet ik hier niet vergeten te vermelden. De derde muskietier die het lab en daarbuiten onveilig maakte. En Pieter, ik denk dat ik nu wel de middag vrij heb verdiend, of niet? Graag wil ik hier ook Frans (3x), Koen, Jasper, Marloes, René v. W., Werner, Sjaak, Louis, Paul, Astrid, Kitty en Karin bij naam noemen. Naast deze specifieke personen

wil ik graag de rest van de Dräger Best bedanken voor mijn fijne tijd daar. Jammer dat het moest ophouden!

Komen we aan bij de collega's van Experimentele Cardiologie. Dirk, net als Arnold ben jij iemand die ik erg respecteer. Hoewel het onderwerp waar dit boekje over gaat niet direct aansluit op jouw onderzoeklijn, heb je me wel altijd kunnen helpen door de juiste vragen te stellen en suggesties te geven voor het onderzoek. Daphne, ook jou moet ik natuurlijk danken voor de ondersteuning van dit onderzoek. Ik heb geen idee hoe vaak we om tafel hebben gezeten voor de bespreking van een draak van een tekst die dan werd gekneet en geschaafd tot iets wat (veel) beter paste. Monique, ik moet jou natuurlijk bedanken voor het inplannen van tijd bij Dirk, alsook voor alle zaken rondom het werk!

De medische omgeving was ook een hele fijne afwisseling op die van Dräger. Door met enkel 5 dames op een kamer werken is er een wereld voor me open gegaan. Als ik een cyclus zou hebben, loopt ie nu synchroon... Maar, alle gekheid op een stokje: Martine, als er iemand goed is om een vrolijke sfeer op de kamer te brengen ben jij het wel! Vooral met de ochtend muziekjes begon de dag goed. En als we alle negatieve dingen maar "de-Boeren", dan komt alles goed... Of zo... Elza, hoeveel tonnen zout ik al wel niet heb gebruikt bij jouw opmerkingen. Ik ben maar gestopt met tellen. Ook heb ik me toch altijd verbaasd over hoe goed je bent in uitslapen of in het delen van spullen (of niet, Martine ;). Maaïke, zonder jou had dit proefschrift er niet gelegen. Ik ben je dan ook erg dankbaar voor het uitvoeren van de proeven, waar ik het dier dan niet mocht aanraken (een ervaring die ik niet zou hebben willen missen ☺). Inge, het gevecht om de temperatuur op de kamer werd continu gevoerd, met af en toe een uitstapje naar het gooien van zachte voorwerpen. Gelukkig was het dan snel goed te maken met een biertje, als dat nog in de koelkast lag. Shanti, het is wel erg makkelijk om jou te plagen met een dode muis, of met het idee van iets met bacteriën... Rob, gelukkig kon ik, als die dames me teveel werden, jouw kant opvluchten. De technische afwisseling op het medische heb ik erg kunnen waarderen, samen met de regel-tripjes naar andere afdelingen! Was je er niet, dan was Roy er wel met een mooi verhaal.

Komen we bij de Rembo en Rembo van de afdeling, Vincent en André. Vincent, vooral de afsluitende periode van de promotie heb ik erg veel aan je gehad, maar daarvoor kon ik je al erg waarderen (staat er toch nog wat onzin in dit proefschrift ☺). En ga nu maar iemand anders lastig vallen! André daar in tegen straalt op de een of andere manier echt rust uit. Totdat je hem samen met

Vincent treft...Heren, bedankt voor Papendal, en de intro into Rembo en Rembo!

Mieke, de BBQ's in het park, de etentjes na een congres of borrel, of juist voorafgaand aan een borrel, waren altijd gezellig! En de zaterdagen op het Erasmus MC: gedeelde smart is halve smart?

Voor de collega's achter de klapdeuren: het hing er vanaf wie er 's ochtends als eerste genoeg had van het werk om te komen vragen wie er mee ging lunchen. Een goede afwisseling op het serieuzere werk. Naast Vincent was ook Dennie goed in het verstoren van het werk, op een plezierige manier (tijdens lunchtijd of daarbuiten). Renate, dankzij jou heb ik vaak naar Florida gewild. Mocht je ooit een oppas voor je katten zoeken... Remco, bij deze voor elke komende morgen een "goede morgen"!

Richard, Ilona, Ihsan, Jeroen, Caroline, Oana, Jaco, Wijnand en Heleen wil ik hier graag ook nog even specifiek bedanken. Daarnaast zijn er natuurlijk veel meer mensen van de afdeling die ik wil bedanken, teveel om bij naam op te noemen (ik ben gewoon bang dat ik iemand vergeet). Echter zonder hen zou de sfeer echter niet zo prettig zijn geweest zoals ik hem heb ervaren!

Verder ben ik Jan Hofland en Robert Tenbrinck dankbaar voor de hulp bij de opzet van de proeven, de bijdrage aan de artikelen, en voor de leermomenten in het ziekenhuis.

Omdat dit stuk tot hier redelijk op chronologische volgorde is geschreven wil ik op deze plaats graag de leden van zowel de kleine als de grote leescommissie bedanken. Prof.dr. W.J. van der Giessen, Wim, Dr. A.H. van den Meiracker, Anton, Prof.dr. F.W. Prinzen, Frits, Dr.ir. M.Siebes, Maria, en Prof.dr. J. Bakker, allen hartelijk bedankt voor het deel willen nemen aan de commissies. Ik hoop dat we een leuke discussie tijdens de verdediging kunnen gaan voeren!

In het dankwoord komen natuurlijk ook de mensen naar voren die je hebben kunnen afleiden van het denkwerk (waarvoor overigens de hierboven genoemde mensen ook verantwoordelijk zijn geweest). Als lid van Junior Kamer De Kempen heb ik veel geleerd op het gebied van organisatie. Nog belangrijker, de leden zijn ook erg aardig en gezellig. Vooral Martijne, Mirjam en Anne wil ik graag bedanken voor de lekkere etentjes en de gezellige tijd! Ik hoop echt dat ik nu weer meer tijd ga hebben om gezellig iets te doen met de Kamer!

Now the English part of this acknowledgement. As everyone knows I really like Florida for 3 reasons. Of course for the temperature and sun, but much more important, the friends I have started to consider as family. Jim, I admire you for what you represent. Together with Susan you make sure that all the big cats, but also the livestock have the best life that is possible! But next to that, you are fun to hang out with off property. Susan, without you the Wildlife Sanctuary probably would not have existed. Thanks for all the good times, and I hope there will be many more to come! Dale, I thank God for meeting you the very first day I came over. It has been so much fun since then working together at the sanctuary, but also at your church! Laura, when will we finally practice Yoga together? Finally, I would like to thank all the cats, next to the dogs and livestock, for taking my mind of work.

Iris, bedankt voor alle lessen Yoga. Zoals je weet zie ik het voornamelijk als een sport, en ben dus ook minder in voor het “zweverige” aspect. Al spreekt de term karma me erg aan, gezien de link met mijn “eigen” geloof. Ik hoop dat ik nog lang van je lessen mag genieten, en de gesprekken eromheen!

De paranimfen verdienen natuurlijk een eigen paragraaf. René, graag wil ik je bedanken voor de leuke uurtjes in het lab bij Dräger. Daarbij is vaak gebleken dat onze verschillende denkpatronen elkaar goed aanvullen. Ook buiten Dräger was het altijd gezellig. Hoewel we tegelijkertijd bij elektrotechniek zijn begonnen, zijn we pas bij ODIN dingen samen gaan doen. Daar heb ik je dan ook leren kennen als een slimme gozer met gevoel voor humor!

Vincent, ik vraag me wel eens af wat er gebeurd zou zijn als ik in die ene zomer geen witbier zou hebben aangeboden... Als ik iemand als goede vriend beschouw dan ben jij het namelijk wel. Tijdens strandwacht heb ik je natuurlijk goed leren kennen. Ook al zijn we daar nu “te oud” voor, het altijd erg fijn om een weekendje in Middelburg te zitten. Hoe je samen met Sabine voor Nova zorgt, laat zeker zien hoe je in elkaar steekt. I salute you! Ik hoop dat we nog vaak een borrel kunnen drinken en een goede sigaar mogen verbranden!

Aankomende bij de familie betekent dat het schrijven ook bijna gedaan is. Allereerst wil ik hier graag Rian en Kees bedanken. Dankzij hun heb ik in Maastricht rustig een eigen plekje kunnen zoeken. Ons Opa en Oma, Pake en Beppe wil ik graag bedanken voor hoe ons pa en ma (je bent Brabander of je bent het niet) hun levenslessen hebben opgedaan. En natuurlijk voor alle wijze lessen!

Johan en Stephen, broers, ik ben erg benieuwd wat er voor ons elk in de toekomst ligt. Hoewel we op veel vlakken het zelfde zijn, zijn er ook hele duidelijke verschillen. Ik geloof dat ik als naamgenoot van ons pa de technische kant heb mee gekregen. Jullie duidelijk meer het figuur (sorry ik kon het niet laten, daarvoor heb je broers). Mede dankzij de rivaliteit tussen ons 3-en ligt dit boekje er nu ook. Ondanks de rivaliteit waren jullie er wel altijd als ik jullie nodig had. Uit de grond van mijn hart, bedankt! Ook Lisette en Joyce wil ik graag bedanken voor interesse naar hoe het met de werkzaamheden stond. En natuurlijk Isabelle en Annefiene voor het laten smelten van mijn hart (en voor de shirts vol kwijl).

Pa en ma, laat het duidelijk zijn dat dit zonder jullie nooit gelukt was. Ik acht me erg gelukkig met de opvoeding die jullie me gegeven hebben. Duidelijk, liefdevol. En stimulerend. Hoewel ik de nodige dingen heb mee gemaakt, jullie hebben me er altijd doorheen gesleept (soms bewust, soms onbewust). Ma, bedankt voor het lezen, pa, bedankt voor de techniek. Beide voor het inzien dat er eerst een plan gemaakt diende te worden. Ik denk dat deze zaken de hoekstenen zijn van dit boekje. En de toekomst die gaat volgen. Ik houd van jullie!

Curriculum Vitae

Marcus Jan van Houwelingen was born September 27th, 1979 in Eindhoven. From 1991 to 1997 he attended the Christiaan Huygens College in Eindhoven and received both his HAVO (1996) and VWO (1997) diploma. He subsequently started an education in Electrical Engineering at the Eindhoven University of Technology (1997). His external traineeship was performed in Berkeley (Florida) at the Life Sciences department in the Poly-PEDAL lab run by Professor Robert Full, where he worked on artificial muscles. In his Master of Science project he developed a computer simulation model that simulated the interaction of the human respiratory and circulatory system. This model was used to explain the behavior of the arterial blood pressure under influence of hemodynamic and ventilatory changes. In 2003 he received the degree of Master of Science in Electrical Engineering at the Eindhoven University of Technology.

In 2004 he started working on a PhD at Maastricht University at the Biophysics department, with Arnold Hoeks and Jan Meinders as respectively his Promoter and Co-Promoter. At their lab, he studied the arterial pressure waveform using ultrasound, and found that the isovolumic contraction period could be determined using a small pre-systolic pressure perturbation in this waveform. Due to personal circumstances he decided to switch to Dräger Medical, for which he designed and tested patient ventilators and automated test setups. Moreover, as an employee of Dräger Medical he continued his PhD at the Erasmus University at the Experimental Cardiology lab of Dirk Duncker and Daphne Merkus, with financial support by both Dräger Medical and the Dutch government. This lab offered the possibility of high fidelity invasive measurements in controlled experiments to investigate the origin of the arterial pre-systolic pressure perturbation and its possible applications described in this thesis. With his start at Finapres Medical Systems, he will be able to continue his research concerning the arterial pressure waveform, in cooperation with the Erasmus MC.

Publications

Articles

van Houwelingen MJ, Merkus D, Hofland J, Tenbrinck R, te Lintel Hekkert M, van Dijk G, Hoeks APG, Duncker DJ; *Arterial determination of the left ventricular isovolumic contraction period in the assessment of hemorrhagic shock severity*. (in preparation)

van Houwelingen MJ, Merkus D, te Lintel Hekkert M, van Dijk G, Hoeks APG, Duncker DJ; *Initiation of ventricular contraction as reflected in the arterial tree*. (in preparation)

van Houwelingen MJ, Merkus D, te Lintel Hekkert M, van Dijk G, Hoeks APG, Duncker DJ; *Coronary-aortic interaction during ventricular isovolumic contraction*. Med. Biol. Eng. Comput. 2011 (in press)

Patent 10158025.6-1526 *Indicator for fluid resuscitation*. Inventor **van Houwelingen MJ**, owner Dräger Medical AG & CO. KG (published)

Bender SB, **van Houwelingen MJ**, Merkus D, Duncker DJ, Laughlin MH; *Quantitative analysis of exercise-induced enhancement of early- and late-systolic retrograde coronary blood flow*. J Appl Physiol 2009 December

van Houwelingen MJ, Barenbrug PJ, Hoeberigs MC, Reneman RS, Hoeks AP; *The onset of ventricular isovolumic contraction as reflected in the carotid artery distension waveform*. Ultrasound Med Biol. 2007 March

Presentations

van Houwelingen MJ, Merkus D, Duncker DJ; *Applicability of the Arterial Detected Isovolumic Contraction in Shock*. Cardiovascular System Dynamics Society 2010 (Fukuoka, Japan), Nico Westerhof award session.

van Houwelingen MJ, te Lintel Hekkert M, Merkus D, Hoeks APG, Duncker DJ; *The onset of ventricular isovolumic contraction as reflected in the arterial pressure waveform*. PhD day COEUR 2010 (Rotterdam, The Netherlands).

van Houwelingen MJ, te Lintel Hekkert M, Merkus D, Hoeks APG, Duncker DJ; *The onset of ventricular isovolumic contraction as reflected in the arterial pressure waveform*. Mini Symposium AMC 2010 (Amsterdam, The Netherlands).

van Houwelingen MJ, Meinders JM, Reneman RS, Hoeks APG; *Timing analysis of carotid distension wave*. 13th New England Doppler Conference 2005 (London, UK).

van Houwelingen MJ, Meinders JM, Hoeks APG; *Distension Waveform Analysis*. Erasmus MC Mini Symposium November 2004 (Rotterdam, The Netherlands).

Posters

van Houwelingen MJ, Merkus D, Hofland J, Tenbrinck R, te Lintel Hekkert M, Van Dijk G, Duncker DJ; *Ventilation-induced variation in the arterially determined isovolumic contraction period is an excellent indicator of hemorrhagic shock*. Experimental Biology 2011 (Washington, DC, USA)

van Houwelingen MJ, Merkus D, te Lintel Hekkert M, van Dijk, G, Hoeks AP, Duncker DJ; *Coronary-Aortic Interaction During Ventricular Contraction*. Cardiovascular System Dynamics Society 2010 (Fukuoka, Japan)

van Houwelingen MJ, te Lintel Hekkert M, Merkus D, Duncker DJ; *Determination of ventricular isovolumic contraction solely by means of pulse contour analysis*. Experimental Biology 2010 (Anaheim, FL, USA)

van Houwelingen MJ, Reneman RS, Hoeks APG; *The onset of ventricular isovolumetric contraction as reflected in the carotid artery distension waveform*. International Symposium on Intensive Care and Emergency Medicine 2007 (Brussels, Belgium)

PhD portfolio



Name PhD student: Marc van Houwelingen Erasmus MC Department: Experimental Cardiology Research School: COEUR		PhD period: 1-1-2008 to 1-4-2011 Promotors: Prof D.J.Duncker Prof.dr.ir. A.P.G. Hoeks Supervisor: Dr. D. Merkus	
1. PhD training			
	Year	Workload (ECTS)	
General academic skills			
- Biomedical English Writing and Communication	2004	1.5	
- Laboratory animal science	2011	4.5	
Research skills			
In-depth courses (e.g. Research school, Medical Training)			
- PhD courses at COEUR/CARIM (8x)	2007-2010	9.9	
- Basic Science courses at Papendal/Houthalen (2x)	2004-2008	4.0	
- Basic Anatomy	2010	7.5	
Presentations			
- National/international (6x)	2004-2011		
International conferences			
- National (3x)	2004-2011	1.5	
- International (6x)	2004-2011	7.8	
Seminars and workshops			
- Coeur research seminars (12x)	2008-2011	4.8	
Didactic skills			
Other			
2. Teaching activities			
	Year	Workload (ECTS)	
Lecturing			
Supervising practicals and excursions			
Supervising Master's theses			
Other			

